NTNU

Norwegian University of
Science and Technology

Feasibility study for upgrading the current heat distribution network of an existing building complex to a Smart Thermal Grid

John Clauss

Master's Thesis
Submission date: August 2015
Supervisor: Trygve Magne Eikevik, EPT
Co-supervisor: Armin Hafner, SINTEF Energi AS

Norwegian University of Science and Technology
Department of Energy and Process Engineering

NTNU

Norwegian University of Science and Technology

Department of Energy and Process Engineering

EPT-M-2015-127

MASTER THESIS

for

Student John Clauß

Spring 2015

Feasibility study for upgrading the current heat distribution network of an existing building complex to a Smart Thermal Grid

Mulighetsstudie for å fornye ei eksisterende thermal grid av ei bygningskompleks til ei smart thermal grid

Background and objective

Environmental awareness became a key role in building planning during the last decade. Buildings account for 40% of the total energy use in Norway [1] and can hence help saving a vast amount of energy. On top of that, an increased energy efficiency is one of the most important measures to curb greenhouse gas emissions (GHG) and secure future energy supply. According to Trondheim Municipality the potential for energy savings in residential buildings within the borders of the municipality is about 387 GWh using existing and available technology [1]. The goal in building projects, where several residential buildings are connected, is the utilization of surplus heat and efficient interaction between energy demand, surplus heat/cold and thermal storage in building complexes.

The objective of this project is the evaluation of the possibility of a smart thermal grid (STG) for the Risvollan housing cooperative in Trondheim. The existing distribution grid of the cooperative utilizes district heating directly, often at unnecessary high temperatures. This thesis will look into the possibility of low-temperature distribution and different ways for heating and hot water production, such as heat pumps, solar thermal and thermal energy storage. In this way, the energy efficiency would be increased as well as the share of renewable energy sources.

[1] Trondheim Kommune, Trondheim SmartCity Energy Efficiency, 2007

The following tasks are to be considered:

1. Literature research on STGs, state-of-the-art technology, current energy situation and the existing distribution grid, etc.
2. Structuring the technologies available (heat/cold supply, recovery, storage, etc.)
3. Describing feasible technologies considering the existing distribution grid (solar thermal, geothermal storage, heat pumps, smart meters, etc.)
4. Developing a model to simulate the operation of the STG including different technologies
5. Setting up a model for heat pumps with EES and a model for geothermal storage with EED
6. Analyzing the data and suggesting measures
7. Report and presentation (making a scientific paper with the main results from the thesis)
8. Making a proposal for further work

Within 14 days of receiving the written text on the master thesis, the candidate shall submit a research plan for his project to the department.
When the thesis is evaluated, emphasis is put on processing of the results, and that they are presented in tabular and/or graphic form in a clear manner, and that they are analyzed carefully.

The thesis should be formulated as a research report with summary in English, conclusion, literature references, table of contents etc. During the preparation of the text, the candidate should make an effort to produce a well-structured and easily readable report. In order to ease the evaluation of the thesis, it is important that the cross-references are correct. In the making of the report, strong emphasis should be placed on both a thorough discussion of the results and an orderly presentation.

The candidate is requested to initiate and keep close contact with his/her academic supervisor(s) throughout the working period. The candidate must follow the rules and regulations of NTNU as well as passive directions given by the Department of Energy and Process Engineering.

Risk assessment of the candidate's work shall be carried out according to the department's procedures. The risk assessment must be documented and included as part of the final report. Events related to the candidate's work adversely affecting the health, safety or security, must be documented and included as part of the final report. If the documentation on risk assessment

represents a large number of pages, the full version is to be submitted electronically to the supervisor and an excerpt is included in the report.

Pursuant to "Regulations concerning the supplementary provisions to the technology study program/Master of Science" at NTNU §20, the Department reserves the permission to utilize all the results and data for teaching and research purposes as well as in future publications.

The final report is to be submitted digitally in DAIM until September 7th 2015. An executive summary of the thesis including title, student's name, supervisor's name, year, department name, and NTNU's logo and name, shall be submitted to the department as a separate pdf file. Based on an agreement with the supervisor, the final report and other material and documents may be given to the supervisor in digital format.

☐ Work to be done in lab (Water power lab, Fluids engineering lab, Thermal engineering lab)
☐ Field work

Department of Energy and Process Engineering, April 24th 2015

Prof. Olav Bolland
Department Head

Prof Trygve M. Eikevik
Academic Supervisor
e-mail: Trygve.m.eikevik@ntnu.no

Research Advisor:
Armin Hafner, SINTEF Energy Research

e-mails
Armin.hafner@sintef.no

Declaration

Hereby I assure to have written this Master Thesis without unallowable help of others and only with the quoted sources. All information from external sources is marked as such.

(City, Date) (Signature)

Abstract

A feasibility study on upgrading an existing heat distribution network to a low-temperature distribution grid has been carried out during this project. The integration of a solar thermal system combined with a borehole thermal energy storage (BTES) for covering the space heating demand of the buildings as well as the application of CO_2 heat pumps and water storage tanks for domestic hot water (DHW) production were investigated in order to apply more renewable energy sources.

The energy analysis included several measures, such as modeling the energy demand of the buildings, finding a reasonable number of solar collectors to be installed and dimensioning a ground source heat pump (with the use of CoolPack and Engineering Equation Solver EES) and a geothermal storage (Earth Energy Designer Software EED) as well as CO_2 heat pumps (CoolPack/EES).

An economic analysis of all proposed measures has been carried out based on the Net Present Value (NPV) and Net Present Value Quotient (NPVQ). Initial costs, annual costs, annual savings as well as the payback time of the energy systems have been calculated.

It is found that it is not feasible to invest in the proposed energy system for space heating because the payback time (28 years) of the system is longer than the lifetime of the solar thermal system. Furthermore, the solar gain from the solar collectors is not sufficient for recovering the ground temperature of the BTES with solar energy only which is why external sources would be needed for supplying the remaining energy needed to recover the ground temperature.

Results show that an integration of CO_2 heat pumps and water storage tanks for DHW production is very promising as the payback time for the investigated system is only 4 years which is why this part should be investigated further.

Acknowledgements

First of all I would like to thank my family, especially my brother and my parents because they always supported me during all my studies. I know that it has not always been easy for them because I studied so far away from home most of the time, but they still supported me with whatever was needed. They made me who I am today and if I would start studying again, I would do everything exactly the same way. I am grateful and thankful for the last 6 years.

I thank Prof. Björn Palm, the Head of the Department of Energy Technology at KTH Stockholm, for giving me the opportunity to do my Master Thesis abroad.
Special thanks go to Dr. Armin Hafner, Senior Scientist at SINTEF Energi AS in Trondheim, for accepting me as a Master Thesis student at his department as well as to Trygve M. Eikevik who accepted me as a Master Thesis student at NTNU.

Moreover, I want to thank Dr. Armin Hafner and PhD Hanne Kauko for their supervision and their professional knowledge and advices which always promoted my thesis.

As a last point, I want to thank Eric Höfgen for his interest in my project and his thoughts on my Master thesis.

Table of Contents

List of Figures

List of Tables

List of Abbreviations and Symbols

Latin symbols

a_1	$\frac{W}{m^2K}$	Linear heat loss coefficient
a_2	$\frac{W}{m^2K^2}$	Quadratic heat loss coefficient
C_n	NOK	Costs in year n including operation, maintenance and fuel
c_p	$\frac{kJ}{kgK}$	Heat capacity of the storage medium
C_t	NOK	Net cash inflow during the time period
C_0	NOK	Initial investment costs
e		Rate of price increase
E	W	Operating energy of the compressor
G	$\frac{W}{m^2}$	Global irradiance
h		Hour, Enthalpy
i		Inflation rate
L, l		Liter
m		Meter, Mass
K		Kelvin
kJ		Kilo-Joule
p		Pressure
Q_n		Produced energy in year n
Q_1	W	Heat output of the heat pump
Q_2	W	Heat transferred to the heat pump cycle
r		Real interest rate
r_n		Nominal interest rate
s		Tax rate, Seconds
t	$°C$	Temperature
T_1	K	Temperature of the heat sink
T_2	K	Temperature of the heat source
W		Watt

Greek symbols

Δ	Delta
η_0	Conversion factor
Σ	Sum

Subscripts

amb	Ambient
B, Brine	Brine
C, Cond.	Condenser
E, Evap.	Evaporator
fl	Fluid
GC	Gas cooler
in	Inlet
out	Outlet
R	Refrigerant
S	Suction line
SH	Superheater

Abbreviations

ATES	Aquifer thermal energy storage
BTES	Borehole thermal energy storage
CHP	Combined heat and power
COP	Coefficient of performance
COP_1	Coefficient of performance of a heat pump
COP_2	Coefficient of performance of a refrigeration system
CO_2	Carbon dioxide
DC	District cooling
DH	District heating
DHC	District heating and cooling
DHW	Domestic hot water
DOT	Design outdoor temperature
EED	Earth energy designer
EES	Engineering equation solver
EN	European norm

GHG	Greenhouse gas
GSHP	Ground source heat pump
GTR	Ground temperature recovery
GWh	Gigawatt-hour
GWP	Global warming potential
HCF	Heat carrier fluid
HDG	Heat distribution grid
HP	Heat pump
HVAC	Heating, ventilation and air-conditioning
ICT	Information and communications technology
kWh	Kilowatt-hour
LEA	Low-energy architecture
Log	Logarithmic
LTDG	Low-temperature distribution grid
MEG	Monoethylenglycole
MPG	Monopropylenglycole
MW	Megawatt
MWh	Megawatt-hour
NH_3	Ammonia
NGU	Norges geologiske undersøkelse
NOK	Norwegian Kronor
NPV	Net present value
NPVQ	Net present value quotient
PCM	Phase change material
RBL	Risvollan Borettslag
R717	Refrigerant 717 (Ammonia)
R744	Refrigerant 744 (CO_2)
SH	Space heating
SPF	Seasonal performance factor
SS	Substation
STG	Smart thermal grid
TEK87	Building standard from 1987
TES	Thermal energy storage
VDI	Verein Deutscher Ingenieure

1. Introduction

Environmental awareness became a major factor in building planning during the last decade. Buildings account for 40% of the total energy use in Norway [1] and increasing building efficiency can hence help saving a vast amount of energy. On top of that, an increased energy efficiency is one of the most important measures to curb greenhouse gas (GHG) emissions and secure future energy supply. According to Trondheim Municipality the potential for energy savings in residential buildings within the borders of the municipality is about 387 GWh using available technology. The goal in building projects, where several residential buildings are connected, is an efficient interaction between energy demand, surplus heat/cold and thermal storage in building complexes.

A local heat distribution grid can be customized in order to meet the heating demand of the area in question. A low-temperature distribution grid as well as innovative thermal storage systems which consider the local heat load predictions and available renewable energy sources are a reasonable measure to supply heating energy. In general, district heating (DH) grids distribute heat efficiently from the generating plant to the customer. A broad range of energy generation technologies can be combined in order to meet the heating demand of the end-users, but supply temperatures are at high temperatures of up to 120°C so that hot water for residential buildings can be provided. A low-temperature grid can be run at supply temperatures of around 45°C. This temperature is sufficient for space heating, whereas additionally installed heat pumps can heat up DHW of a residential building to up to around 70°C.

There are around 7000 DH grids in Europe, and 14% of the energy is from renewable energy sources. The share of renewable sources in DH and district cooling (DC) is expected to reach 21.4% by 2020. The most promising approaches are Smart City initiatives which include DH and DC applications as well as off-grid small-scale applications. The aim of these initiatives is often the combination of off-grid systems and DH systems into a whole system which can lead to a so-called “Smart Thermal Grid (STG). [2]

The application of a STG can help reducing the energy consumption of a district. STGs are

defined as a network of pipes connecting buildings in a neighborhood, town center or an entire city, so that they can be served from centralized plants as well as from a number of distributed heating and cooling production units including individual contributions from connected buildings [3].

The objective of this Thesis is the evaluation of the possibility of applying a STG for the Risvollan housing cooperative in Trondheim. Risvollan is a district in Trondheim with about 1300 apartments, most of them owned by the housing cooperation Risvollan Borettslag (RBL). The existing distribution grid of the cooperative utilizes district heating directly, often at unnecessary high temperatures. This thesis will look into the possibility of a low-temperature distribution and different solutions for space heating and hot water production, including for instance heat pumps, solar thermal and thermal energy storage. In this way, the energy efficiency as well as the share of renewable energy sources could be increased.

2. Objectives

This thesis is part of an innovation project “Development of Smart Thermal Grids” between SINTEF Energy Research, Statkraft Varme and Trondheim Municipality. The project will be carried out on behalf of SINTEF Energy AS and the aim is a feasibility study for upgrading the current heat distribution network of the existing housing cooperative to a Smart Thermal Grid. The focus is mostly on the evaluation of the different technologies to be used, such as CO_2 heat pumps for hot water heating as well as solar thermal and geothermal energy storage for space heating. All evaluations are made under the consideration of the given energy situation in Risvollan and characteristics of the area, such as the current heating demand, the orientation of the buildings (important for solar thermal) and solar irradiation and the properties of the soil (important regarding geothermal storage).

Maintaining the desired temperature level in buildings is a key characteristic when modeling the system to be installed. Assuming that the current heating demand for space heating and DHW needs to be met in the future as well, the energy systems have to be planned accordingly. By maximizing the renewable energy share and reducing the energy use, the demand of purchased energy of the building complex is expected to be reduced significantly compared to conventional solutions. Energy exchanges with the DH network of Trondheim are still possible in order to meet the peak heating and cooling demand of the building complex.

This Thesis has the following main objectives:

- Literature research on STGs, state-of-the-art technology, current energy situation and the existing distribution grid
- Structuring the technologies available (heat supply, recovery, storage, etc.)
- Describing feasible technologies considering the existing distribution grid (solar thermal, geothermal storage, heat pumps, etc.)
- Modeling the energy demand of the buildings applying SIMIEN software tool
- Setting up a model for ground source heat pumps (Engineering Equation Solver EES) and a model for geothermal storage (Earth Energy Designer Software EED)
- Setting up a model for CO_2 heat pumps (Engineering Equation Solver EES) for domestic hot water (DHW) heating

3. Boundaries and methodology

The system boundaries and the applied methodologies go hand in hand and interfere with each other. This chapter describes the general methodologies used and discusses the boundaries of this thesis. Detailed descriptions of the procedures of each of the simulations and calculations are given in the respective chapter.

3.1 Methodology

Figure 1 gives an overview of how the project is approached. After the objectives have been outlined, system boundaries need to be defined. A literature research is carried out focusing on STGs, state-of-the-art technology, the current energy situation and the existing distribution grid.

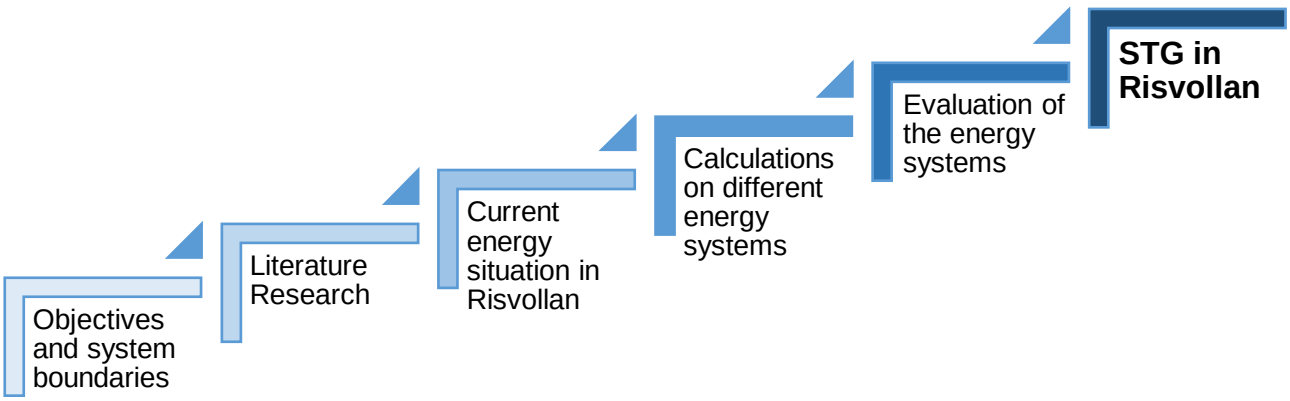

Figure 1 - Methodology for the feasibility study of a STG in Risvollan

New technologies may be implemented into the existing buildings in the future. The energy savings potential of each measure is calculated and evaluated from an energy point of view as well as from an economic point of view. Since this thesis focuses on the STG and not on the building envelopes, measures like insulation of walls/roofs or replacement of windows and doors are not considered in the project planning. The main objective is the feasibility study of a low-temperature distribution network which includes centralized heat production at low temperature as well as a seasonal thermal energy storage.

SIMIEN is used to model the energy demand and peak load demand of buildings, EED is

used to model a seasonal geothermal storage, EES software is applied to create a model for heat pumps and the solar gain is calculated in Excel.

In the end, the implementation of the different technologies will be discussed and measures for further work will be suggested.

3.2 System boundaries of the project

System boundaries can be of different orders [4]. A “physical boundary” can depend on the geography, capacity or energy transfer properties. In this project the physical boundary includes the houses which are connected to the local heat distribution network. The basis of drawing the boundary around this area is a map of the heat distribution grid owned by the Borettslag. The map is given in Figure 2.

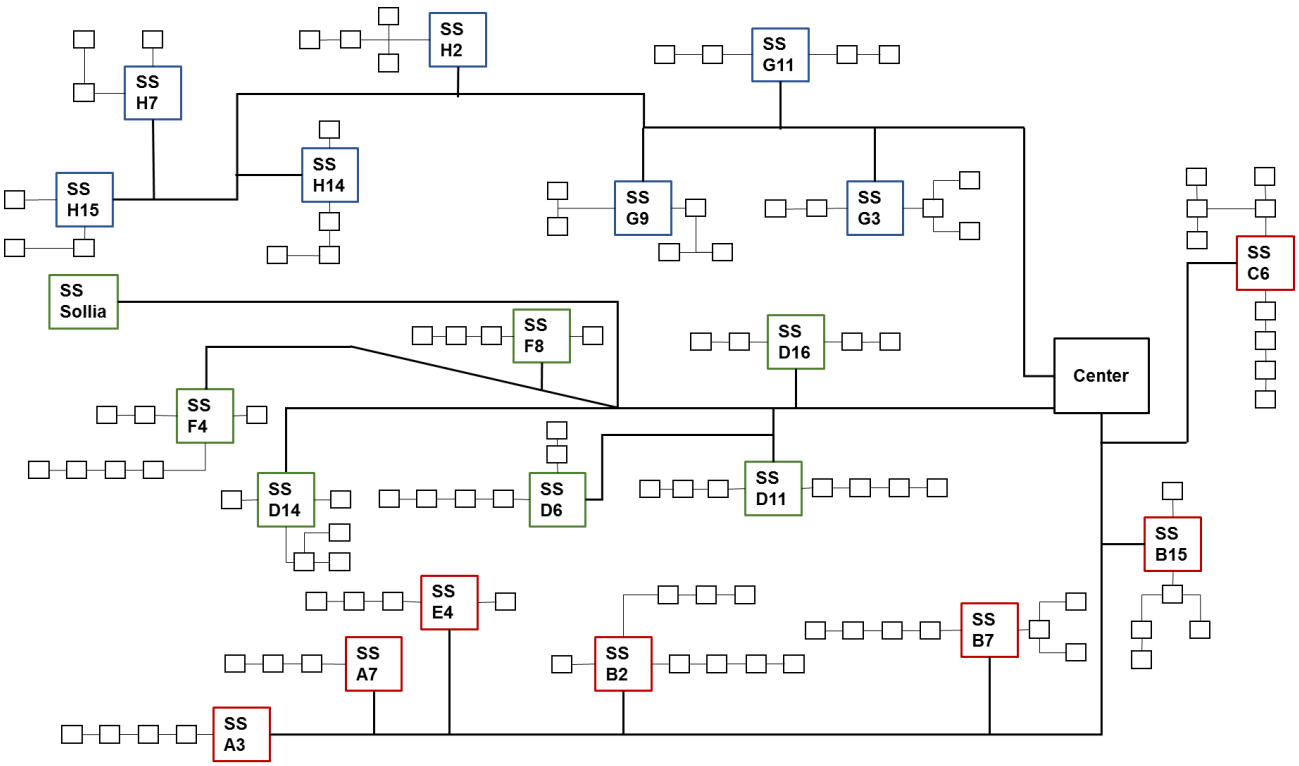

Figure 2 - Sketch of the heat distribution grid in Risvollan

Using this map it is possible to determine the buildings which are to be investigated. From an energy point of view, the usage of district heating/cooling and electricity are a part of the system because it is up to the Borettslag what to use and how to use it. It should be mentioned that this project does not consider any transport matters.

A second boundary is the “impact boundary” which depends on emissions and economy,

that is, energy market prices and costs. As this thesis is a feasibility study, there is no real boundary from an economic point of view. Many measures can be investigated, but a decision of what is feasible and what is not feasible is up to the stakeholders. From an economic point of view, the prices for electricity and DH/DC are not part of the system because they are regulated by the market and set by the provider; however all investments and costs which are introduced by the different energy efficiency measures are part of the system.

The “political boundary” is dependent on laws, permits and/or building regulations [4]. Political decisions affect the system to a great extent (for example tax systems), but as decisions from policy makers cannot be influenced, they are not a part of the system. Building regulations on the other hand, can be a part of the system, if they are changed in a way that it affects the choice of which kind of energy system to use.

4. Background information

This chapter gives a brief introduction to smart thermal grids, district heating, solar thermal, heat pump technology and thermal energy storage technologies.

4.1 Smart thermal grids

Smart thermal grids can ensure a reliable supply of heating and cooling using renewable energy such as solar thermal, geothermal, biomass or waste as a heating source. On top of that, it can adapt to demand changes at a low response time and thus make sure that as little energy as possible is used. Typical requirements/characteristics of a STG are presented in Table 1.

Table 1 - Characteristics of a Smart Thermal Grid [2]

Flexible	• Short-term: adapt to energy supply and demand situation • Medium-term: adapt by adjusting the temperature level in existing networks and through the installation of new distributed micro-networks • Long-term: adapt by aligning the network development with urban planning
Intelligent	• Planning and operation, end-users interaction with the heating and cooling system
Integrated	• Urban planning and urban networks – electricity, sewage, waste, Information and communications technology (ICT), etc.
Efficient	• Optimal combination of technologies and cascade usage
Competitive	• Cost-effective, affordable
Scalable	• For neighborhood-level or city-wide application depending on energy demand
Securing energy supply	• Using local energy sources for energy supply

In order to make the installation of a STG reasonable, several challenges have to be overcome. The main challenges are [5]:

- Cost-effective operation of district heating grids (costs for fossil fuels are increasing)
- Supply of renewables to district heating and cooling (DHC) grids (competition between renewables; additional investment for seasonal storage; limited potential for renewables in populated areas)
- Demand side management (customers and network operators need to be motivated)
- Planning of innovative networks (very complex systems; no standard planning

procedure)

- Implementation of innovative networks (new infrastructure may be needed; contractual conditions need to be fixed)
- Supply of industrial waste heat to DHC networks (additional investment costs and sites often far away from populated area)

On the other hand, STGs have many opportunities for increased energy efficiency. Heat pumps can be applied in buildings in order to utilize low temperature heat as well as smart meters that will be one of the steps towards a more advanced energy management. Other measures are the integration of ICT systems and thus demand side management or the operation of seasonal storages [5]. ICT systems can ease the control of the interaction of the different energy technologies and optimize the energy use from an economic point of view. Figure 3 gives a summary of what it means to run a smart thermal grid.

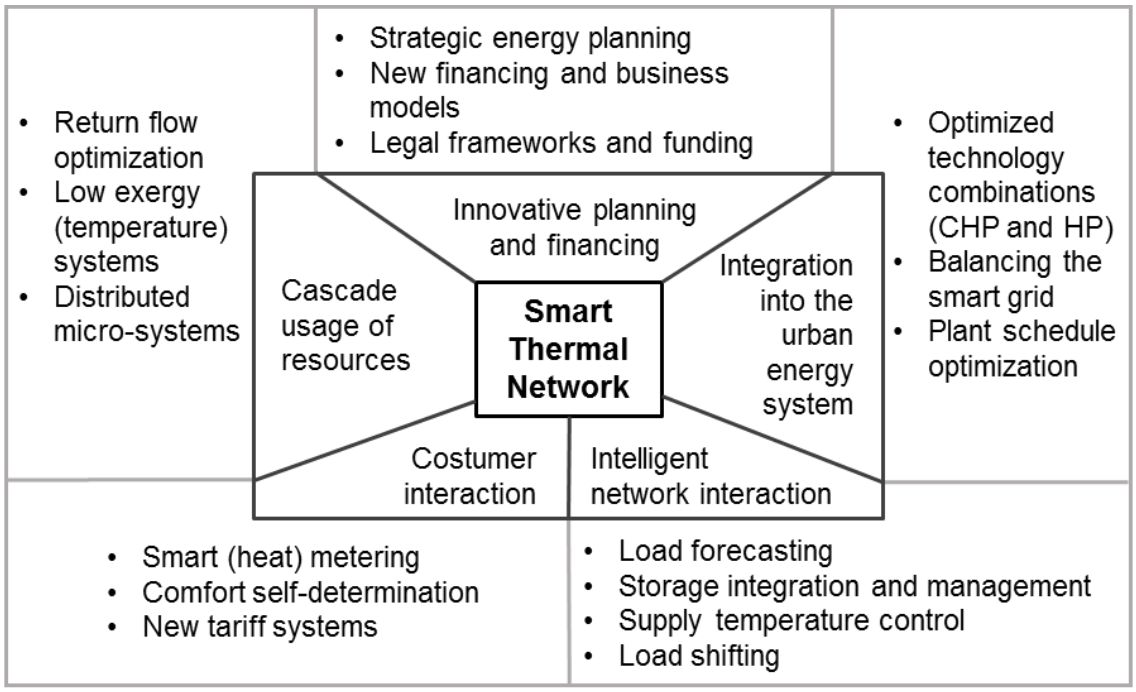

Figure 3 - Characteristics of a smart thermal grid [5]

As a pilot project TU Delft is looking into the transition from a high-temperature heating grid (≈ 130°C) towards a smart thermal grid working as a medium-temperature grid (≈ 70°C) applying waste heat recovery as well as geothermal storage as a long-term thermal energy storage and phase change materials (PCM) as a short-term storage. The study showed that the PCM storage inside the buildings is not feasible because the total heat demand reduction gained with this measure is calculated to be 1% which does not justify

the high investment costs [6].

Furthermore, buildings in this pilot project were renovated and connected in series meaning that high-temperature buildings are provided first and afterwards medium-temperature buildings. This is called a cascade system. The new heating system is expected to decrease the primary energy supply by 18-47% with respect to the present system [7].

4.2 District heating

The principle of DH is the same in each city and therefore, general information on DH is provided first and afterwards the DH network of Trondheim is discussed.

The heat for DH is generated in a central incineration plant and is then distributed to the customers via a pipeline network using water as a working medium. The generation plant can be a combined heat-and-power (CHP) plant and/or boilers using a variety of fuels (depending on their availability and prices), renewable energy systems or heat pumps. Normally, the circulating water in the DH pipelines is connected to the customer´s network (a single building or apartment block) via a heat exchanger which extracts heat from the DH water for heating purposes and hot water preparation. In general, the water is forwarded to the customer at a temperature between 80°C and 120°C depending on the surrounding temperature, pressure, location and heat losses in the pipeline, whereas the return water temperature ranges from 45°C to 75°C. The working principle is shown in Figure 4. [8] [9]

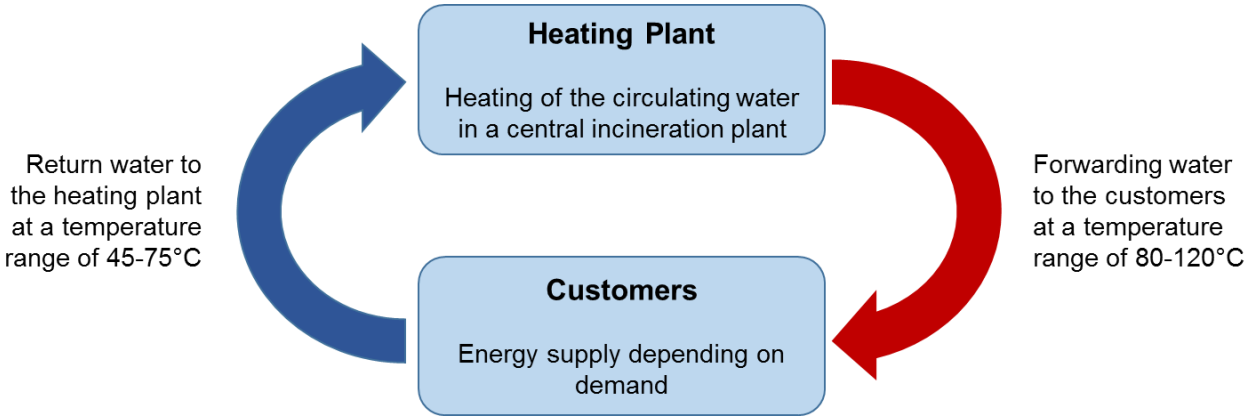

Figure 4 - Working principle of district heating [9]

District heating in Trondheim

Statkraft Varme AS is the local energy provider for DH in Trondheim covering about 30% of Trondheim´s heating demand. Statkraft´s annual heat production in Trondheim is 576 GWh using a waste incineration plant mostly [10]. Statkraft runs several power plants of different capacities: waste (78 MW), biomass (9 MW), biogas (2 MW) and heat pumps (1 MW) for base load production and electrical boilers (65 MW), oil (50 MW), LNG (30 MW) and LPG (75 MW) for peak load production [11]. In total, there are ten heating plants and a pipeline distribution grid of 250km. A sketch of the distribution grid is presented in Figure 5.

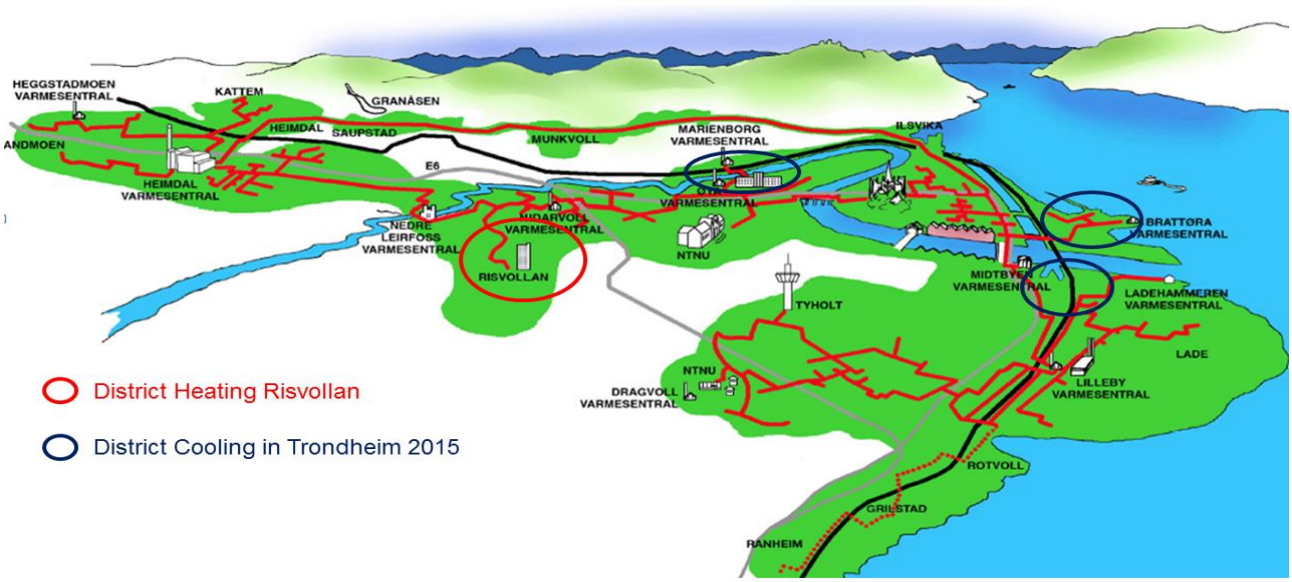

Figure 5 - Map of the DH and DC network in Trondheim [11]

The pipeline system is designed for a pressure of 16 bar (in 1982), a forwarding temperature of 120°C and a return temperature of 70°C. In order to minimize pressure losses, the network is divided with heat exchangers into several sub-systems coupled in parallel. Statkraft is planning to re-design the existing system for pressures up to 25 bar in the upcoming years. A waste incineration plant is favored over a combined heat-and-power (CHP) plant because the price for heat is about the same as the price for electricity which makes a CHP plant not feasible [12].

In the Risvollan area, Statkraft provides DH to a heating central of Risvollan housing cooperative which distributes the heat via their own pipeline network. The network plan was shown in Figure 2.

4.3 Solar heating system

A solar heating system harnesses solar radiation by converting the incident solar flux to useful heat. A low-temperature solar thermal power system operates at temperatures below 120°C and can be applied for local DHW production and/or space heating [13]. Incoming solar radiation is absorbed by a solar collector in order to heat up a fluid which circulates in the solar collector. A typical solar collector type is the flat-plate collector which operates at a temperature range of 20°C to 80°C. An illustration of a flat-plate collector is presented in Figure 6.

Figure 6 - Image of a flat-plate solar collector [14]

Such a collector has a glass cover as a protection for the underlying absorber. The absorber can be of aluminum which is coated with a highly selective material which absorbs sunlight and converts it into heat which is transferred to the solar collector fluid. The collector is insulated on each side and the back in order to decrease heat losses [15]. The efficiency of a flat-plate collector is typically in the range of 50% to 90% [16]. The solar gain of a solar collector system is calculated in Chapter 6.2.2 and therefore not further discussed here.

A combisystem for space heating and DHW production is often applied in residential buildings. A sketch of a combisystem is shown in Figure 7 and discussed in Chapter 4.5.3.

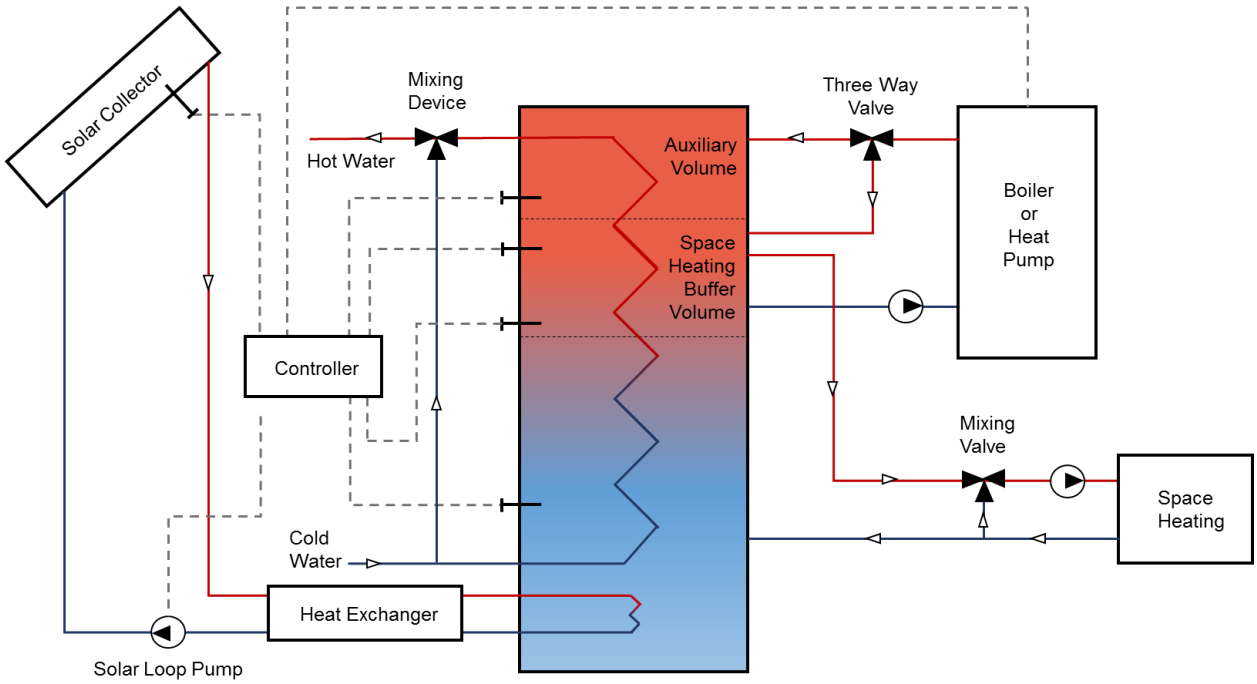

Figure 7 – Combisystem for space heating and DHW heating [13]

4.4 Heat pump technology

This chapter gives an introduction to heat pump technology as well as typical applications and common heat sources for heat pump systems.

4.4.1 General information about heat pump technology

A heat pump is used to “pump” energy from a heat source to a heat sink. The heat source contains low temperature heat energy, which can be from ambient air, the ground, lake or sea water. A heat pump provides a temperature lift and delivers heat to the heat sink at higher temperature levels, for instance for space heating or for DHW use. Heat pumps are often used as “heating, ventilation and air-conditioning” (HVAC) heat pumps, which means that they can be applied for heating and cooling purposes which is also more beneficial from an economic point of view. According to Havtun [17] favored conditions for heat pump applications are:

- High temperature of the heat source
- Heat source close to the heat demand
- Demand at moderate temperature levels
- Many working hours per year
- Relatively high energy price since this emphasizes the annual economic savings

4.4.2 Working principle and characteristic parameters

Figure 8 shows the working principle of a heat pump from a more technical point of view where Q_1 is the heat output of the heat pump, T_1 the temperature of the heat sink, E the operating energy, Q_2 the heat transferred to the cycle and T_2 the temperature of the heat source.

The coefficient of performance for a heat pump, COP_1, can be defined as

$$COP_1 = \frac{Q_1}{E} \tag{4.1}$$

With an energy balance over the system

$$Q_1 = Q_2 + E \tag{4.2}$$

the coefficient of performance for a refrigeration system, COP_2, is

$$COP_2 = \frac{Q_2}{E} = COP_1 - 1 \tag{4.3}$$

COP_2 is mentioned because a heat pump can be run in heating mode as well as in cooling mode. It has to be pointed out that the equations for COP_1 and COP_2 are only valid, if all the rejected heat from the system is included in Q_1 [17].

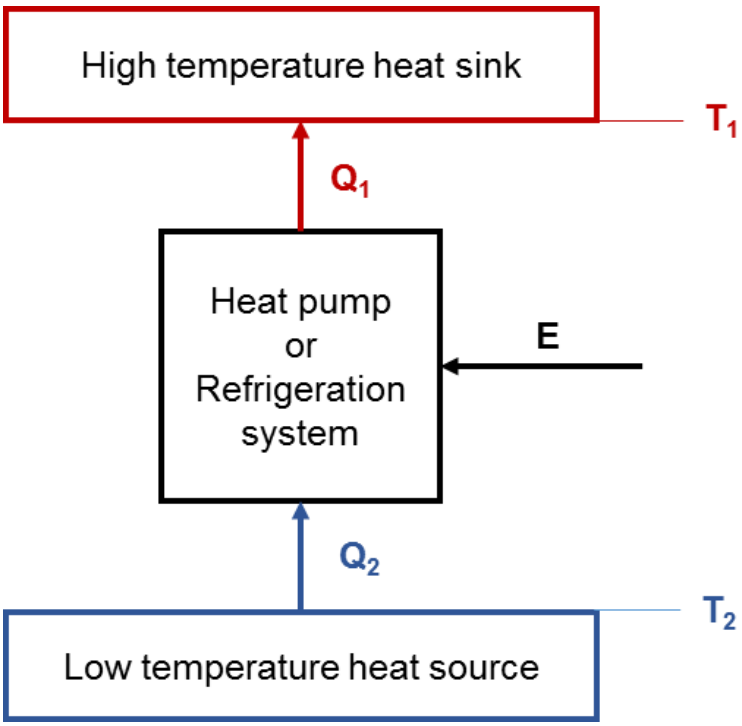

Figure 8 - Principle of a heat pumping system

A characteristic parameter for practical applications of heat pumps is the seasonal performance factor, SPF. The SPF is related to the COP_1 as it describes the performance of a heat pump over a whole year, thus leading to

$$SPF = \frac{\sum Q_1}{\sum E} \tag{4.4}$$

where $\Sigma\ Q_1$ is the total useful heat energy delivered from the heat pump and Σ E is the total operating energy for the system during a whole year.

A typical heat pump uses the working principle of a vapor-compression-cycle shown in Figure 9. A refrigerant absorbs heat from a heat source in the evaporator. The now gaseous refrigerant is compressed and afterwards condensed in the condenser while rejecting heat to an external water or brine cycle. After the condenser the refrigerant is expanded back to the evaporation pressure and flows back to the evaporator completing the cycle.

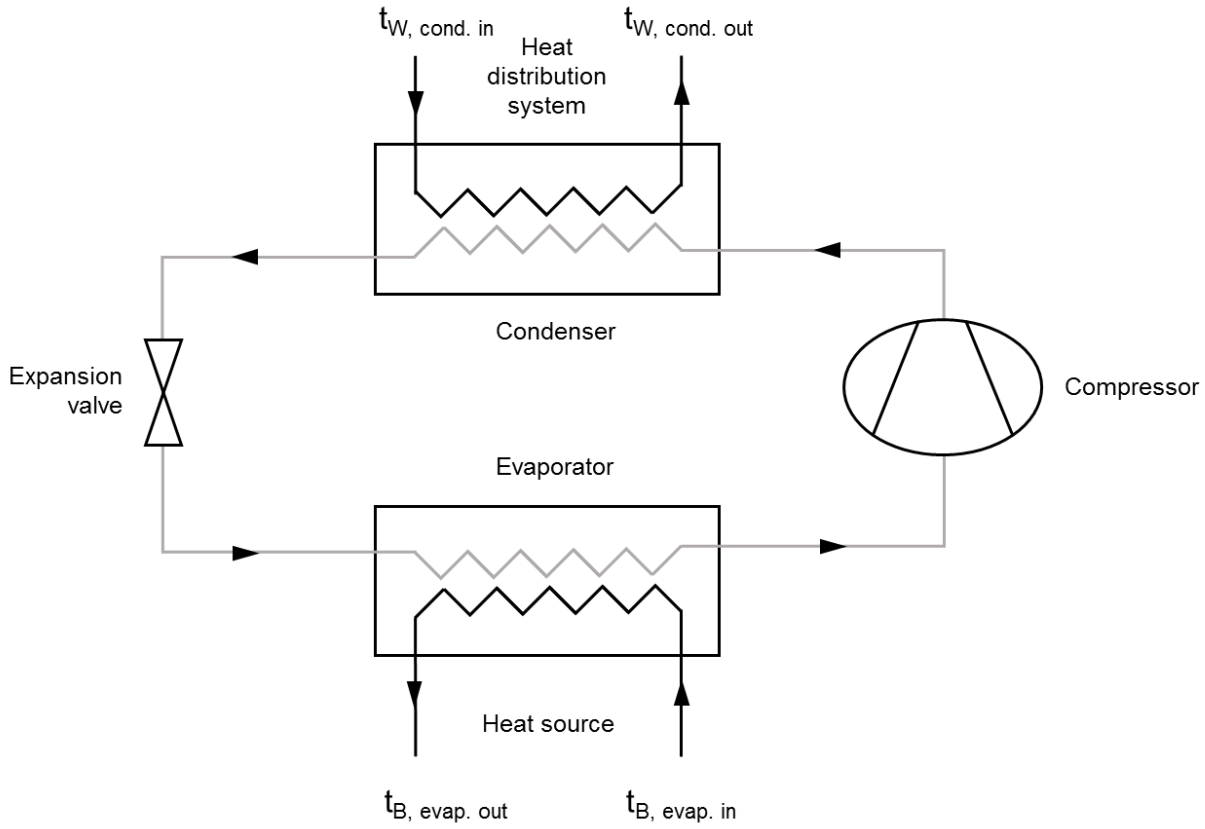

Figure 9 - Sketch of a vapor-compression-cycle

4.4.3 Integration of heat pump systems for heating applications

In general, the process efficiency is highly dependent on the temperature in the evaporator and the condenser. When installed for heating purposes in buildings, the heat pump systems should work at the lowest possible temperature for heat distribution also maintaining the desired indoor temperature meaning that the temperature for the circulating heating water is controlled by the indoor temperature. If a heat pump is used for space heating as well as for DHW heating, the condenser should consist of several sections (hot gas cooler, condenser, sub cooler) where one section is either used for space heating or DHW heating. An advanced solution for a heat pump application for residential buildings is given in Figure 10 combining space heating and DHW heating. In order to increase the heating capacity of a heat pump system, a hot gas cooler and a sub-cooler can be installed before and after the condenser. The sub-cooler is a heat exchanger which can be used in the ventilation system for heating the inlet air to a building as it uses the low-temperature energy from the refrigerant after the condenser. The hot gas cooler uses the high temperature of the refrigerant after the compressor and can be used for heating up the water to even higher temperatures than the condensing temperature. Figure 10 presents a working scheme for a heat pump system which could be integrated into a residential building complex for tap water heating as well as space heating.

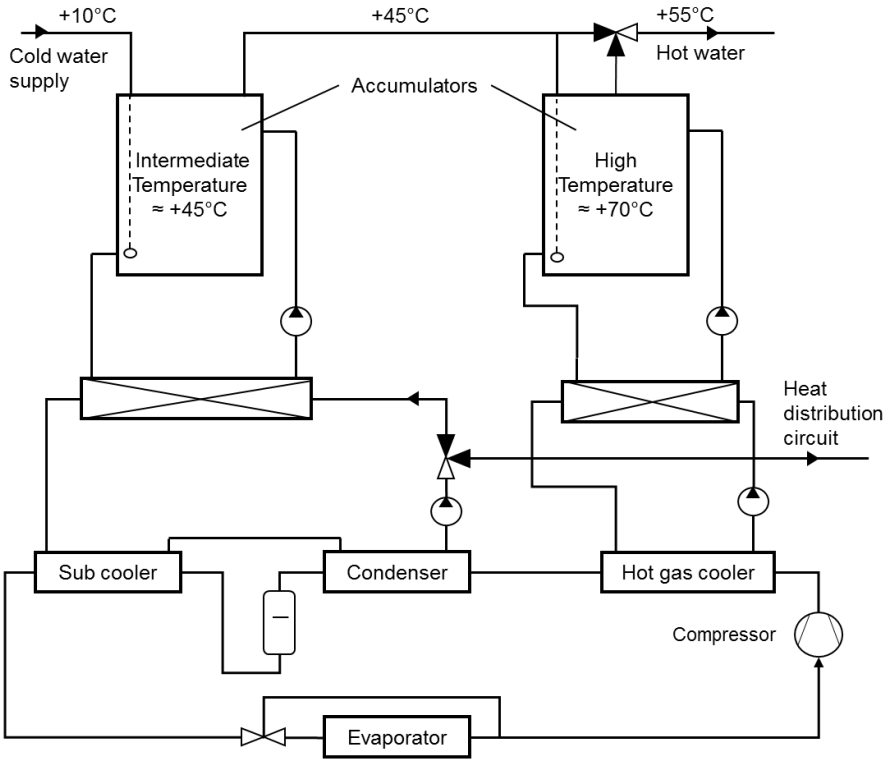

Figure 10 - A heat pump system for space heating and DHW heating [17]

4.4.4 Heat sources in Risvollan

If ambient air is used as a heat source, it is usually necessary to install a supplementary heat source because the heating capacity is lowest during the coldest days of the year which means that the heat pump is most probably not able to cover the heating demand in those cold days [17].

In Norway, a ground source heat pump (GSHP) is more reasonable, using either shallow ground coil or bedrock as the heat source. Shallow ground coil requires a rather big area which limits the use in urban areas. As a rule of thumb it can be said that an area of 500m^2 is required for covering the heating demand of a typical one-family house. A capacity of about 20 $\frac{W}{m_{tube}}$ and an energy storage capability of about 30 $\frac{kWh}{m^2*year}$ are common characteristics of such systems in Scandinavia. Systems which use a vertical borehole in the bedrock are more common in urban areas as they require less space. Those systems can be fit to the site´s heating demand specifications. If many boreholes which are located close to each other are applied, the system needs to be recharged during summer time because the ground temperature will decrease, if heat is extracted from the ground during winter time [17]. Boreholes can also be applied as a cooling source during summer time. The borehole drilling technique highly depends on the ground conditions and can be very expensive depending on the length of the borehole, the ground conditions and the technology/equipment used for drilling.
Furthermore, lake, river or sea water can be used as a heat source. They have a huge potential due to their large volumes, but the change in water temperature needs to be considered because it may change depending on the heating/cooling capacity. Since there is no lake and neither a river close to the Risvollan area, this technology is not described any further, but more information is provided by Havtun [17].

4.4.5 Ground source heat pumps

GSHPs use the heat of the bedrock as a heat source and can be applied for space heating applications. It is common to use an indirect system design which is a closed pipeline system, where a pump circulates a brine (anti-freeze-fluid) between the bedrock heat exchanger and the evaporator of the heat pump transferring heat from the heat source. A principle design of such a system is shown in Figure 11.

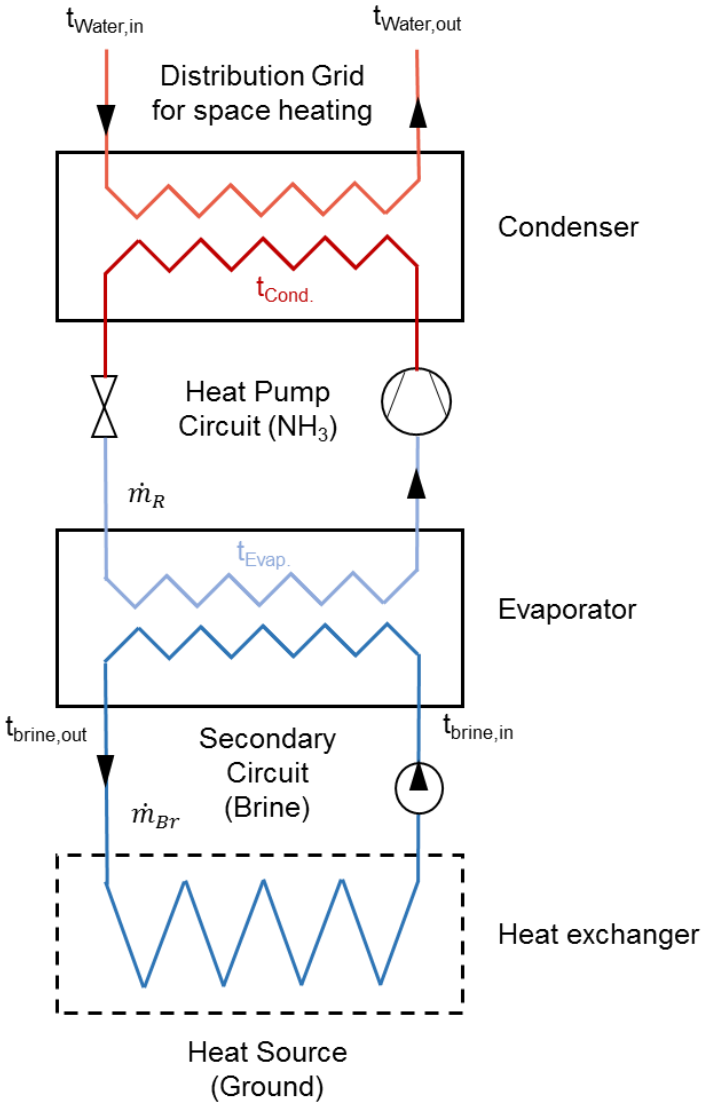

Figure 11 - Principle design of an indirect heat source system [18]

A working fluid well-suited for the low temperature levels of a GSHP is ammonia (NH_3, R717). Ammonia heat pumps can achieve high energy efficiencies, especially for non-residential buildings with large heating/cooling demands, if they are applied for heating and cooling [19]. Despite ammonia´s toxic behavior, it has been commonly used in Norway ranging from heat pump capacities of 200 kW to 8 MW.

For the Risvollan project the maximum supply temperature is of importance. Ammonia has a normal boiling point of -33.3°C and a critical temperature of 132.2°C and thus covers a big range of heat pump applications. The GSHP is supposed to heat up the water of the distribution grid to around 45°C. This happens at the condenser side of the heat pump. On the evaporator side of the heat pump, the brine inlet temperature is in the range of 0°C to 12°C depending on the month of the year and the demand conditions. The choice of the

evaporator/condenser temperatures is based on the log p-h diagram for R717 which is presented in Figure 12.

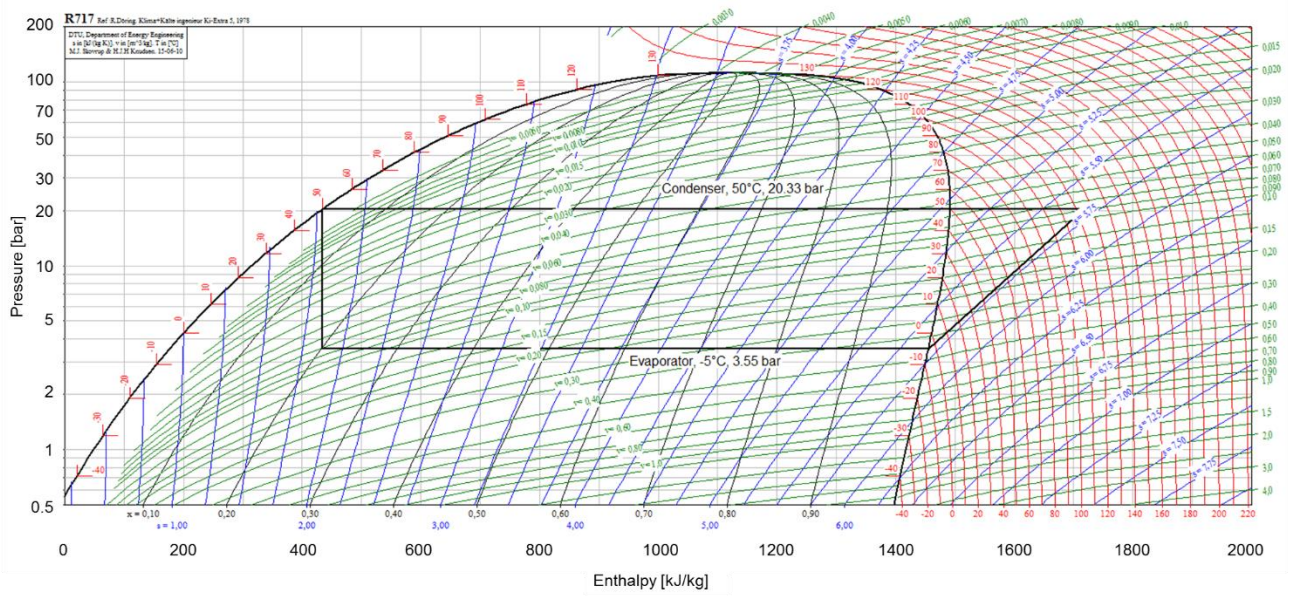

Figure 12 - Log p-h diagram of R717

General advantages of using ammonia as a refrigerant are its very low global warming potential (GWP) [20] and its high heat of evaporation [21]. A detailed description is given in Chapter 6.3.4.

4.4.6 CO_2 heat pumps

When it comes to heat pump applications at a higher temperature level (around 80°C) more and more priority has been given to CO_2 heat pumps during the last few years. Nekså [22] investigated a CO_2 heat pump for DHW heating. According to Nekså, typical evaporation temperatures of a CO_2 heat pump cycle are around -5°C to 0°C. After the compressor, the CO_2 passes the gas cooler, where it cools down from around 85°C to 15°C depending on the pressure. If water is heated up to 65°C, the pressure inside the condenser needs to be about 90 bar in order to still have a slight pinch point temperature difference to the water. After the gas cooler the CO_2 passes an internal heat exchanger where it cools down to an even lower temperature. A throttle valve is used to set the pressure of the evaporator to 35 bar which corresponds to an evaporation temperature of 0°C. The CO_2 takes the heat from the heat source and evaporates inside the evaporator before it passes the internal heat exchanger and the compressor. A common heat source

for an evaporation temperature of 0°C is sea water. The internal heat exchanger is used to superheat the vapor at the compressor inlet in order to make sure that no liquid is entering the compressor. The cycle is shown in a T – s – diagram in Figure 13.

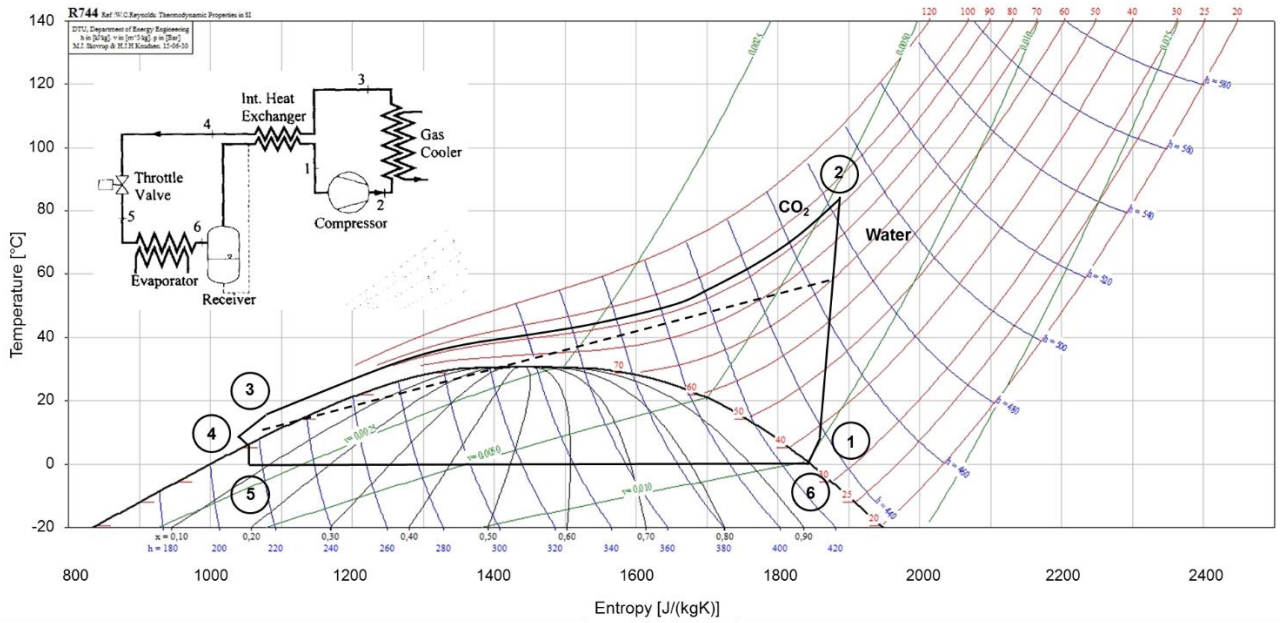

Figure 13 - Typical CO_2 heat pump cycle [22]

Because of the low critical temperature of CO_2 (R744), 31.3°C, the system is operated in trans-critical mode which means that the refrigerant passes a subcritical as well as a supercritical state. The CO_2 heat pump cycle for DHW heating is shown in a log p-h diagram in Figure 14 where the evaporation temperature is 0°C and the condensing temperature is 85°C.

Stene [23] tested a CO_2 heat pump under different modes: for space heating (up to 40°C), DHW heating (up to 80°C) and in a combined DHW and space heating mode. It was found that the SPF of a CO_2 heat pump is equal or higher than the SPF of conventional synthetic refrigerants. The investigated heat pump consisted of a tripartite gas cooler using two gas coolers for preheating and reheating the DHW and a gas cooler in the middle for space heating.

A principle of the investigated system is shown in Figure 15. A COP of 4.2 was reached, if the heat pump was used for DHW heating only, heating it from 10°C to 60°C. It was emphasized that the DHW storage tank should be designed for each system individually including movable insulating plates or having two different tanks for hot water and cold city water storage.

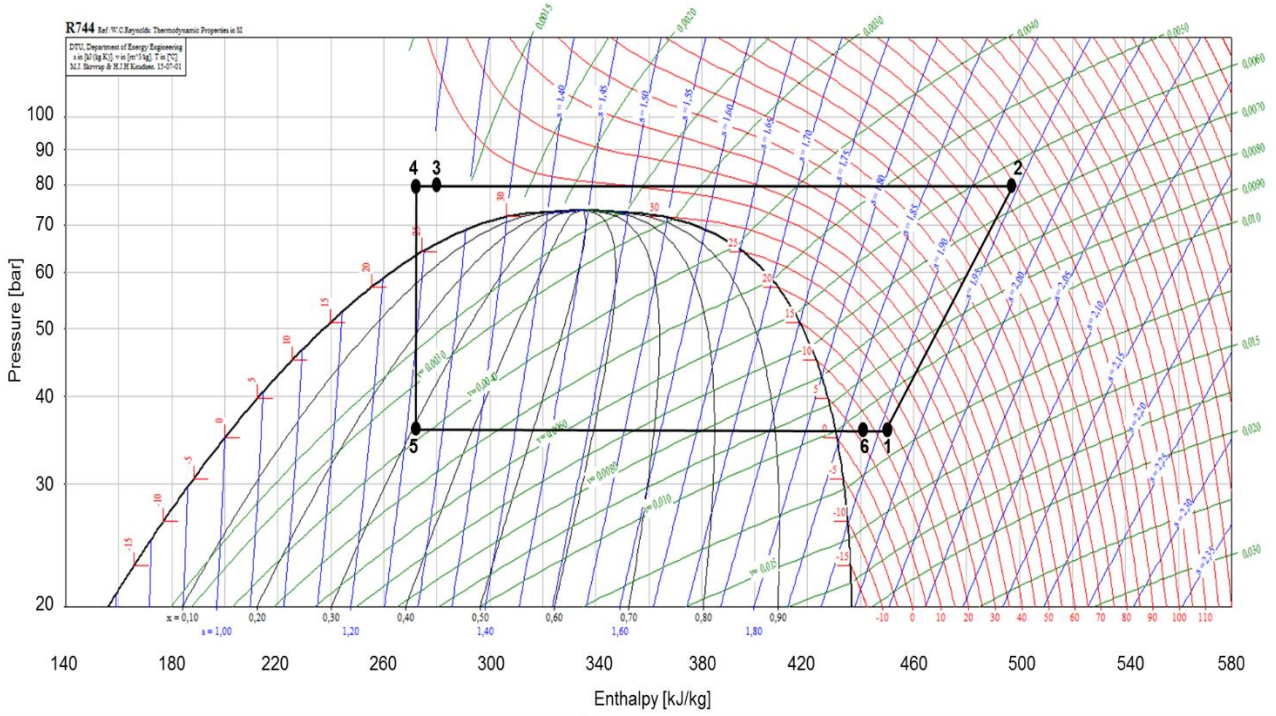

Figure 14 - Log p-h diagram of a CO_2 cycle for DHW heating

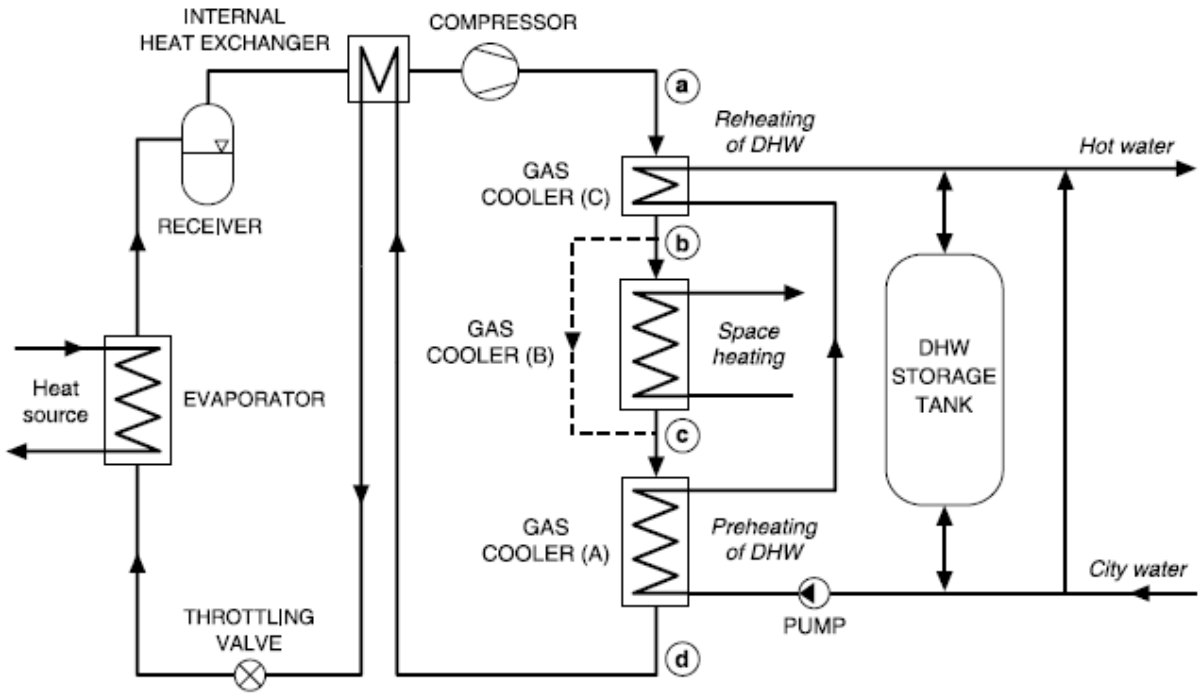

Figure 15 - Principle of a residential CO_2 heat pump system [23]

4.5 Thermal energy storage

Thermal energy storage (TES) is a possibility to increase the share of renewable energy sources in order to meet the energy demand delivering heat or cold to the system when it is needed.
With the help of TES peak heating loads as well as peak cooling loads can be reduced [24]. This chapter gives a brief introduction to some TES technologies available nowadays and selected measures are described in more detail.
In general, TES can be categorized into Passive Storage and Active Storage where passive systems are considered as systems without any mechanically moving parts and active systems have mechanical moving parts and an active control system. Passive systems are integrated into the built environment, whereas active storage is more of an auxiliary component of the system. A passive storage system depends on the surrounding climate conditions and is generally dependent on the thermal mass of a building. Active storage on the other hand, is usually connected to a heat sink/source which means it can be charged whenever possible and discharged when energy is needed *[25]*.

According to Heier [24] “the combination of TES and building types […] has a significant potential for increased energy efficiency in buildings”. It also is a good way to implement renewable energy sources into the building sector because the building´s energy demand can be decreased, if stored energy is used instead of directly produced energy in case of peak load demands. An overview over different TES possibilities is presented in Figure 16.

4.5.1 Types of TES technologies

As it can be seen in Figure 16, TES can be divided into the different types [25]:

- Sensible heat storage
- Latent heat storage
- Thermochemical storage.

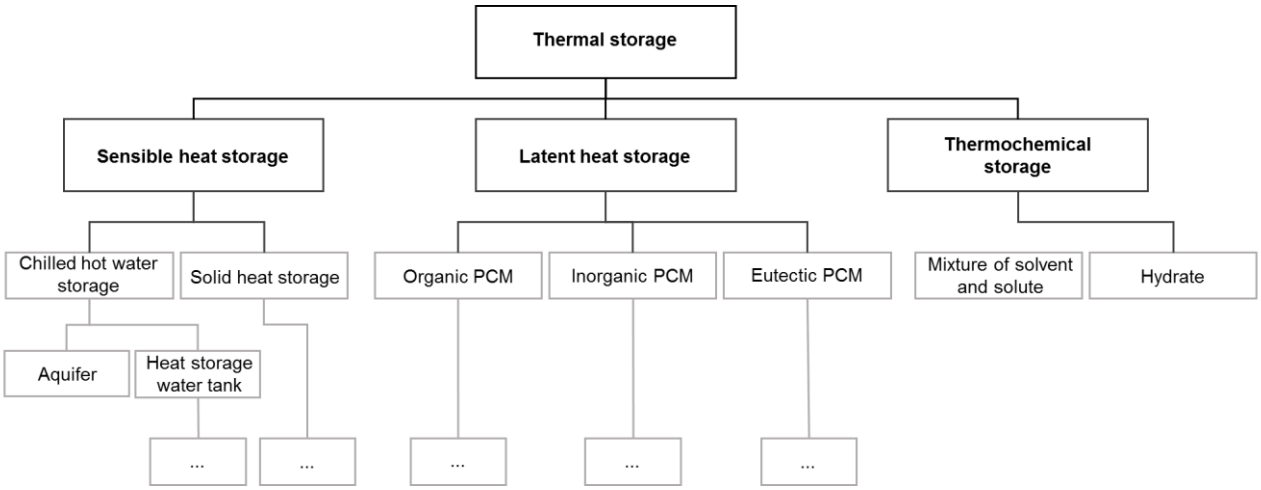

Figure 16 - Classification of thermal energy storage [26]

Sensible heat storage

Sensible heat storage uses a heat storage medium which changes its temperature when heat is added to or removed from the medium. The most commonly used medium is water, but oil, bedrocks, sand and soil are other possible storage media. The stored heat depends on the storage medium´s temperature rise/drop and its heat capacity leading to Equation (4.5) [25]:

$$\Delta H = m * c_P * \Delta T \tag{4.5}$$

ΔH … Enthalpy / Stored Energy [kJ]

m … Mass [kg]

c_P … Heat capacity of the storage medium $\left[\frac{KJ}{kg*K}\right]$

ΔT … Temperature difference [K]

There are several types of sensible heat storage systems, such as concrete tanks, aquifers, vertical tubes or drilled wells. More detailed information on characteristic properties of the systems is presented in Appendix B – Table B1.

The most common type of sensible heat storage is the hot water tank which usually is installed as a short-term storage in a residential building. This system as well as underground thermal energy storage (UTES) is described in more detail in Chapter 4.5.3. UTES can be applied as a seasonal storage.

Latent heat storage

A latent heat storage medium changes its phase in case of heat being added to or removed from the medium. The stored heat depends on the latent heat (specific enthalpy change) and mass of the phase change storage medium. It can be calculated from Equation (4.6):

$$\Delta H = m * \Delta h_{phase\ change} \quad (4.6)$$

Latent heat storage can be characterized by a constant phase change temperature, for instance the melting temperature or evaporation temperature of water. The system can be run at a small temperature difference during the charging and discharging process and can therefore allow lower space requirements, lower weight requirements and a higher temperature stability of the system compared to a sensible heat storage system. In general, latent heat storage materials are able to store 5-14 times more heat per unit volume than common sensible heat storage materials, but because of their higher energy density, they also have higher costs. Latent heat storage materials can be phase change materials (PCM). Typical PCMs are salt hydrates, water/ice, hydroxides or carbonates [25]. Ice storage is another common latent heat storage system. It is a possibility for seasonal storage. It can be used for heating as well as for cooling depending on the surrounding temperature. Alternatively, a snow storage can be used, however an ice storage requires a smaller volume.

Thermochemical storage

In a chemical reaction, thermal energy is absorbed or released through the formation or breaking of chemical bonds. If heat is added to a chemical compound, the compound reacts and chemical bonds are broken. Both components of a compound are stored under stable conditions and when heat is needed, the storage is discharged by mixing both components which leads to an exothermic reaction where the basic chemical is formed again and heat is released. Thermochemical storage is a potential technology for seasonal storage because the two components can be stored without any heat losses [24].

4.5.2 Design considerations for TES

There are several aspects which should be considered when it comes to the design of a TES such as the temperature range, the required capacity, physical constraints and costs.

More importantly, the meaningfulness of the technology has to be given consideration that for instance the integration of a solar thermal system and thus water storage tanks only make sense, if there is enough sun and a geothermal energy storage is reasonable only with adequate ground conditions. Furthermore, heat losses should be considered for all storage systems when systems are to be designed.

4.5.3 Technologies of interest for Risvollan

Solar thermal combined with DHW storage tanks

One of the most common storage technologies is the active storage in a water tank. This solution is for instance applied when using solar collectors to heat up the water which is used for space heating and DHW as indicated in Figure 17.

Sensible hot water storage is most common in residential buildings whereas sensible cold water storage is used in commercial buildings where lots of cooling is required. A system which includes a storage tank for DHW can work as a peak shaving device and decrease the energy consumption. An alternative system consists of a tank which stores water heated up by solar energy (from the collector) and a second source which could be a boiler or a heat pump. The water can be used for DHW and space heating [24].

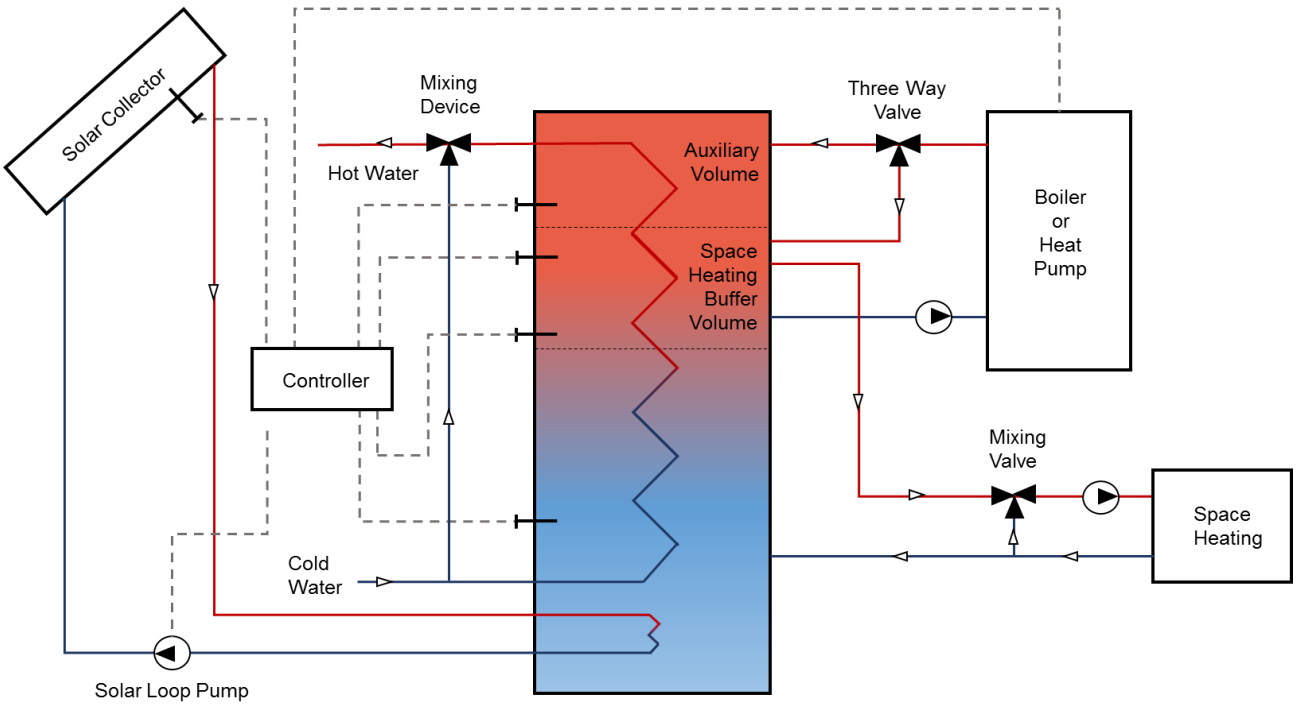

Figure 17 - Combination of DHW and space heating supported by solar energy [13]

Geothermal energy storage

UTES is suitable for seasonal storage, where the most common technologies are Aquifer Thermal Energy Storage (ATES) and Borehole Thermal Energy Storage (BTES). Both systems depend to a great extent on the underground characteristics of the place in question.

Aquifer thermal energy storage

ATES uses groundwater as heat storage medium and has possibilities for large, invisible storage. Most importantly, underground conditions have to be suitable for aquifer storage and the heating and cooling loads should be balanced in order to make full use of the ATES.

Since aquifers can have a large storage capacity, they can be used for seasonal heating and cooling storage [27]. According to Paksoy et al. [28] very high heating and cooling rates can be achieved because the water pumps can be run at high rates. Therefore, ATES can be applied in areas with a high heating and/or cooling demand as well as for a group of buildings. An ATES is operated through two drill holes, a hot and a cold one, as shown in Figure 18. In summer time, the waste heat can be injected into a hot drill hole and water from the cold drill hole can be used for cooling, whereas in winter time, the water is taken from the hot drill hole in order to meet the heating demand.

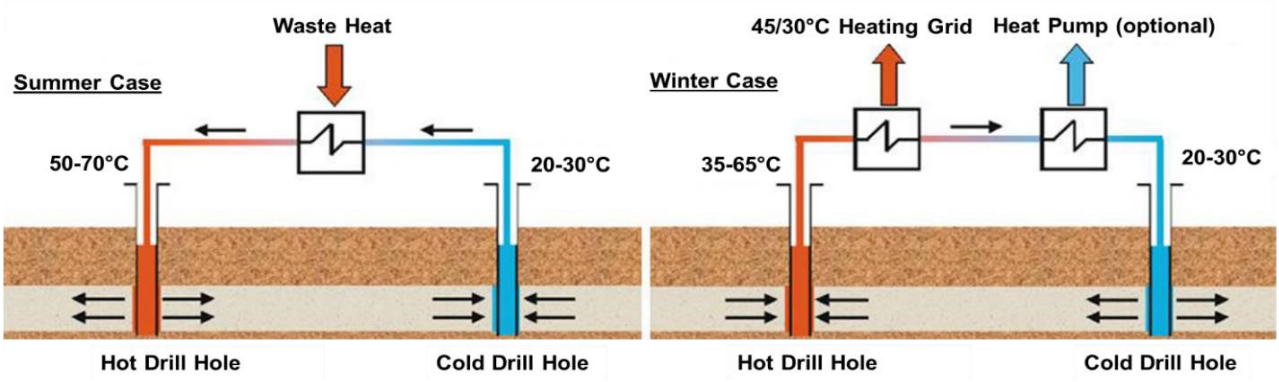

Figure 18 - Simplified functional scheme of an aquifer storage during charging (left) and discharging (right) [27]

Borehole thermal energy storage

The main advantage of BTES is the possibility to have many boreholes in a rather small area. The boreholes which act as a heat exchanger contain a U-tube with a recirculating heat transfer fluid which is a glycol solution in many cases. In order to increase the thermal contact between the tube and the soil, a grouting material with a high thermal conductivity

can be filled into the borehole. Groundwater can be a very good filling material compared to a fixed filling material because it improves the thermal properties of the system not only through an increased thermal conductivity, but also through natural convection [29]. For a big BTES system, a building which has the function of an energy center, houses all the pumps and valves of the water-distribution grid. In principle, the temperature of a BTES field is highest in the center and gradually decreases towards the outer part of the area.
When heated water is to be stored, it is pumped into the center of a BTES field where the heat is transferred to the surrounding rock decreasing the water temperature as it gets closer to the outer border of the field before it flows back to the energy center of the BTES field. If the houses are in need for heat, cold water is pumped into the outer area “of the field and as the water flows [back] to the [energy] center, it picks up heat”, the water temperature is increased and the warm water passes a short-term storage in the energy center from where it is distributed to the homes via the local pipeline network [30]. An example of such a BTES field is presented in Figure 19, although this is only one possible arrangement of the boreholes.

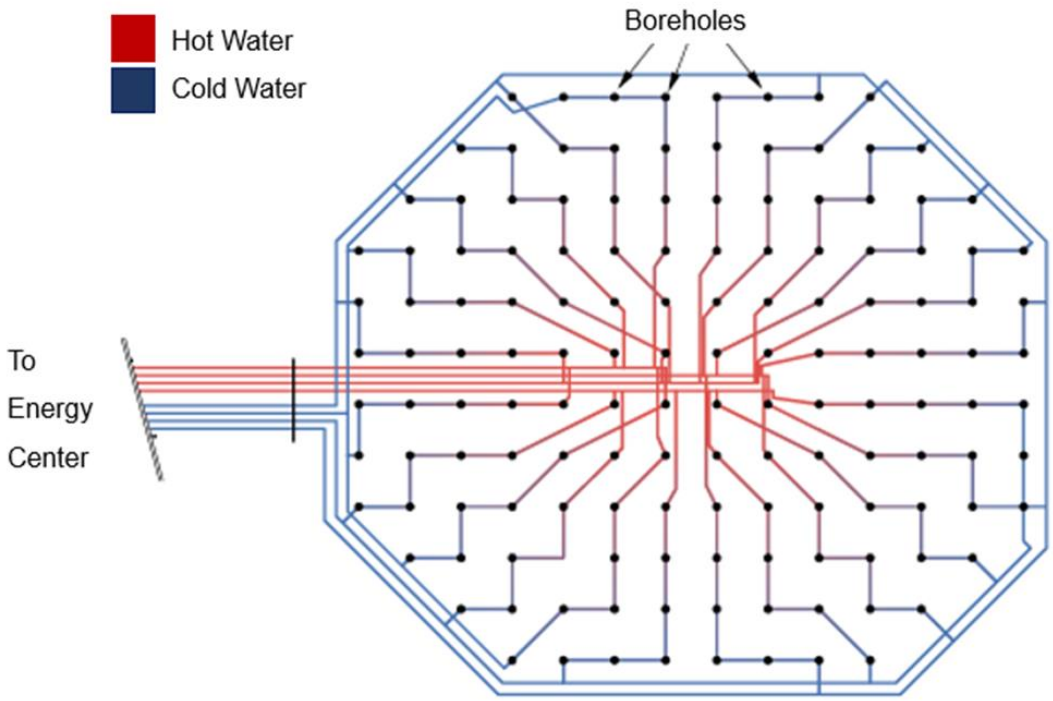

Figure 19 - Sketch of a BTES field [30]

The boreholes can be coupled in many different ways. As it can be seen from Figure 19, boreholes are coupled in parallel and in series as well. From the center, the boreholes are

connected in line towards the outer part of the geothermal storage field having a temperature decrement from the center to the outer border. In this way the heating losses are decreased leading to a higher efficiency of the field. Furthermore, there are many borehole strings starting in the center and ending at the outer rings of the borehole field. Every second string ends up in the outer most ring, where the water is pumped back to the energy center. The other lines in between circulate the water into the other direction. In this way, the geothermal storage field acts as a huge heat exchanger.

When it comes to the design of such a BTES field, the spacing between the boreholes needs to be considered as well as recovering the ground temperature. If the boreholes are drilled too close to each other, they influence the temperature of the neighboring borehole which can lead to a lower COP of the GSHP. Solar energy is a reasonable way for recovering the ground temperature and studies show that it is also beneficial to do so. [29] [31]

4.5.4 Combination of solar thermal and geothermal storage

A combination of BTES and solar energy application has been studied and applied in several projects [30], [32]. According to Trillat-Berdal [31], the COP of the heat pump is increased, if boreholes are charged with excess solar heat. Wang et al. [33] did a case study on a hybrid solar/geothermal system and pointed out that the matching of the size of the water storage tank and the tank volume is of great importance for the performance of the system. They found that the optimum ratio between the water tank volume and the solar collector area is about 20 – 40 $\frac{L}{m^2}$.

A possible system configuration is presented in Figure 20. This system is installed in Drake Landing in Okotoks, Canada and was completed in 2007. Solar collectors are used to harvest solar energy and heat up water which is transferred to the short-term thermal storage tanks at the system´s energy center. Surplus heat can be stored in the BTES and can be released in times of higher heating demand. This system can lead to significant energy savings, especially in cases of high solar radiation and beneficial soil conditions. 90% of the total heating demand of Drake Landing is provided by solar energy. Preliminary simulations on the energy system in Drake Landing have been done with the TRNSYS software tool and were proven to be accurate. Compared to a non-combined system, results show that the BTES efficiency increases from 9% to 41% and the solar fraction from 66% to 89% over five years [34].

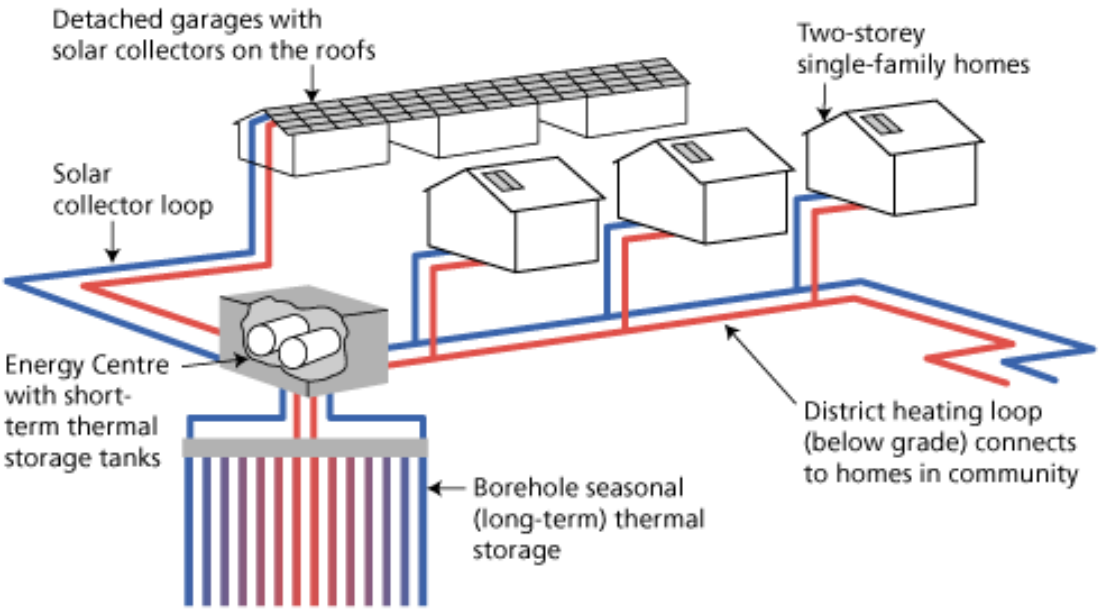

Figure 20 - Scheme of combined solar energy use and BTES [35]

Another example of a hybrid solar/BTES system is Crailsheim in Germany. It contains 80 boreholes with a depth of 55m as well as 5400 m^2 solar collector area. A huge water tank is considered in addition to the BTES because the hot water from the solar collectors has to be distributed to the BTES over a longer time period. It is heated up to 65°C by the end of September whereas the temperature is 20°C at the end of the winter. A maximum temperature of 90°C is reached during the charging process. The whole BTES covers a heating demand of 4100 MWh, which is the heat consumption of 260 houses and two schools. A GSHP of a capacity of 530 kW is installed. [36]

DMA Engineering [37] developed a geothermal/solar hybrid system for the Colorado region. Given the ambient conditions in Colorado the operation time of the GSHP can be reduced by 8% and the payback time of each technology of the combined system is lower than if each technology was installed separately.

A more detailed hybrid geothermal/solar system is presented in Figure 21. A GSHP and solar collectors are used for DHW production and space heating. This system is an expansion of the system introduced in Figure 17.

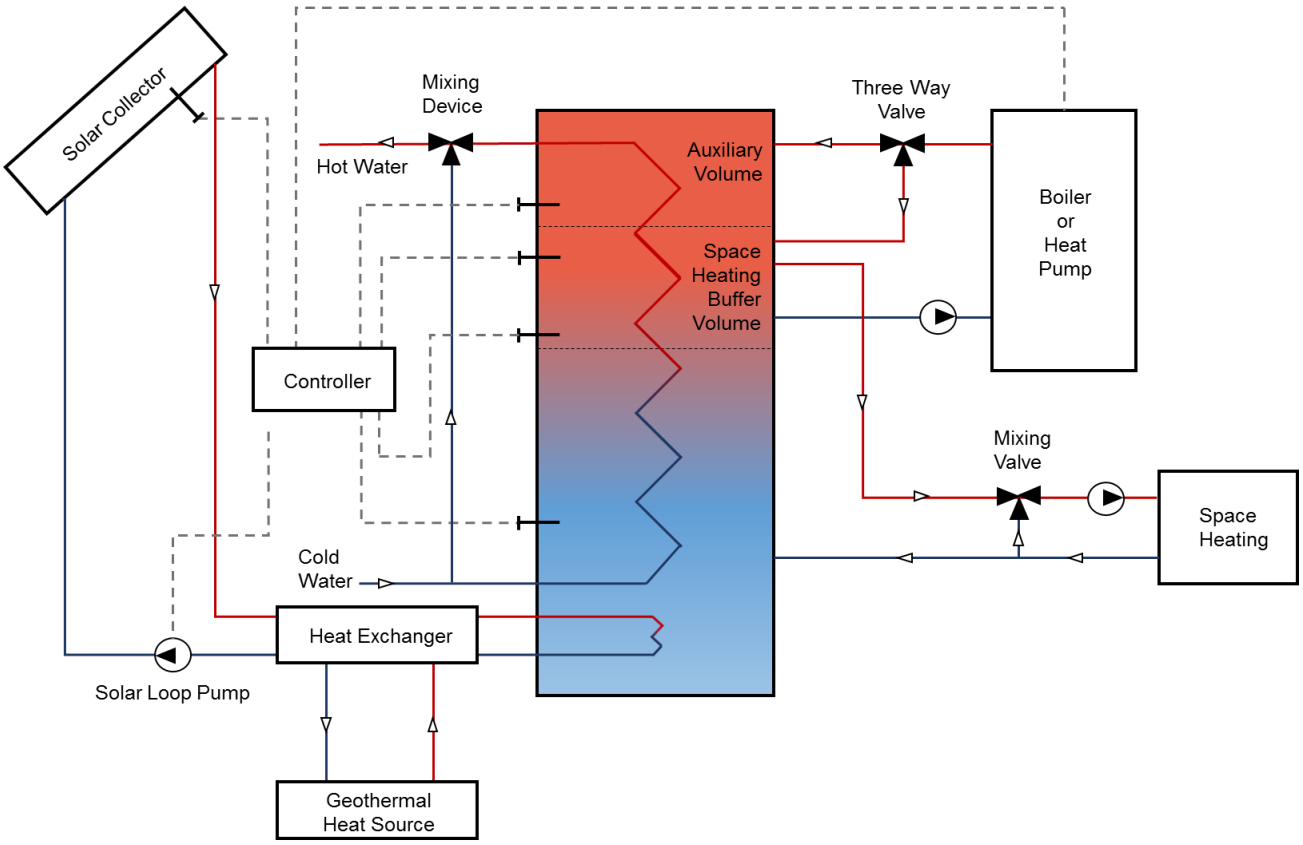

Figure 21 - Sketch of a hybrid geothermal/solar system for DHW and space heating [13]

5. Risvollan today

Risvollan is a neighborhood which consists of around 1300 apartments, where 1113 are owned by RBL. There are further apartments which are connected to the same heat distribution grid and therefore are also considered for the feasibility study. A map of the whole area is presented in Figure 22. The housing blocks were built in the 1970s and were refurbished (improved insulation) in the 1990s.

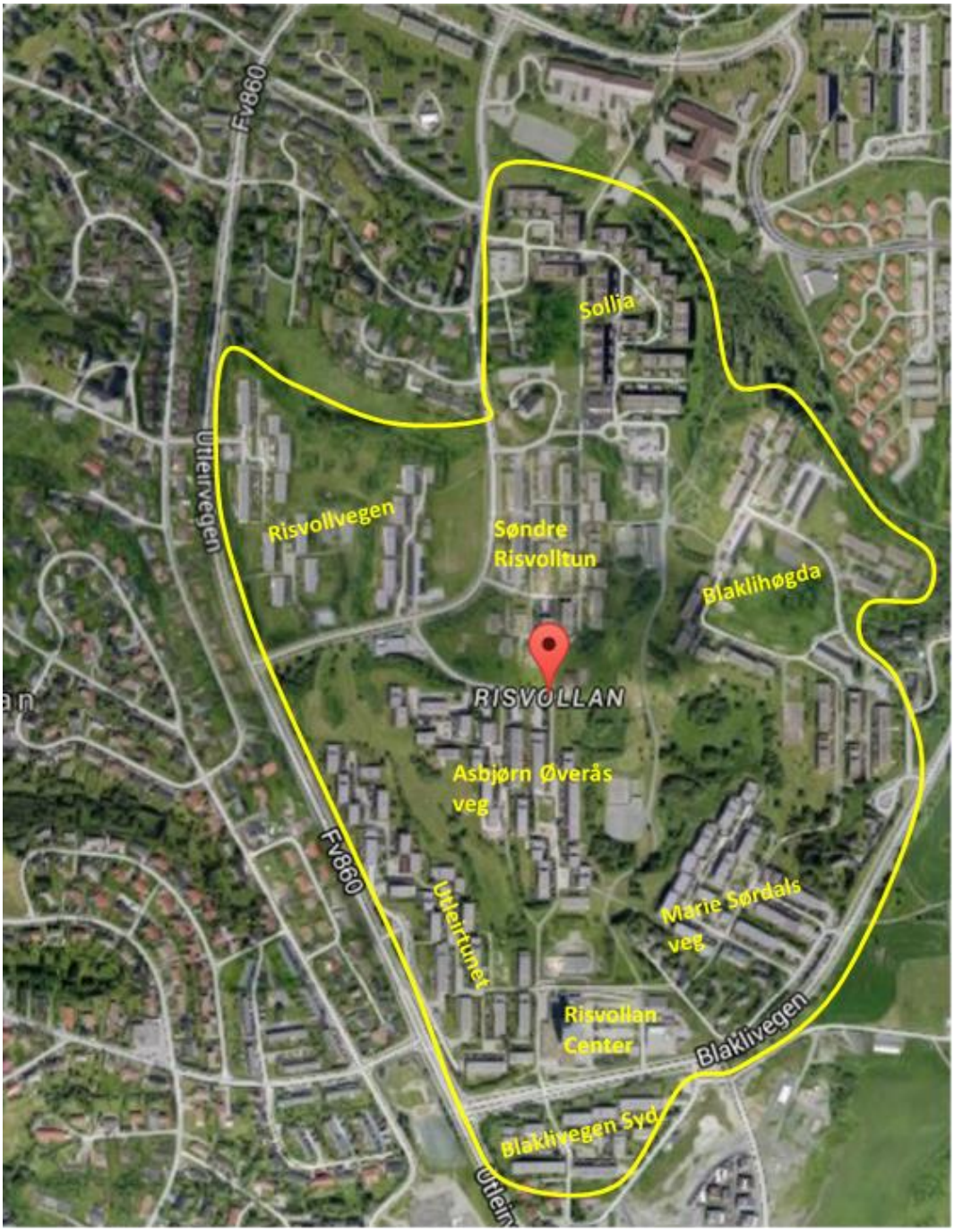

Figure 22 - Map of Risvollan area

Information about the current distribution grid and a summary of the current energy situation in Risvollan is given in this chapter based on real consumption data from 2014 provided by the RBL, followed by prospects for a possible future energy system. The houses are aligned along North-South or East-West. The orientation has to be considered for the calculations of the solar radiation gain because it has an impact on the amount of collectors which can be installed, also considering the optimum inclination angle of the collectors and the optimum orientation towards the sun.

5.1 Information on the current distribution grid

Risvollan has an existing distribution grid which is owned by the cooperative (RBL) and which utilizes district heating directly, often at unnecessary high temperatures. The distribution grid was introduced earlier in Figure 2 and is presented again in Figure 23.

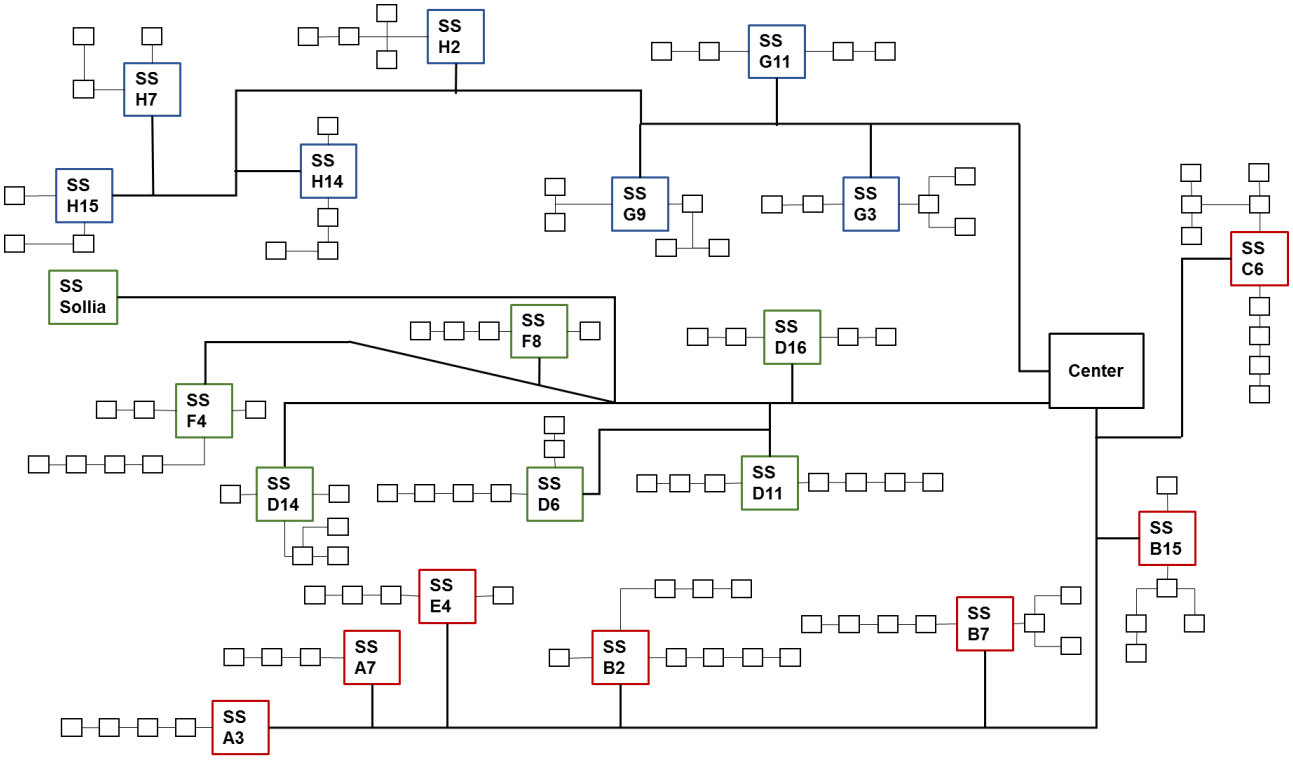

Figure 23 - Sketch of the heat distribution grid in Risvollan

There are three loops which are called Loop ABCE (red), Loop FDSollia (green) and Loop GH (blue). The substations (SS) of each loop are marked with the same color in the figure. The heating demand data for one loop provided by RBL is the smallest classification made meaning that more detailed data is not available.

5.2 Overview of the current heating demand

The total heating demand of the apartments of the Risvollan district is made up of the demand for heating the apartments and of heating the warm water. Table 2 presents the monthly heating demand of all the buildings.

Table 2 - Heating demand in Risvollan in 2014

	Heating demands [MWh]		
	Space Heating	**DHW**	**Total Demand**
January	1623.1	695.6	2138.7
February	1143.7	490.1	1633.8
March	1199.6	514.1	1713.7
April	980.9	420.4	1401.3
May	855.4	366.6	1222.0
June	308	205.3	513.3
July	292.3	73.1	365.4
August	408.2	174.9	583.1
September	603.9	258.8	862.7
October	889.2	381.1	1270.3
November	1026	439.7	1465.7
December	1278.8	852.5	2131.3
Total	**10609.1**	**4872.2**	**15481.3**
% from total	**69**	**31**	**100**

The annual specific energy demand of the apartments in $\frac{kWh}{m^2}$ is calculated for each Loop based on the total heated floor area of the buildings. The data is shown in Table 3.

Table 3 - Heating demand per heated floor area

Loop	Floor area [m^2]	Total heating demand [kWh]	Specific Heating demand $\left[\frac{kWh}{m^2}\right]$	Share of the total heating demand [-]
ABCE	33631	4894400	145.53	0.334
FDSollia	37500	5450300	145.34	0.372
GH	30105	4319600	143.48	0.294

The annual specific heating demand is almost equal for the three loops being roughly 145 $\frac{kWh}{m^2}$. As can be seen from Table 2, space heating accounts for 69% of the total heating demand and DHW for 31%. Data for space heating and DHW is provided as a sum for all

apartments of the housing cooperative only, but not per Loop and therefore, the share of space heating and DHW is assumed to be constant throughout all apartments. This data is provided in Table 4.

Table 4 - Share of DHW and space heating

	Total floor area [m2]	DHW demand [kWh]	Specific DHW demand $\left[\frac{kWh}{m^2}\right]$	Space heating demand [kWh]	Specific space heating demand $\left[\frac{kWh}{m^2}\right]$
RBL	101236	4872200	**48.13**	10609100	**104.80**

The data on the specific heating demand is important for the comparison with the building regulations as well as for the simulations in SIMIEN and needs to be calculated prior to the modeling. SIMIEN is applied in order to model the energy demand of buildings and thus getting the peak load demand which is needed for the simulations in EED.

5.3 Solar irradiation in Trondheim

The data for solar irradiation is taken from the SODA website (**SO**lar irradiation **DA**ta) [38]. It provides the total monthly irradiation of a place in question. Irradiation data of 15 years has been averaged and is then used for further calculations. The global irradiation in Trondheim is presented in Figure 24. The global solar irradiation is a measure of the rate of total incoming solar energy on a horizontal plane [39].

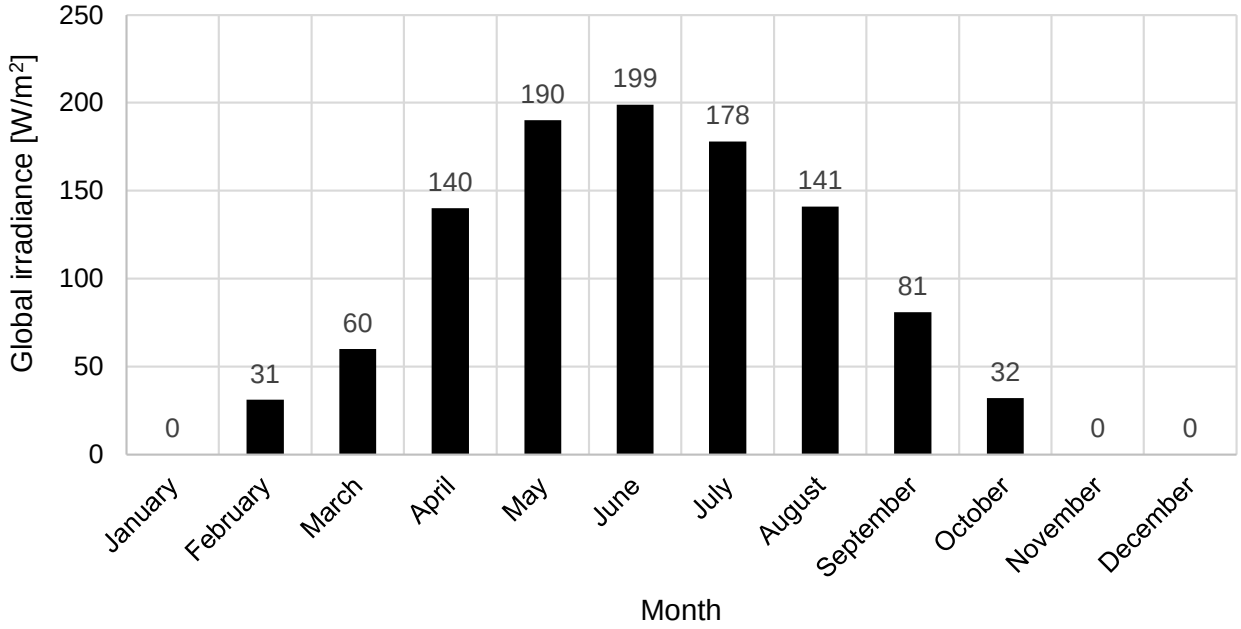

Figure 24 – Monthly global irradiance in Trondheim

These data are the basis for the calculations of the solar gain from the solar collectors. The calculations will be presented in Chapter 6.2.

5.4 Ground conditions in Risvollan

The subsurface of the area has been investigated by Multiconsult, Rambøll Norge AS and Trondheim Kommune in 2013 [40]. The ground consists of a quick clay layer which is more than 20m thick, which is not good considering the use of a BTES because drilling the boreholes will be very expensive. The first 2 – 3m consist of recalcitrant clay and the underlying layer of a more dense clay. According to Norges geologiske undersøkelse (NGU) the bedrock is mainly quartz-diorite, but areas of greenstone, greenschist and arkose exist as well [41]. A map is provided in Figure 25 with buildings being ochre-colored, quartz-diorite being red and greenstone being ruby-colored.

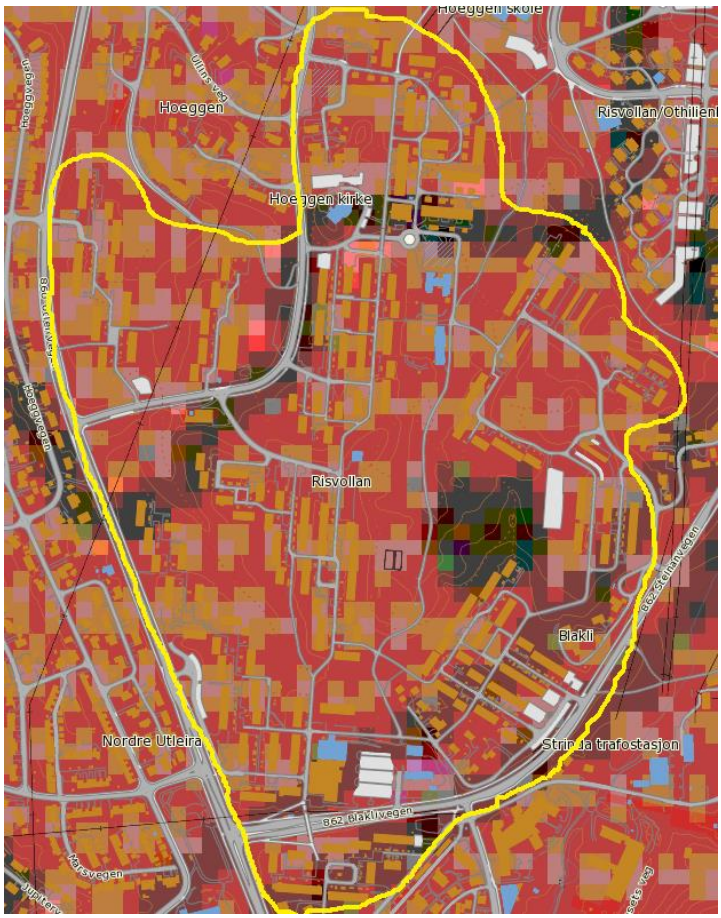

Figure 25 - Geological map of Risvollan [41]

Diorite is chosen for the simulations in EED. This is important because each bedrock has characteristic thermal properties.

6. Smart thermal grid in Risvollan

The idea of changing to a low-temperature grid in Risvollan consists of several measures. This chapter focuses on the description of the investigated measures required for a conversion to a STG. The approach taken consists of the following steps:

- Investigating the feasibility of running the local heat distribution network at a lower temperature and uncoupling it from the public DH network
- Modeling the energy demand of the buildings using the SIMIEN software tool
- Investigating the possibility of using solar thermal
- Investigating geothermal storage possibilities using EED
- Investigating a heat pump technology for GSHP and DHW heating

Among other measures, a combination of all the mentioned technologies can lead to a STG in Risvollan. As mentioned in Table 5, a STG should be flexible, intelligent, integrated, efficient, competitive, scalable and use local energy sources. At this point it has to be mentioned that this thesis does not look into the integration of ICT technologies. Table 5 shows the STG features investigated in this thesis.

Table 5 - STG features investigated in this thesis

Flexible	• Short-term: adapt to energy supply and demand situation	✓
	• Medium-term: adapt by adjusting the temperature level in existing networks and through the installation of new distributed micro-networks	✓
	• Long-term: adapt by aligning the network development with urban planning	-
Intelligent	• Planning and operation, end-users interaction with the heating and cooling system	-
Integrated	• Urban planning and urban networks – electricity, sewage, waste, ICT, etc	-
Efficient	• Optimal combination of technologies and cascade usage	✓
Competitive	• Cost-effective, affordable	✓
Scalable	• For neighborhood-level or city-wide application depending on energy demand	✓
Securing energy supply	• Using local energy sources for energy supply	✓

6.1 Heating demand simulations in SIMIEN

SIMIEN can be applied for modeling the energy demand of buildings based on building properties as well as the climatic conditions in the considered location.

6.1.1 Approach and methodology

Since no detailed data for the building properties (used materials, type of insulation, etc.) was available, proposed data from the building code from 1987, TEK87, is used as input data [42] because the buildings have been restored in the 1900s and therefore need to fulfil the requirements of TEK87. The code proposes U-values for different construction elements, such as external walls, windows, doors, roofs and floors. SIMIEN is used to simulate the energy demand of all buildings of Loop GH (blue substations in Figure 23). This loop is chosen as an exemplary case. The main goal of the application of SIMIEN is to get the peak load heating demand of the substations because these results are needed to dimension the heat pump and for the simulations of the ground temperature in EED.
Each building is sized reasonably in SIMIEN and the heating demand is made fit to the actual demand data provided by RBL, namely the DHW demand of 48 $\frac{kWh}{m^2}$ and the space heating demand of 105 $\frac{kWh}{m^2}$ respectively. There are several parameters which are varied until these specific heating demands are obtained ± 5% accuracy. These parameters are:

- Number of windows per building
- Window area per building
- Number of doors per building
- Heat gain from lighting
- Heat gain from electrical appliances

It has to be pointed out that the final value for these parameters might not agree with the real properties of the building, but the focus is strongly on reaching the two heat demand values in order to be able to simulate the peak power demand. The heating power for DHW is set to 5.50 $\frac{W}{m^2}$ in order to reach a demand of 48.2 $\frac{kWh}{m^2}$. A flowchart for the procedure of modeling the heating demand in SIMIEN is presented in Figure 26.

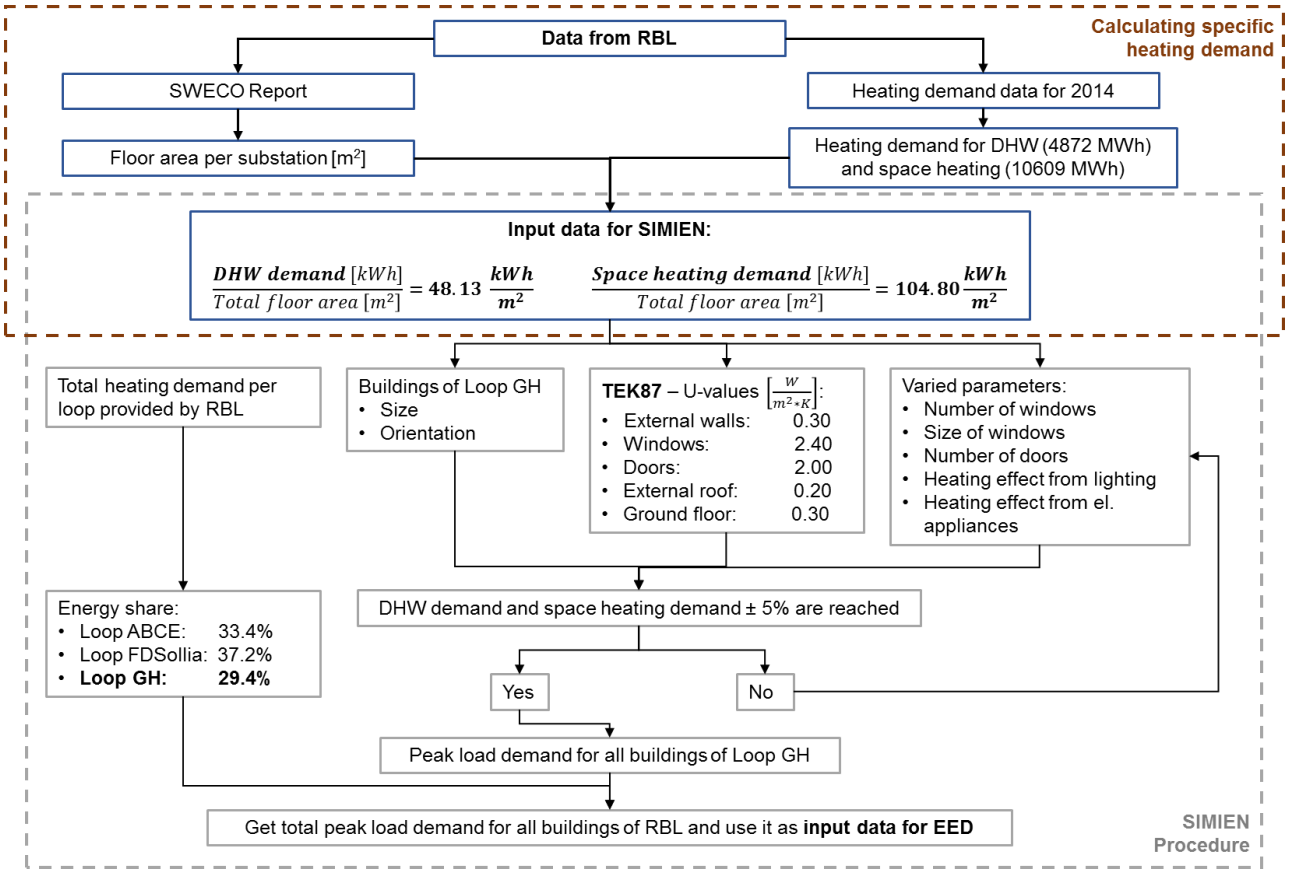

Figure 26 - Procedure for heating demand calculations and modeling in SIMIEN

6.1.2 Results from SIMIEN simulations

The simulation in SIMIEN is done for Loop GH only which is why the results have to be up-scaled in order to get the energy demand and thus the peak load of all houses that are connected to the local distribution grid in Risvollan. In general, the simulation results from SIMIEN match the energy demand data for Loop GH provided by RBL. The final results from SIMIEN give a specific energy demand of 104 $\frac{kWh}{m^2}$ for space heating and 48 $\frac{kWh}{m^2}$ for DHW heating and thus leading to an energy demand of 3169.3 MWh and 1469.1 MWh respectively. The actual data from RBL states a total heating demand of 4320 MWh for Loop GH. The simulation does not consider cooling of the buildings and neither the electricity demand of the buildings.

In order to get the peak load demand of Loop GH, the coldest day of the year is modeled based on the climate data of the SIMIEN database. The minimum temperature at the coldest day is -19.5°C (design outdoor temperature DOT) leading to a peak load demand of 1524.5 kW. The peak load of each of the substations can be compared to the report from SWECO as SWECO did a study on the buildings in 2011. They used a more general

approach for the calculations as they assumed a specific power demand of 40 $\frac{W}{m^2}$ and multiplied this number with the floor area which gives a heating demand of 1204 kW. If the same approach is applied for a specific power demand of 52 $\frac{W}{m^2}$ as it is proposed by COWI AS and TEK87 [43], the heating demand would be 1565.5 kW, which confirms the results of the simulations in SIMIEN.

This means that the findings from SIMIEN are reasonable and that they can be used as input data for simulations in EED. As mentioned Table 3, the energy share of Loop GH is 29.4% from all three loops and therefore, the total peak load of the area is

$$Total\ peak\ load = \frac{1524.5\ kW}{0.29} = \mathbf{5185\ kW} \tag{6.1}$$

6.2 Applying solar thermal technology

An investigation of implementing solar thermal into the system has been done. This chapter describes the applied methodology, the calculations and the reasoning applying solar collectors.

6.2.1 Approach and methodology

The first step is to find out which houses are inside the area. This is done by aligning google maps and the map of the existing pipeline system in Risvollan (Figure 22 and Figure 23). For the calculations it is considered that solar collectors are to be installed on the roof of each residential building. In order to make the calculations more comprehensible, all houses are numbered (Appendix A) and based on the size of a typical solar collector and the available roof area, it is decided how many collectors are to be installed on top of each building. Furthermore, it was found that the optimum inclination angle for solar collectors in Trondheim is 43° [44], which has an impact on the spacing between collector rows and thus on how many rows could be installed at each building. On top of that, it was found that the optimum orientation of the collectors is 172° (8° off direct south) [45], with North being 0°. Using a web-based solar collector spacing calculator, it is found that the minimum spacing between each collector row should be around 25m [46]. In the end, an estimation of the solar gain is provided which also considers shading effects between the collector rows. An example which includes these considerations is presented in Figure 27 based on building 53.

Figure 27 - Example sketch for the installation of solar collectors

6.2.2 Calculating the solar gain per month

There will be an exemplary calculation for building number 53 in order to show the calculation procedure.

Calculating the solar collector area

As a first step, the available roof area of each building is calculated based on the maps (Appendix A). From those pictures the number of houses, the orientation, the total roof area and the number of levels of the roof can be determined. Table 6 presents these characteristics for the exemplary building 53.

Table 6 - Characteristics of Building 53

Building	Estimated Total Roof Area [m^2]	Roof area [m^2]	Alignment	Nr. of roof levels
53 (Utleirtunet)	540	54m*10m	North/South	2

The size of a typical solar collector is about 2.6m^2 for a Solar Collector L20 AR from Wagner Solar which was chosen for the feasibility study. It has to be pointed out that the calculation is of exemplary nature and it is assumed that the results would be in the same range, if another solar collector of the same type and size was installed. The specific data of the collector is presented in Table 7, where the parameters are:

η_0 Conversion factor according to EN 12975-2 [47]

a_1 Linear heat loss coefficient according to EN 12975-2 $\left[\frac{W}{m^2*K}\right]$

a_2 Quadratic heat loss coefficient according to EN 12975-2 $\left[\frac{W}{m^2*K^2}\right]$

By considering the orientation of the building, the number of levels of the roof and the collector width, a theoretical number of collectors to be installed next to each other can be determined.

Table 7 - Solar collector specifications *[48]*

Collector name	Wagner Solar Collector L20 AR
Collector area [m^2]	2.613
Collector width [m^2]	1.215
η_0 [-]	0.848
a_1 $\left[\frac{W}{m^2*K}\right]$	3.46
a_2 $\left[\frac{W}{m^2*K^2}\right]$	0.0165

Since Building 53 is 10m wide, the width of the collector row is assumed to be 8m so that it is still possible to pass the collectors on either side which is of interest for maintenance. The theoretical number of collectors can be calculated from

$$Theor.\ nr.\ of\ collectors = \frac{Width\ of\ the\ collector\ row}{Collector\ width} \tag{6.2}$$

$$\frac{8m}{1.215m} = 6.58$$

which is then rounded down to the next even number in order to get the real number of collectors. This leads to six solar collectors being installed in one row at the roof of Building 53. As the building is 54m long, several collector rows can be installed. A spacing of 15m is assumed in this case in order to minimize/avoid shading or blocking losses. A total number of four rows can be installed on the roof of this particular building since it has

a two-leveled roof. This leads to small shading losses in the overall annual performance, but since the sun is high up during summer time anyways, it is assumed that no shading losses will appear during that time. The next step is the calculation of the total collector area which can be installed per roof. This is simply done by

$$\begin{aligned} Total\ collector\ area = Real\ nr.of\ collectors\ per\ row * Solar\ collector\ area \\ * Nr.of\ collector\ rows\ per\ roof \\ 6 * 2.613m^2 * 4 = 62.71m^2 \end{aligned} \quad (6.3)$$

This procedure is carried out for each of the buildings. The total solar collector area in Risvollan is 6958m^2 resulting from 2663 installed collectors.

Calculating the solar gain

The total monthly solar gain per roof is calculated by

$$\begin{aligned} Total\ collector\ area\ per\ roof\ [m^2] * Averaged\ monthly\ irradiation\ \left[\frac{kWh}{m^2}\right] \\ = Total\ solar\ gain\ per\ month\ [kWh] \end{aligned} \quad (6.4)$$

For June it is

$$62.71m^2 * 144\frac{kWh}{m^2} = 9030.53\ kWh$$

The collector efficiency [49] can be calculated from

$$\eta = \eta_0 - \left(a_1 * \frac{T_{fl} - T_{amb}}{G}\right) - \left(a_2 * \frac{\left(T_{fl} - T_{amb}\right)^2}{G}\right) \quad (6.5)$$

where

G Global irradiance $\left[\frac{W}{m^2}\right]$

T_{fl} Mean fluid temperature [°C]

T_{amb} Ambient air temperature [°C]

The mean fluid temperature level depends on the intended use, either space heating or for DHW heating and influences the efficiency of the collector and thus the useful solar gain. Nevertheless, calculation results show that the efficiency changes over temperature are small and therefore the temperature is assumed to be 50°C for this calculation. The solar gain as a function of the mean fluid temperature in the collector are shown in Figure 28.

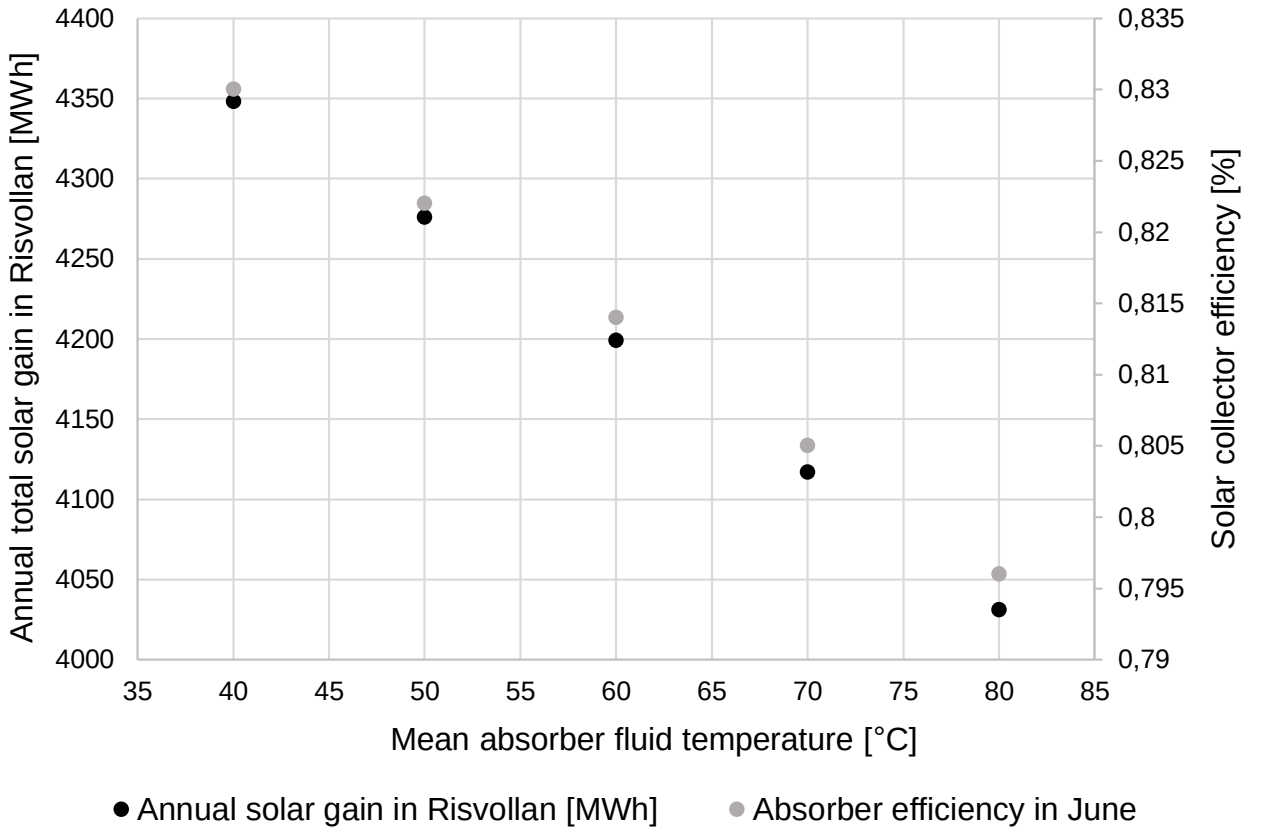

Figure 28 - Annual solar gain in Risvollan and collector efficiency as a function of the mean absorber fluid temperature

In general, the collector efficiency decreases with an increase in difference between mean fluid temperature T_{fl} and the ambient temperature T_{amb}. The data for the ambient air temperature is taken from the website climate-data [50] which contains weather data from the last 30 years. The ambient temperatures are averaged for each month and then used for the calculations. The collector efficiency in June is calculated from

$$\eta = 0.848 - \left(3.46 * \frac{50-12}{5970}\right) - \left(0.0165 * \frac{(50-12)^2}{5970}\right) = \mathbf{0.82} \tag{6.6}$$

Also considering the collector efficiency, the useful solar gain per roof and per month is then calculated by

$$\begin{gathered} Total\ solar\ gain\ per\ month\ [kWh] * Collector\ efficiency \\ = Useful\ solar\ gain\ [kWh] \\ 9030.53\ kWh * 0.82 = \mathbf{7405\ kWh} \end{gathered} \tag{6.7}$$

Thus the useful solar gain from Building 53 in June is 7405 kWh.

6.2.3 Useful solar gain for the Risvollan area

Applying the described procedure for each building the annual solar gain can be calculated. Figure 29 presents the total monthly solar gain for Risvollan area. The annual solar radiation is about 4276 MWh for the Risvollan area. The last point that has to be considered is the shading effect in case the solar collector rows are placed too close to each other. An optimum distance of 25m between the collector rows has been calculated for Trondheim. Due to limited space on the roofs, distances of 8m to 25m have been chosen depending on the specific building/roof. Another reasoning for placing the solar collectors closer than 25m is the high sun angle during summer time. A distance of 25m between the collector rows avoids blocking during winter time when the sun´s angle is lowest, but since there is no useful irradiation during winter time, the collector rows can be put closer to each other as the sun has a high angle during summer time. That means that more collectors could be put on the roof which would also increase the total useful solar gain.

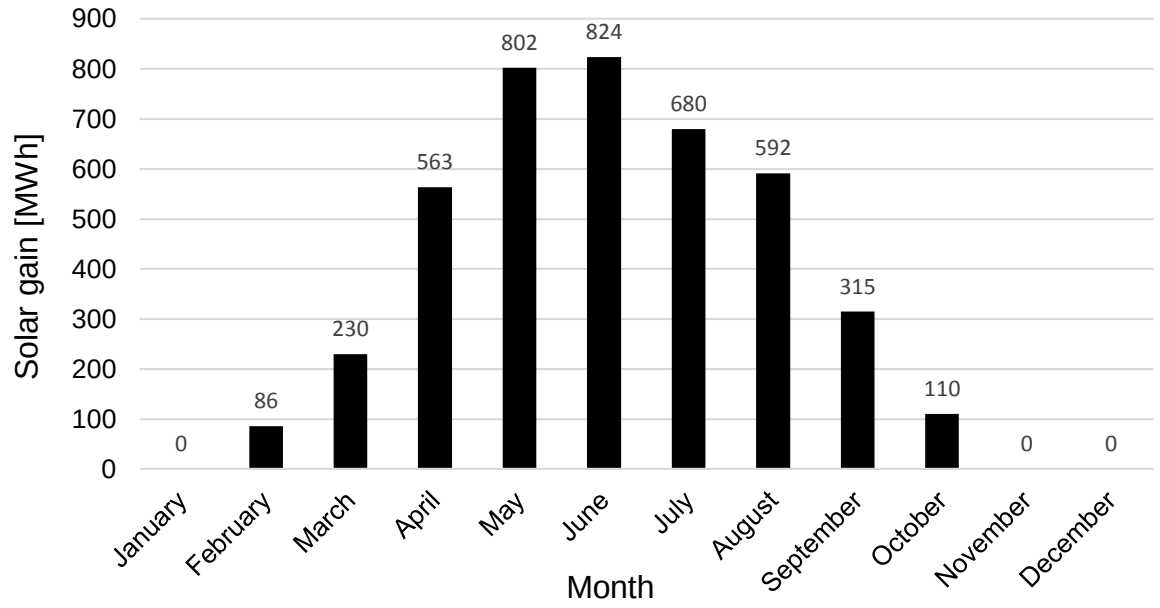

Figure 29 - Estimated monthly solar gain for Risvollan

6.2.4 Discussion of solar results and solar application

The energy gained from the solar collectors could either be used for direct DHW heating or for recovering the ground temperature of the geothermal storage.

Solar energy for DHW heating only

In case of solar heating of DHW, high temperatures (≈ 70°C) and huge storage tanks are required in order to cover the whole heating demand. The annual solar gain at 70°C is 4117 MWh. The solar gain per loop based on the DHW supply temperature is shown in Figure 30. As is can be seen from Figure 30, the solar gain is different for each loop. This is due to the different number of buildings and building sizes and thus different roof and collector areas.

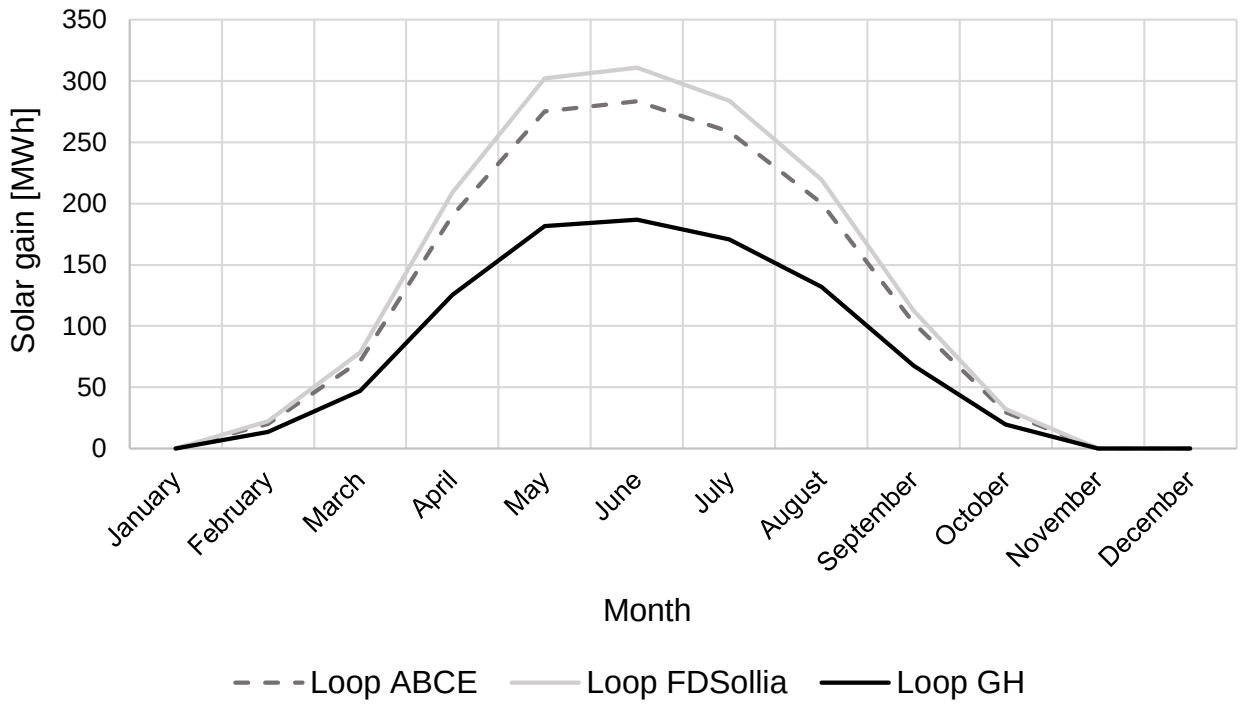

Figure 30 - Expected solar gain per loop [MWh]

Figure 31 shows the total solar gain and total heating demand of Risvollan. If the solar energy is used to heat up DHW only, it is able to cover the entire DHW demand from April to September for each of the three loops assuming that sufficient space heating is supplied by the low-temperature grid. DHW consumption is very low in July which is assumed to be the result of holiday season in Norway.

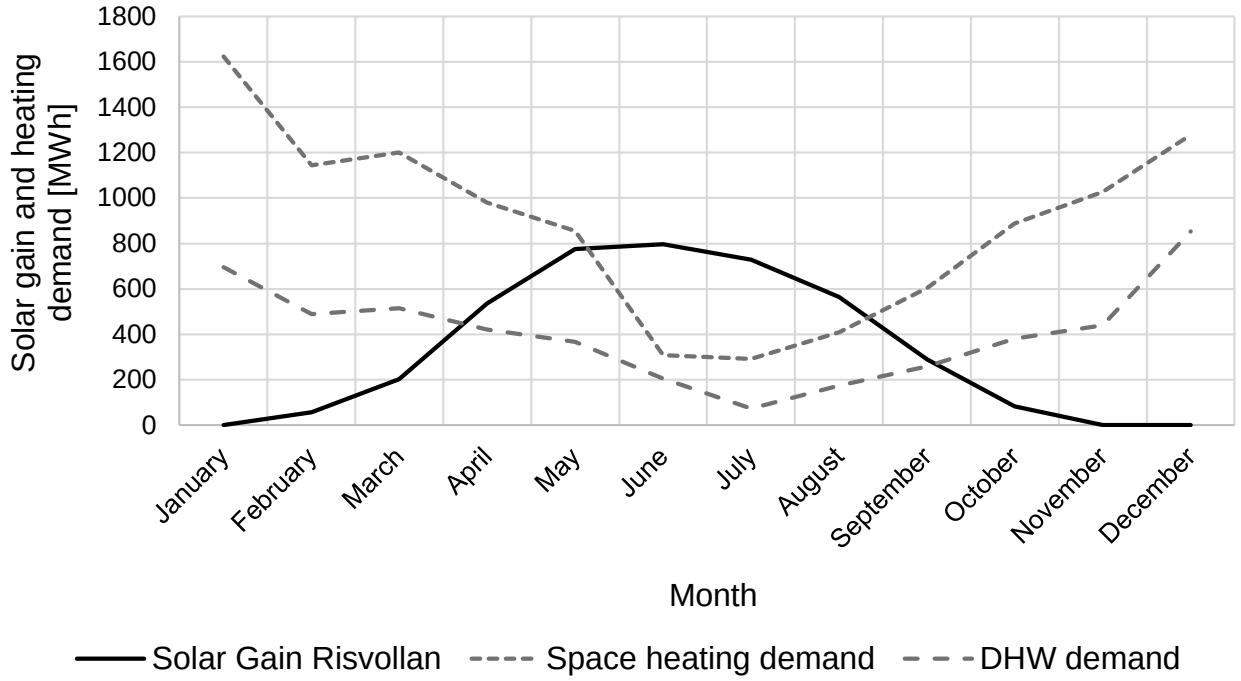

Figure 31 - Solar gain and heating demand of the whole district

The calculated solar gains and heating demands are additionally presented in Table 8.

Table 8 - Heating demand and solar gain of the investigated district

	Heating demands [MWh]			**Solar gain [MWh]**
	Space Heating	**DHW**	**Total Demand**	
January	1623.1	695.6	2138.7	0
February	1143.7	490.1	1633.8	57.1
March	1199.6	514.1	1713.7	201.7
April	980.9	420.4	1401.3	535.9
May	855.4	366.6	1222.0	775.0
June	308	205.3	513.3	797.4
July	292.3	73.1	365.4	728.5
August	408.2	174.9	583.1	563.4
September	603.9	258.8	862.7	288.5
October	889.2	381.1	1270.3	83.1
November	1026	439.7	1465.7	0
December	1278.8	852.5	2131.3	0
Total	**10609.1**	**4872.2**	**15481.3**	**4030.6**
% from total	**69**	**31**	**100**	**-**

Figures 32, 33 and 34 present the solar gain and the space heating demand as well as the demand for DHW per loop. The trend of each loop follows the trend for the whole district. Each of the three areas can supply enough solar energy to cover the DHW demand of the loop from April to September.

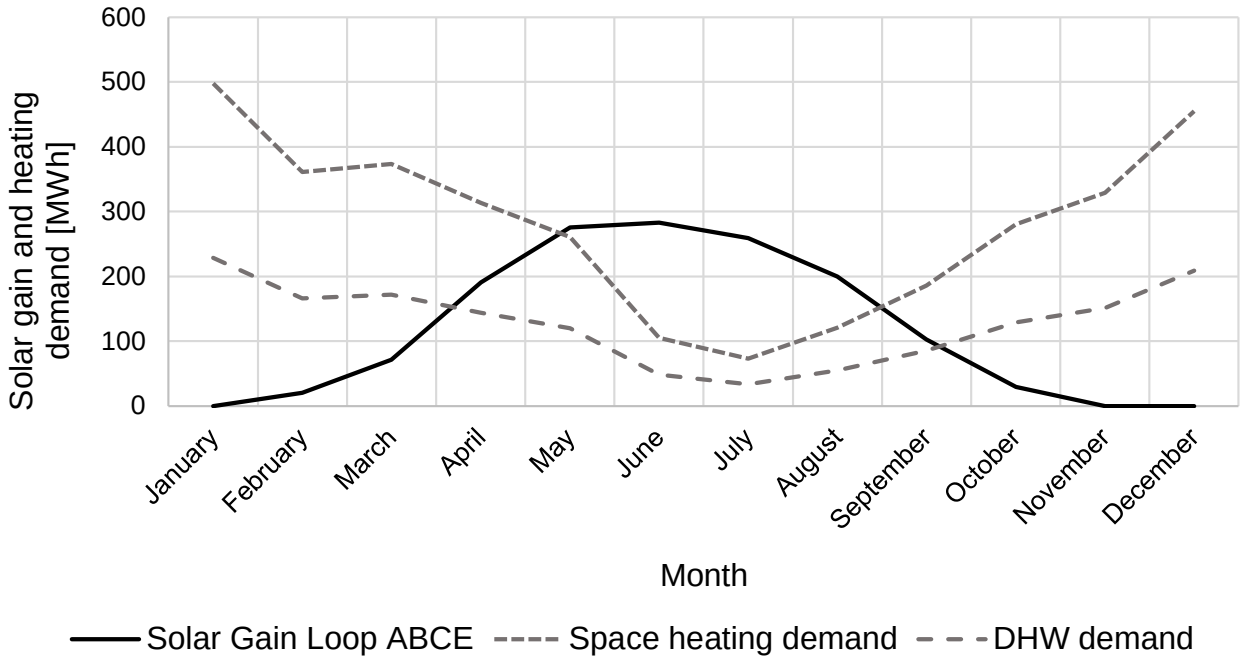

Figure 32 - Solar gain and heating demand of Loop ABCE

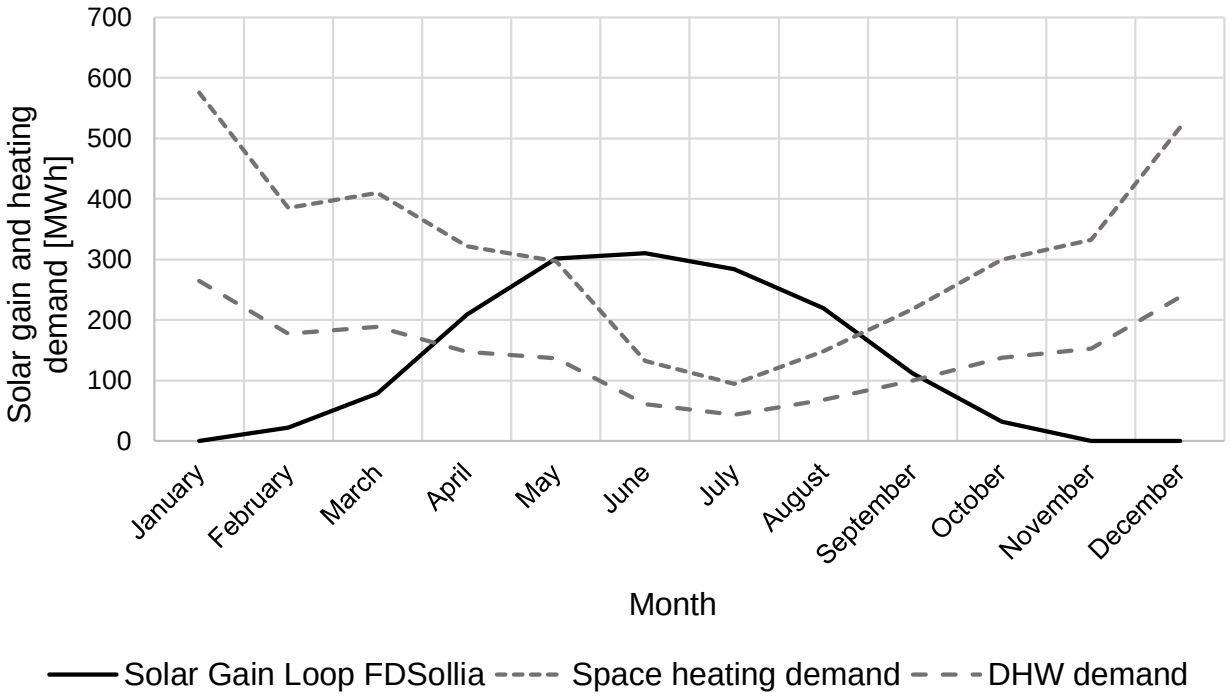

Figure 33 - Solar gain and heating demand of Loop FDSollia

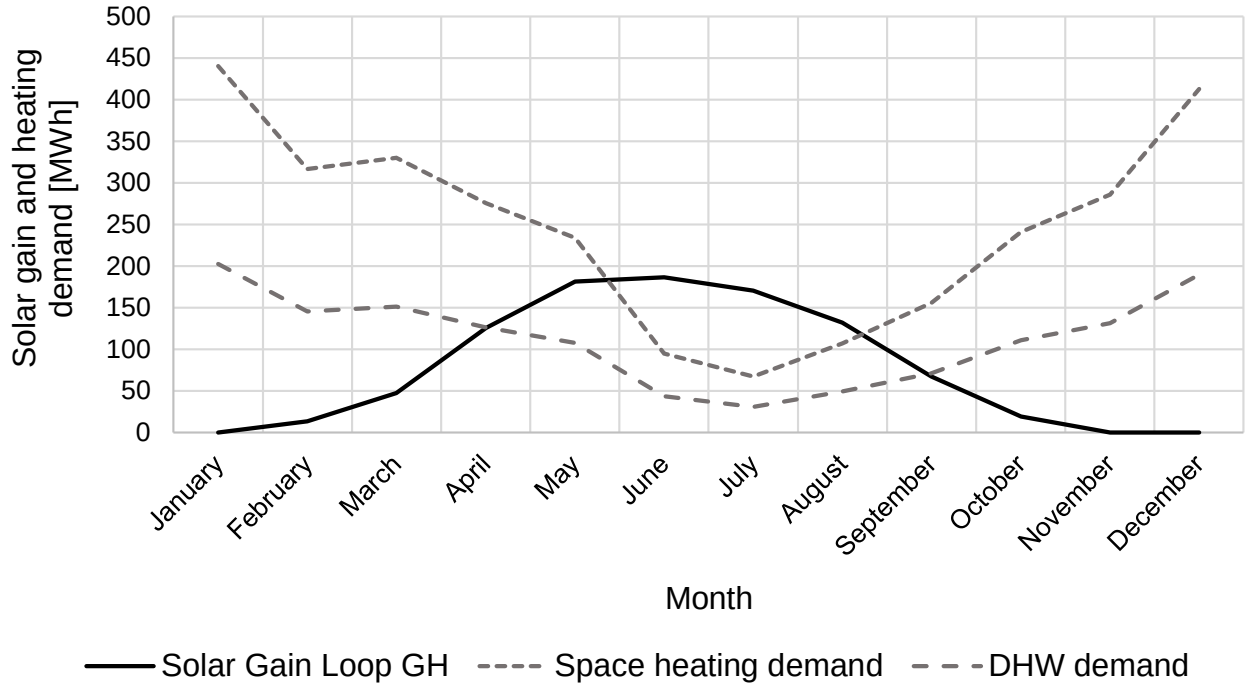

Figure 34 - Solar gain and heating demand of Loop GH

The results show that about 26% of the total heating demand could be supplied by solar energy, confirming the results of the SWECO report from 2011 which came to a solar share of 30%. The assumptions for the current report are rather conservative because it considers big distances between the collector rows. In practice, it would be possible to place the collector rows closer to each other and thus install more collectors per roof than it is considered in this study which would lead to a higher total solar gain for the district. Furthermore, the roof area of garages is not considered in this study either.

Solar energy for recovering the ground temperature of the geothermal storage only

Instead of using solar energy for DHW heating only, it can be used to recover the ground of the geothermal storage. If heat is taken from the ground to cover the heating demand of the buildings, the temperature of the ground will drop. In order to maintain a constant temperature in the bedrock, it has to be recovered during summer season and therefore solar energy can be supplied to the geothermal storage. For the calculations of this scenario, a water temperature of 50°C is assumed leading to an annual solar gain of 4276 MWh for the Risvollan district. The ground temperature is modeled using EED software and therefore, it is discussed at a later stage of the report how much energy is needed to recover the ground temperature and whether the solar gain is sufficient.

Combining solar energy use for DHW heating and ground temperature recovery

Solar energy can be used in a combined system for DHW heating and ground temperature recovery (GTR), but the main focus during this project is on the application for GTR and therefore, a combined case is not discussed further.

6.3 Simulation of the geothermal storage in EED

According to VDI 4640-2 (Verein Deutscher Ingenieure) it is necessary to model the design of a geothermal storage for heat pump systems >30kW and more than 2400 working hours per year in order to dimension the system. This can either be done by analytical or by numerical calculations. EED is an analytical software tool for modeling the temperature changes in the ground as well as the temperature of a heat carrier fluid (HCF). The software validates whether the chosen system leads to the ground going hypothermic which would lead to a less efficient system operation. The software is based on algorithms which are derived from models and parameter studies from numerical simulations. Analytical equations, called step response equations, for the heat flow of several combinations of borehole configurations and their geometry have been derived. These equations depend on the distance between the boreholes and the borehole depth. [51]

Recommendations for the ground temperature during seasonal heat extraction are provided by VDI 4620. The temperature change of the HCF should not exceed ±11K during base load operation compared to the undisturbed ground temperature. During peak load operation the temperature change should be within ±17K. Furthermore, the minimum temperature of the HCF at base load extraction should be around 0°C. [52]

6.3.1 Approach and methodology

For the simulations of the Risvollan area, several parameters are set and others are varied in EED (see Figure 35) in order to find a reasonable system configuration. The set values are based on findings from literature whereas other parameters are varied within a reasonable range. The key point of the simulations is a constant mean fluid temperature of the HCF. The procedure for the EED simulations is presented in Figure 35.

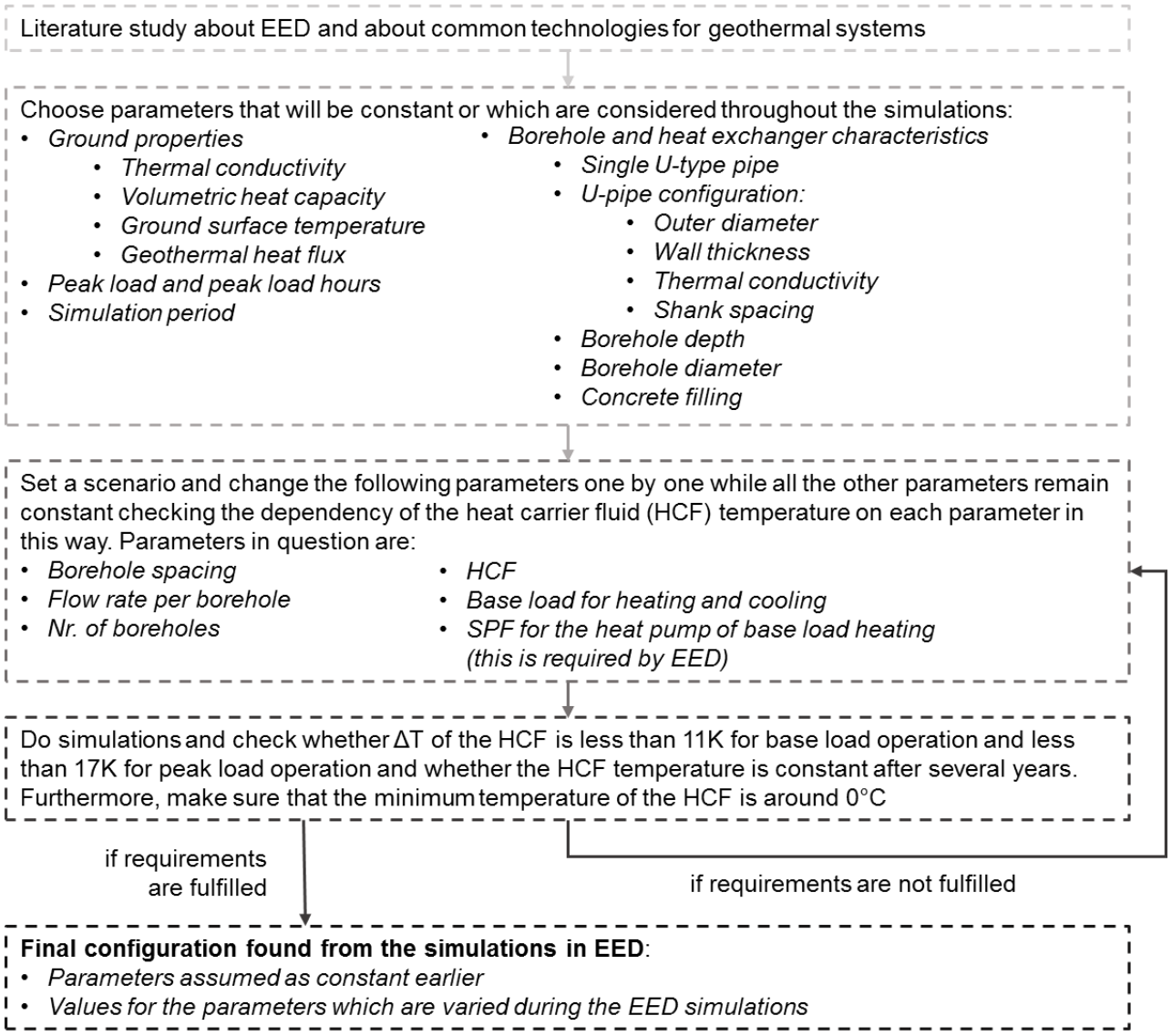

Figure 35 - Procedure for EED simulations

Therefore, a first case is set including all the data from literature as well as assumed parameters which are to be changed during the simulations. For the simulation of the first case the main focus is on finding a constant temperature level of the HCF which is within the 11K and 17K temperature range for base load and peak load operation respectively.

Based on the first case several parameters are varied in order to see the effect on the mean temperature of the HCF for each parameter. Only one parameter is changed per simulation, except for the evaluation of different heating and cooling base loads and SPFs because both base loads go hand in hand. If more heat is extracted during winter time (heat load), more heat is needed to recover the ground temperature during summer time (cooling load). The same applies for the SPF of the heat pumps for heating and cooling.

The parameters to be varied are the spacing between the boreholes, the type of HCF, heating and cooling loads, the borehole configuration and thus the number of boreholes and the SPFs. The whole process is an iteration where a model for the best-case is suggested in the end.

6.3.2 Input data for EED

There are seven categories where parameters can be inserted, namely: ground properties, borehole and heat exchanger, borehole thermal resistance, heat carrier fluid, base load, peak load and the simulation period.

Ground properties

As introduced in Chapter 5.4 the predominant ground is diorite. Table 9 summarizes characteristic properties of quartz-diorite as well as the ground surface temperature (from EED database) and the geothermal heat flux in Trondheim.

Table 9 - Characteristic properties of diorite and the ground in Trondheim

Thermal conductivity $\left[\frac{W}{m*K}\right]$	2.60
Volumetric heat capacity $\left[\frac{MJ}{m^3*K}\right]$	2.10
Ground surface temperature [°C]	4.70
Geothermal heat flux $\left[\frac{W}{m^2}\right]$	0.05

Borehole and heat exchanger characteristics

The chosen parameters are based on literature research and recommendations from Randi Kalskin Ramstad (NTNU).

Set/constant parameters of this category are

- Single U-type pipe (Double U-type applied for high cooling demands)
- Borehole depth of 280m
- Borehole diameter of 139.7mm
- Concrete filling with thermal conductivity of 1.6 $\frac{W}{mK}$

A typical U-pipe configuration can be chosen in EED:

- Outer diameter of 40mm
- Wall thickness of 2.4mm

- Thermal conductivity of 0.42 $\frac{W}{mK}$
- Shank spacing of 88mm

A configuration is shown in Figure 36.

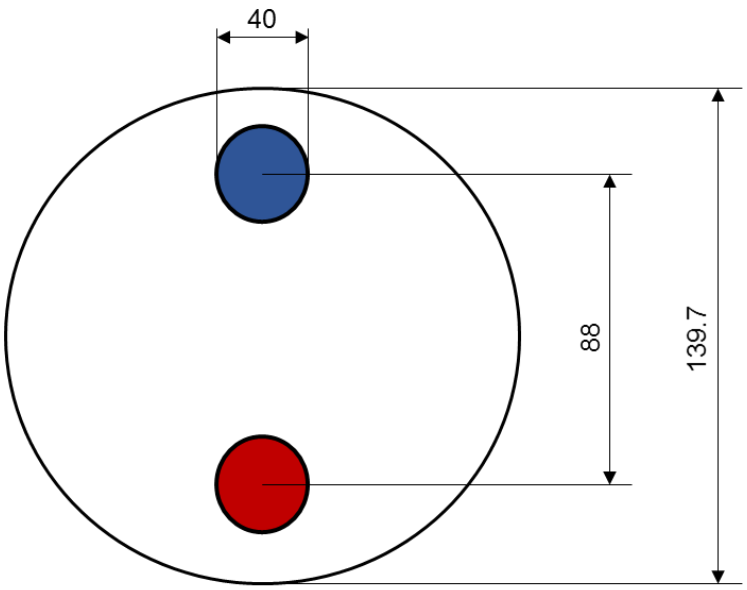

Figure 36 - Configuration of the chosen U-pipe

Varied parameters are

- Spacing between boreholes (6m – 9m)
- Flow rate per borehole (0.5 $\frac{l}{s}$ – 3 $\frac{l}{s}$)

Heat carrier fluid

The HCF is chosen based on its characteristic freezing temperature. The mean temperature of four different HCFs is modeled. The fluids are Monoethylenglycole 25% (MEG), Monopropylenglycole 25% (MPG), Ethanol 25% and Potassium carbonate 25%. They differ in thermal conductivity, specific heat capacity, density, viscosity and freezing point. All these properties are included in the EED database.

Base load

In order to model the base load, the total annual heating and cooling demands as well as the monthly share of the energy demand have to be inserted into EED. The monthly share is calculated from the data provided by RBL. There is no cooling system in Risvollan, however the solar gain can be assumed to be equal to the cooling demand in case of the

solar energy being used to recover the ground temperature. The heating demand is varied from 6000 MWh up to 10600 MWh always varying the cooling demand accordingly since the mean fluid temperature of the HCF has to be kept at a constant level. 6000 MWh is chosen because it is the required heating demand for a solar gain input to the ground of 4000 MWh which is the solar gain for heating the boreholes from solar collectors in Risvollan as calculated in Chapter 6.2.2. 10600 MWh is chosen because it is the heating demand for space heating in Risvollan. The annual heating demand does not need to cover the DHW heating assuming that this is covered by CO_2 heat pumps.
The SPF is varied between 3 and 5 because those are typical values according to Orlikowski [51]. If the SPF is changed, the heating demand has to be changed accordingly in order to get a constant HCF level assuming the cooling demand / solar gain to be constant.

Peak load

The peak load for heating the apartments in Risvollan is 5185 kW as it was modeled with SIMIEN. Furthermore, the duration of peak load required can be set in EED where time durations are chosen freely between 2 hours in April and October and 12 hours in January. The cooling peak load is not considered in this project.

Simulation period

The simulation period is chosen to be 25 years and starts in May leading to heat being transferred to the ground first, before it is extracted for heating purposes.

6.3.3 Simulation results

The results are based on the simulations of the parameters described previously. Table 10 gives an overview of the chosen parameters resulting in a steady temperature level of the HCF.

Table 10 - Parameters leading to a HCF temperature within the given ΔT limit of 11K

Parameter	Chosen value
Number of boreholes	300
Spacing between boreholes	7m
Flow rate of the HCF per borehole	$1 \frac{l}{s}$
HCF	Ethanol

SPF Heat	3
SPF Cool	Direct
Heat base load I	6000 MWh
Cool base load I	4000 MWh
Heat base load II	10600 MWh
Cool base load II	7050 MWh

A “direct” SPF Cool means that there is no heat pump applied, but that all solar gain from the collectors is sent to the geothermal storage directly. The test results of each of the simulations are presented in Appendix B. The variation of the fluid temperature per month is shown in Figure 37.

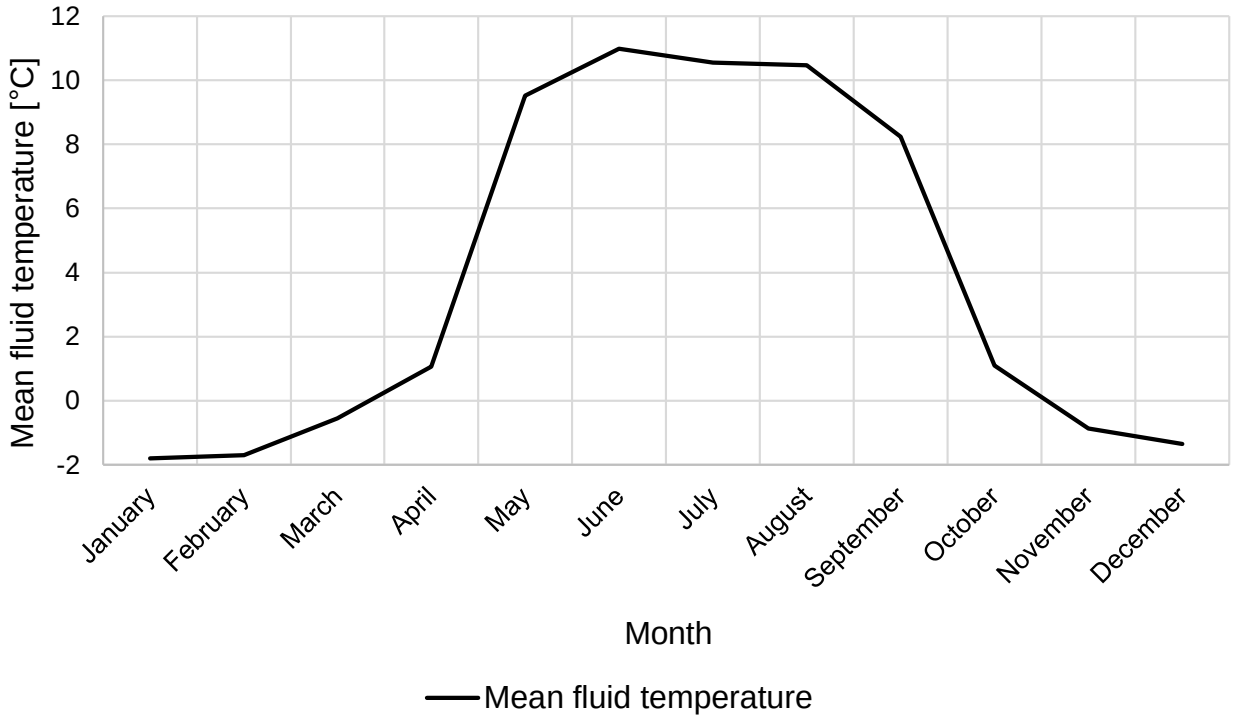

Figure 37 - Mean fluid temperature for peak loads in year 25

As it can be seen from Figure 37, the minimum temperature of the HCF is above -2°C and both, minimum and maximum temperature are well within the ±17K or even ±11K temperature range from the undisturbed ground as recommended by VDI 4640. The temperature is higher during summer because the ground is charged with heat from the solar collectors. A temperature of -1°C is not critical because this temperature occurs only during peak load periods which is assumed to occur for a short time period not long enough to cool down the ground.

The results for the minimum and maximum fluid temperatures at minimum and maximum base and peak loads are presented in Figure 38.

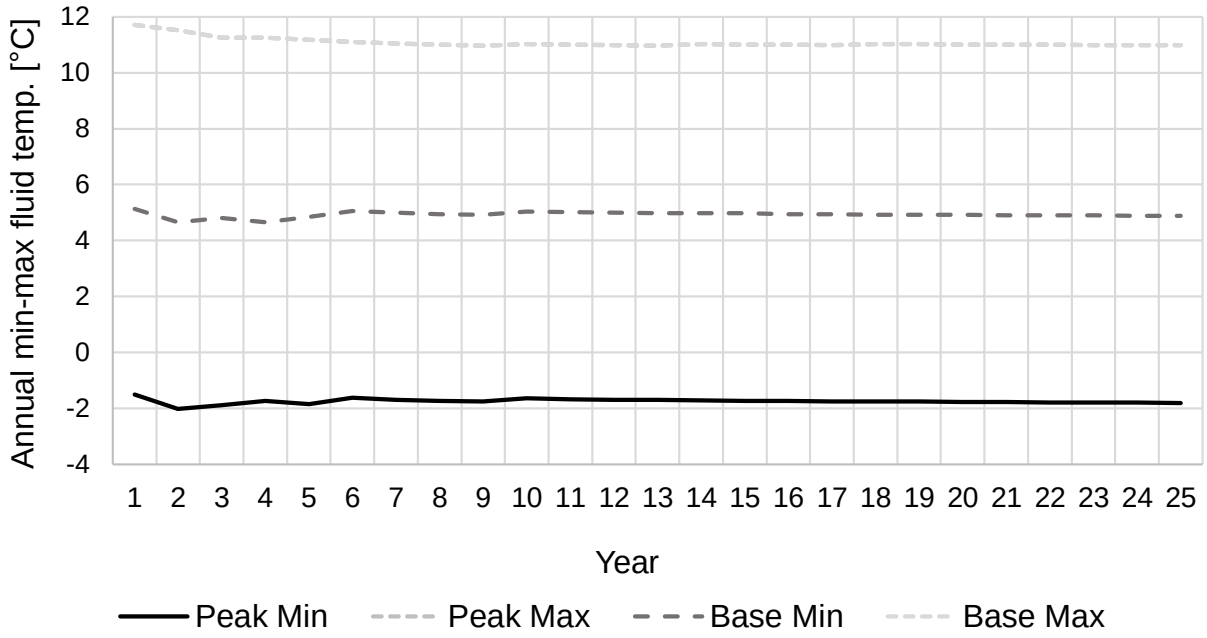

Figure 38 - Annual min-max HCF temperatures

The temperatures reach a steady level after about 10 years. The minimum and maximum mean fluid temperatures of the HCF are the fluid temperatures which occur during base and peak load operations. For instance is the temperature of the “Peak Min” the fluid temperature during peak heating load periods because the highest heat extraction occurs during these times. On the other hand, the fluid temperature during “Peak Max” and “Base Max” operation are equal since there is no peak cooling load, but only the base cooling load. For better understanding of the temperatures, Figure 37 can be checked as well. The temperatures presented in Figure 38 are for a heating base load of 6000 MWh and a cooling base load / solar gain of 4000 MWh. 6000 MWh is about 57% of the current space heating demand of the RBL.

In order to cover the whole space heating demand, a solar gain of 7050 MWh is required to recover the ground during summer season. Either the ground temperature is recovered from solar energy only, but that would require more solar collectors to be installed, partly from solar collectors and partly by heat from DH. According to Åmund Utne [53], Statkraft produces 50-80 GWh surplus heat during summer time (May to September) depending on the outdoor temperatures. Heating from DH should be cheaper during summer time

because there is a surplus of heat in the system. Furthermore, the geothermal storage area could be increased meaning that a larger number of boreholes can be installed, but again this is a matter of costs. An economic analysis will be provided in Chapter 7.

6.3.4 Heat pumps for the geothermal storage system

There are several possibilities when it comes to combining solar energy, geothermal storage and DH depending on how the solar energy is used because the EED results depend to a great extent on how much solar energy is supplied to the ground in order to recover its temperature. Different ideas are introduced in this chapter because the different system designs influence the design of the ammonia GSHPs. Using solar energy for DHW production has already been discussed in Chapter 6.2.4 and therefore it is not discussed here again. Figure 39 presents a simplified design for combining solar energy for supplying heat to the boreholes and the local low-temperature heat distribution grid.

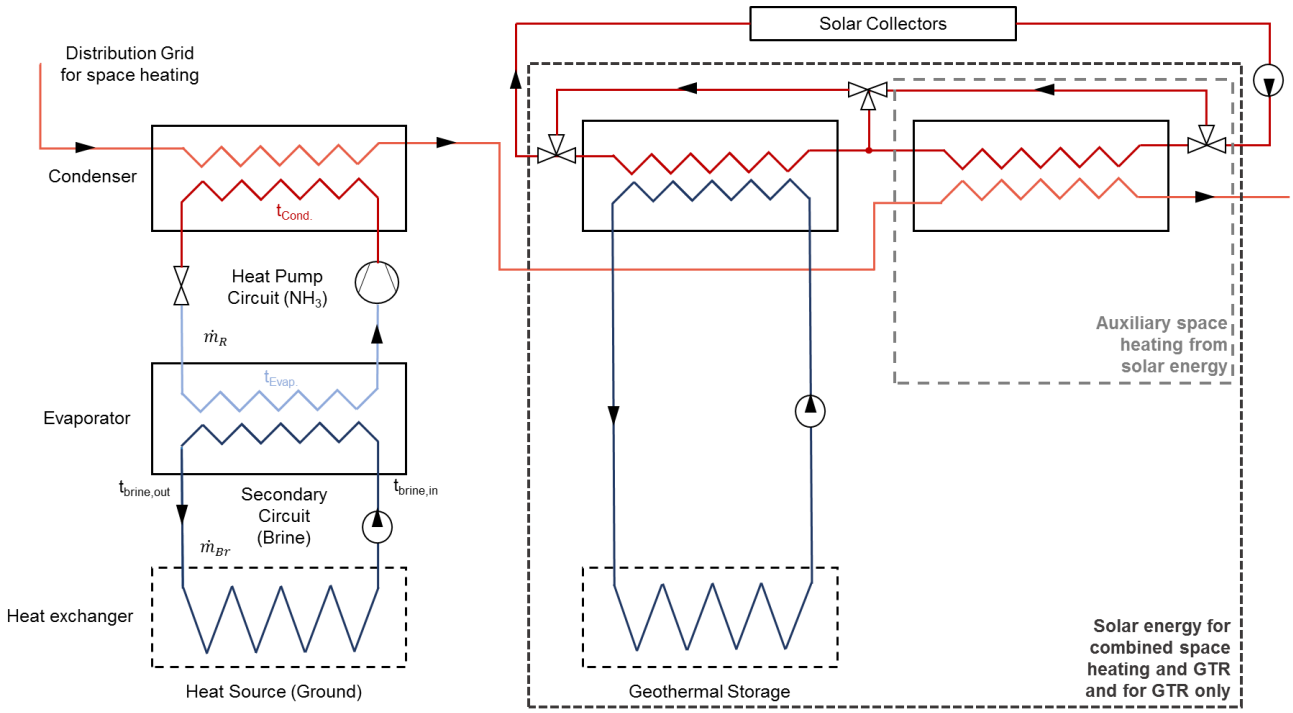

Figure 39 - System design for a hybrid solar thermal / geothermal system

Solar energy for space heating and ground temperature recovery (GTR)

The water of the low-temperature grid can be heated by hot water from the solar collectors depending on the heating demand, the outdoor temperature and the availability of solar energy. If the water of the distribution grid is heated by solar energy, there is less energy available for recovering the ground temperature which has an influence on the design

conditions of the GSHP as well as on the amount of DH needed to recover the ground temperature.

The GSHP has to be designed accordingly because if the water of the distribution grid requires less energy from the GSHP, the ammonia mass flow inside the heat pump as well as the condensing temperature level need to be adjusted.

Solar energy for GTR only

If all of the solar energy is used for recovering the ground temperature, the GSHP needs to cover the heating of the water of the distribution grid to up to 45°C. The design of the GSHP is done using the CoolPack software tool which applies EES. Different cases are investigated in order to find the system with the highest COP. The condenser capacity, evaporation temperature and the condensing temperature are varied. A matrix applied for this work is shown in Table 11. The three columns represent summer, spring/autumn and winter case. Four different condenser capacities are chosen to be examined. Q_{C1} is the peak heating load, Q_{C2} is 60% of the peak capacity and Q_{C3} is chosen randomly whereas Q_{C4} is about half the capacity of Q_{C2}.

It is assumed that the return water temperature of the distribution grid is around 25 °C to 35°C. The condensing temperature of ammonia should be a little higher than 45°C in order to ensure a sufficient heat transfer rate, which is why 49°C is assumed as a design condition for the basic case. In order to get a condensation temperature of 49°C the pressure in the condenser needs to be set to 20.33 bar. The condensation temperature of R717 is varied in order to find the best-fitting temperature. Furthermore, it is known that the peak heating load for space heating which needs to be covered is 5185 kW. Since it is favored to be fully independent from DH, the heat pumps need to cover 100% of the peak load demand. Therefore, the condenser capacity is set to 5.2 MW for the first case. However, it is not favorable to dimension the heat pump to cover the entire peak load, and then to run it on a reduced capacity for most of the year. Usually a heat pump is dimensioned to cover 60% of the peak heating load, in which case it still covers 80-90% of the total annual heating demand [43]. If it is assumed that the GSHP covers 60% of the peak load, the heating load is 3111 kW.

The evaporator conditions depend on the brine temperature. This temperature varies throughout the year as it depends on the heating demands and the season. The mean fluid temperature over a year was presented in Figure 37. The maximum temperature is about 11°C whereas the lowest temperature is about -1°C. Thus the evaporation

temperature of the ammonia needs to be adjusted to this temperature. For a brine temperature of 11°C, the evaporation temperature of R717 should be 7°C and thus the pressure is 5.54 bar. If the brine temperature is -1°C, the evaporation temperature should be -5°C leading to an evaporation pressure of 3.55 bar [54]. These boundary conditions are used as input data for CoolPack for dimensioning the GSHP.

The compressor power E_{Comp} and the capacity of the evaporator Q_{Evap} are given in kW and the mass flow of the refrigerant $\dot{m}_R$ is given in $\frac{kg}{s}$. As it can be seen from Table 11, the COP of the GSHP is highest (3.89) for the lowest condenser temperature and the highest evaporator temperature. The data is taken from CoolPack, but can be confirmed by manual calculations.
The mass flow of the refrigerant R717 can be calculated by

$$\dot{m}_R = \frac{Q_C}{\Delta h_C} = \frac{3111\ kW}{(1770 - 400)\frac{kJ}{kg}} = \mathbf{2.27}\frac{\boldsymbol{kg}}{\boldsymbol{s}} \tag{6.8}$$

The enthalpies are taken from the Log p-h diagram which is presented in Figure 12. Furthermore, the evaporator capacity Q_E for spring and autumn case (with T_E = 2°C) is calculated from

$$Q_E = \dot{m}_R * \Delta h_E = 2.27\frac{kg}{s} * (1500 - 400)\frac{kJ}{kg} = \mathbf{2498\ kW} \tag{6.9}$$

Both values confirm the results from CoolPack marked in Table 11. The temperature difference of the brine (ethanol) in the evaporator is calculated to be 2 K. This is done by

$$Q_E = Q_{Brine} = \dot{m}_{Brine} * c_{p_{Brine}} * \Delta t_{Brine}$$

$$\Delta t_{Brine} = \frac{Q_{Brine}}{\dot{m}_{Ethanole} * c_{P_{Ethanole}}} = \frac{Q_{Ethanole}}{\dot{V}_{Ethanole} * Nr.of\ boreholes * \rho * c_{P_{Ethanole}}} = \frac{2498000\ kW}{0.001\frac{m^3}{s} * 300 * 960\frac{kg}{m^3} * 4250\frac{J}{kg * K}} = \mathbf{2.04\ K} \tag{6.10}$$

A volume flow of 0.001 $\frac{m^3}{s}$ was chosen for the simulations in EED. A temperature difference of the supply and return flow of the brine of 2 K does not cause any problems

for the ground. The SPF for heat extraction can be estimated using the seasonal COPs calculated in Table 11 to be

$$SPF = \frac{3\ months}{12\ months} * COP_{Winter} + \frac{6\ months}{12\ months} * COP_{Spring;Autumn} + \frac{3\ months}{12\ months} * COP_{Summer} = \frac{3}{12} * 3.89 + \frac{6}{12} * 3.35 + \frac{3}{12} * 2.76 = \mathbf{3.34} \quad (6.11)$$

The calculated SPF can be used as an updated input parameter for EED in order to improve the reliability of the results of the EED simulations. As mentioned earlier, the COP/SPF of a heat pump is the COP of a refrigeration system plus one and therefore the final SPF of the GSHP is 4.34.

Furthermore, the size of water storage tanks matters and needs to be investigated. Right now, there are no water tanks applied in the substations of the RBL, but this will be necessary, if solar collectors are used for warm water production.

Table 11 - Matrix for the simulations in CoolPack

			$T_{amb,1}$ = 11°C				$T_{amb,2}$ = 6°C				$T_{amb,3}$ = -1°C			
			T_{E1} = 7°C				T_{E2} = 2°C				T_{E3} = -5°C			
			COP	E_{Comp}	Q_{Evap}	$\dot{m}$	COP	E_{Comp}	Q_{Evap}	$\dot{m}$	COP	E_{Comp}	Q_{Evap}	$\dot{m}$
Q_{C1} = 5185 kW	T_{C1} = 48°C	COP	3,89	-	-	-	3,35	-	-	-	2,76	-	-	-
		E_{Comp}	-	1080	-	-	-	1218	-	-	-	1414	-	-
		Q_{Evap}	-	-	4198	-	-	-	4074	-	-	-	3899	-
		$\dot{m}$	-	-	-	3,86	-	-	-	3,76	-	-	-	3,63
	T_{C2} = 49°C	COP	3,87	-	-	-	3,26	-	-	-	2,7	-	-	-
		E_{Comp}	-	1105	-	-	-	1243	-	-	-	1439	-	-
		Q_{Evap}	-	-	4176	-	-	-	4053	-	-	-	3877	-
		$\dot{m}$	-	-	-	3,86	-	-	-	3,76	-	-	-	3,63
	T_{C3} = 50°C	COP	3,68	-	-	-	3,18	-	-	-	2,64	-	-	-
		E_{Comp}	-	1129	-	-	-	1267	-	-	-	1463	-	-
		Q_{Evap}	-	-	4154	-	-	-	4031	-	-	-	3856	-
		$\dot{m}$	-	-	-	3,85	-	-	-	3,76	-	-	-	3,63
Q_{C2} = 3111 kW	T_{C1} = 48°C	COP	3,89	-	-	-	**3,35**	-	-	-	2,76	-	-	-
		E_{Comp}	-	648,1	-	-	-	730,9	-	-	-	848,7	-	-
		Q_{Evap}	-	-	2519	-	-	-	2445	-	-	-	2340	-
		$\dot{m}$	-	-	-	2,31	-	-	-	**2,26**	-	-	-	2,18
	T_{C2} = 49°C	COP	3,78	-	-	-	3,26	-	-	-	2,7	-	-	-
		E_{Comp}	-	662,8	-	-	-	745,6	-	-	-	863,2	-	-
		Q_{Evap}	-	-	2505	-	-	-	2432	-	-	-	2326	-
		$\dot{m}$	-	-	-	2,31	-	-	-	2,26	-	-	-	2,18
	T_{C3} = 50°C	COP	3,68	-	-	-	3,18	-	-	-	2,64	-	-	-
		E_{Comp}	-	677,4	-	-	-	760,2	-	-	-	877,8	-	-
		Q_{Evap}	-	-	2492	-	-	-	2418	-	-	-	2313	-
		$\dot{m}$	-	-	-	2,31	-	-	-	2,26	-	-	-	2,18
Q_{C3} = 2000 kW	T_{C1} = 48°C	COP	3,89	-	-	-	3,35	-	-	-	2,76	-	-	-
		E_{Comp}	-	416,6	-	-	-	469,9	-	-	-	545,6	-	-
		Q_{Evap}	-	-	1619	-	-	-	1572	-	-	-	1504	-
		$\dot{m}$	-	-	-	1,49	-	-	-	1,45	-	-	-	1,4
	T_{C2} = 49°C	COP	3,78	-	-	-	3,26	-	-	-	2,7	-	-	-
		E_{Comp}	-	426,1	-	-	-	479,3	-	-	-	555	-	-
		Q_{Evap}	-	-	1611	-	-	-	1563	-	-	-	1496	-
		$\dot{m}$	-	-	-	1,49	-	-	-	1,45	-	-	-	1,4
	T_{C3} = 50°C	COP	3,68	-	-	-	3,18	-	-	-	2,64	-	-	-
		E_{Comp}	-	435,5	-	-	-	488,7	-	-	-	564,3	-	-
		Q_{Evap}	-	-	1602	-	-	-	1555	-	-	-	1487	-
		$\dot{m}$	-	-	-	1,49	-	-	-	1,45	-	-	-	1,4
Q_{C4} = 1600 kW	T_{C1} = 48°C	COP	3,89	-	-	-	3,35	-	-	-	2,76	-	-	-
		E_{Comp}	-	333,3	-	-	-	375,9	-	-	-	436,5	-	-
		Q_{Evap}	-	-	1295	-	-	-	1257	-	-	-	1203	-
		$\dot{m}$	-	-	-	1,19	-	-	-	1,16	-	-	-	1,12
	T_{C2} = 49°C	COP	3,78	-	-	-	3,26	-	-	-	2,7	-	-	-
		E_{Comp}	-	340,9	-	-	-	383,5	-	-	-	444	-	-
		Q_{Evap}	-	-	1289	-	-	-	1251	-	-	-	1297	-
		$\dot{m}$	-	-	-	1,19	-	-	-	1,16	-	-	-	1,12
	T_{C3} = 50°C	COP	3,68	-	-	-	3,18	-	-	-	2,64	-	-	-
		E_{Comp}	-	348,4	-	-	-	391	-	-	-	451,4	-	-
		Q_{Evap}	-	-	1282	-	-	-	1244	-	-	-	1190	-
		$\dot{m}$	-	-	-	1,19	-	-	-	1,16	-	-	-	1,12

6.4 Heat pumps for DHW heating

As introduced in Chapter 4.4.6, CO_2 heat pumps are a common technology for DHW heating to temperatures up to 70°C. This chapter gives a description on the methodology used to find a CO_2 heat pump which fits the requirements of the Risvollan project, and presents the results for dimensioning the heat pump.

6.4.1 Approach and methodology

It is assumed that there is one CO_2 heat pump to be installed at each substation of the distribution grid and since each substation has a different heating demand, heat pumps of different capacity need to be installed.
For the Risvollan project it is assumed that the return temperature of the distribution grid is the supply temperature to the evaporator. This temperature is assumed to be 35°C. A simple sketch which shows the general principle of the CO_2 heat pump integration into the heating grid is presented in Figure 40.

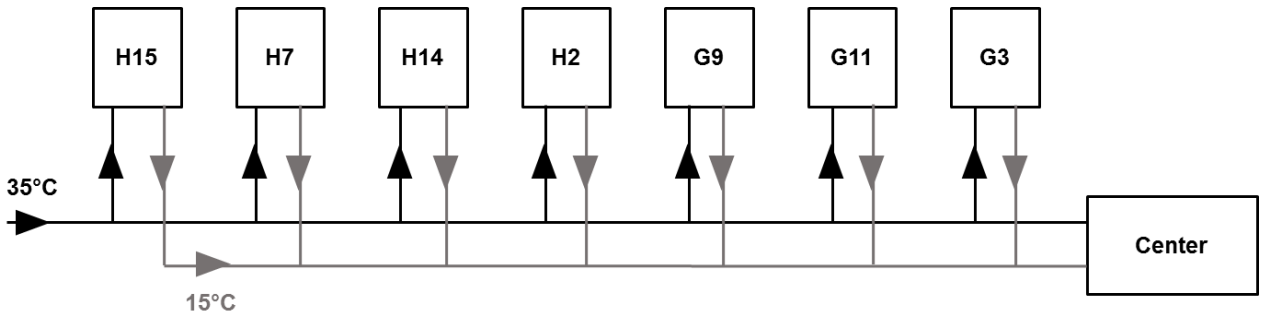

Figure 40 - Principle sketch of CO_2 heat pump integration into the low-temperature distribution grid at each substation of Loop GH

The heat pumps are integrated into the return flow of the low-temperature distribution grid because a rather low temperature on the evaporator side is favorable for the CO_2 heat pump cycle. Typically, the evaporation temperatures of a CO_2 heat pump are around -5°C to 0°C, but since the heat source of the investigated system is the low-temperature grid with a temperature of 25°C to 35°C, the evaporation temperature will be around 20°C. Since the water is supposed to be heated from 8°C to 70°C, but the evaporation temperature is 20°C, the water has to be pre-heated in order to be able to use a CO_2 heat pump. This could be done in a heat exchanger which uses the heat of the return water flow from the evaporator. The principle is presented in Figure 41. Depending on the mass flows

the water can be heated from 8°C to 22°C by the return flow from the evaporator and thus needs to be heated from 22°C to 70°C in the condenser afterwards. The temperatures of the LTDG may be different during summer and winter time depending on the required heating demand.

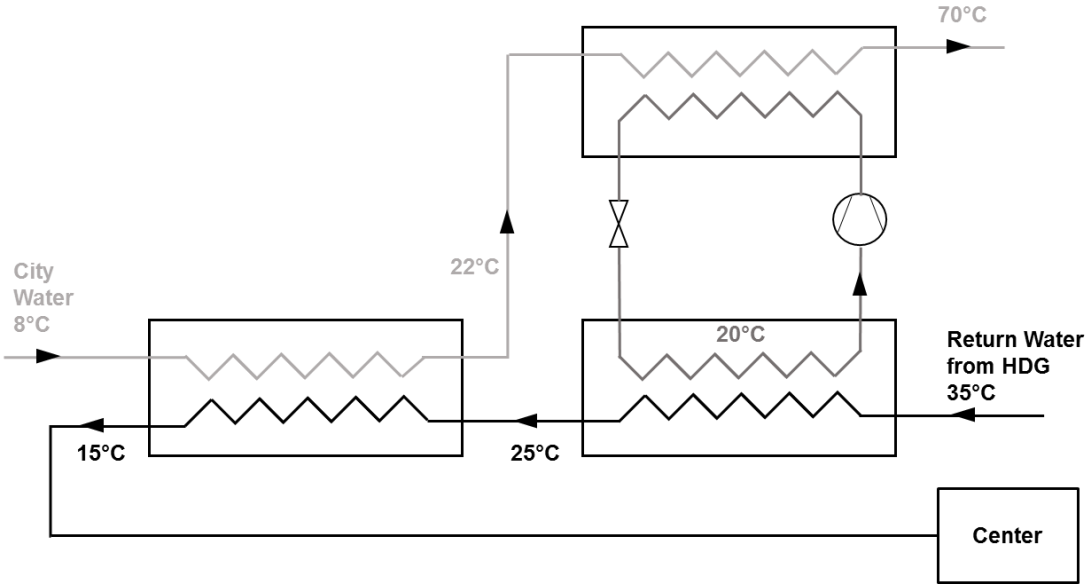

Figure 41 - Principle of CO_2 heat pump integration with pre-heating

By using a heat exchanger for pre-heating the cold supply water, the heat pump can be run at an evaporation temperature of 20°C such that a small temperature difference between the incoming water and the CO_2 is still maintained. The proposed CO_2 cycle is shown in a T-s diagram in Figure 42.

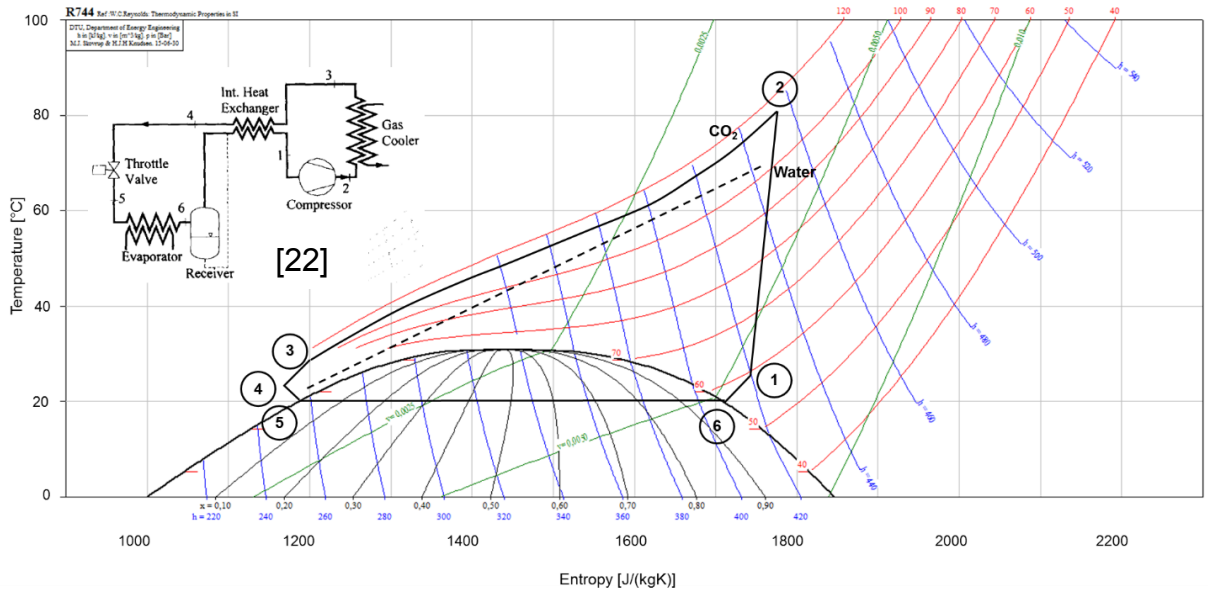

Figure 42 - T – s – diagram of a possible CO_2 cycle for the heat pumps in Risvollan

As it can be seen from Figure 42, the pressure in the condenser should be around 115 bar whereas the pressure in the evaporator is about 57 bar leading a pressure ratio of the compressor of π = 2.02. The temperature difference between the incoming water having a temperature of 22°C and the CO_2 leaving the gas cooler at a temperature of 25°C is therefore assumed to be 3°C. Starting with these assumptions, the CO_2 heat pump cycle can be modeled in CoolPack/EES.

6.4.2 Results of the simulations in CoolPack / EES

The performance of the CO_2 cycle is modeled in CoolPack. The T-s diagram (Figure 42) is used as a starting point and the final input parameters of the chosen cycle are presented in Table 12. A superheating of 3K by the internal heat exchanger is chosen in order to make sure that no liquid is entering the compressor. A high pressure of 115 bar is applied because there needs to be a temperature difference between the CO_2 and the water at the pinch point (see Figure 42) and if the water is to be heated up to 70°C, the pressure needs to be adjusted accordingly. The CO_2 is cooled down to 25°C so that the temperature difference between the CO_2 outlet and the city water inlet is 3K because it is assumed that the water is pre-heated to 22°C before it enters the evaporator.

Table 12 - Parameters of the CO_2 cycle

Parameter	Chosen value
Evaporator temperature T_E [°C]	20
Superheating ΔT_{SH} [K]	3
Condenser pressure [bar]	115
Condenser (Gas Cooler) outlet temperature T_4 [°C]	25
Heating capacity in the gas cooler Q_{GC} [kW]	Depends on the heat pump capacity of each SS
Suction line outlet temperature T_S [°C]	23°C

The capacity of the condenser (gas cooler) depends on the heating capacity of the heat pump at each substation. The suction line outlet temperature is assumed to be 23°C which is 3K higher than the evaporation temperature as the CO_2 passes the internal heat exchanger before the compressor and after the gas cooler. These input parameters lead to a gas cooler inlet temperature of 78.7°C and a COP of 5.711. Depending on the heat pump size, the compressor power can be calculated accordingly. A COP of 5.711 is similar

to the results of Nekså [22]. The CO_2 heat pump cycle is presented in a log p-h diagram in Figure 43.

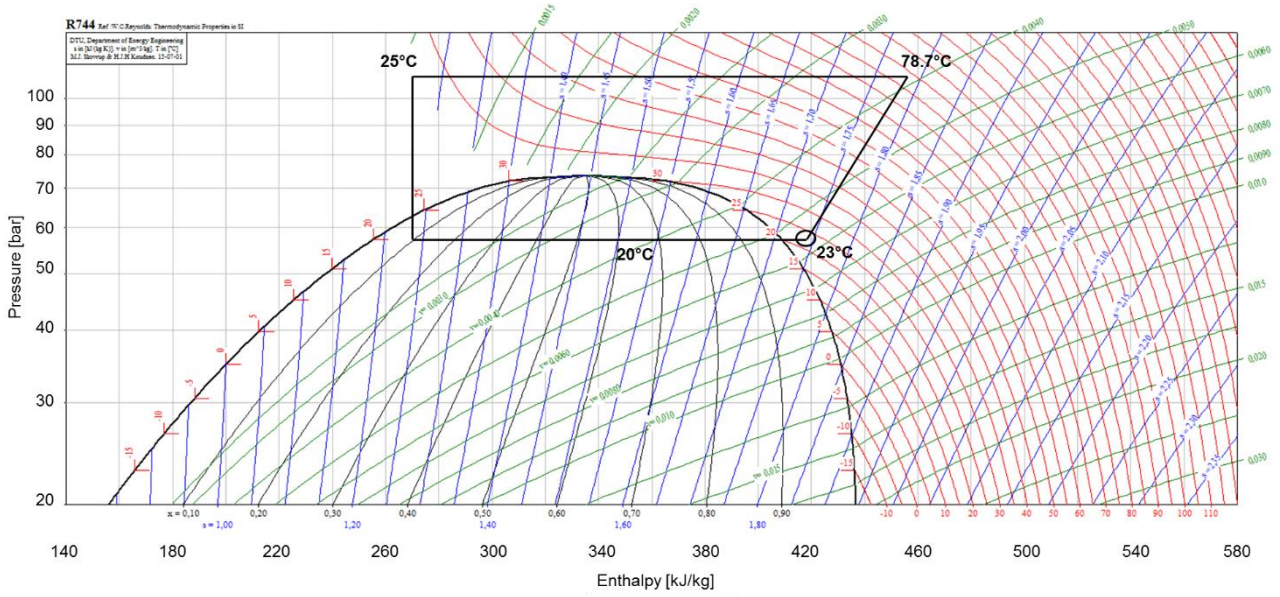

Figure 43 - Log p - h - diagram of the CO_2 cycle

The capacities of the heat pumps for DHW heating are calculated from the results from SIMIEN as well as based on the requirements of regulation TEK87. There are two ways for calculating the heat pump capacity. Both cases are introduced with the aid of an example calculation which is given for Substation SS G9.

<u>Case 1 – Assuming 10% of the total net power demand used for DHW heating</u> [43]

The following data is given or assumed:

- Required heating power for DHW heating [55]: 10% of the total net power demand
- Total Floor Area of Loop GH [56]: 30105 m^2
- Floor Area of SS G9 [56]: 4887 m^2
- Heating power demand after TEK87 [43]: 52 $\frac{W}{m^2}$
- Total heating power of Loop GH: 1524.5 kW (from SIMIEN simulations)

First, a correction factor for the heating capacity is calculated because the calculations based on TEK87 and the results from SIMIEN are slightly different.

$$Total\ floor\ area * Heating\ power\ demand = Total\ heating\ capacity \quad (6.12)$$

$$30105\ m^2 * 52\ \frac{W}{m^2} = 1565408\ W$$

$$\frac{Total\ heating\ capacity\ after\ SIMIEN}{Total\ heating\ capcity\ after\ TEK87} = Correction\ factor \quad (6.13)$$

$$\frac{1524500\ W}{1565408\ W} = 0.974$$

Knowing the correction factor, the heat pump capacity of substation G9 can be calculated.

$$Floor\ area * Heating\ power\ demand * Correction\ factor = Heating\ capacity \quad (6.14)$$

$$4887\ m^2 * 52\ \frac{W}{m^2} * 0.974 = 247483\ W$$

Since it is estimated that the required heating power for DHW heating is 10% of the total heating power demand, the capacity of the heat pump of SS G9 can be calculated by

$$Heating\ capacity * 10\% = Heat\ pump\ capacity \quad (6.15)$$

$$247483\ W * 0.1 = \mathbf{24.75\ kW}$$

The capacities of the heat pumps of all other substations are calculated the same way. The results are presented in Table 13.

Table 13 - Capacities of the heat pumps for DHW heating Case 1

Substation	Heat pump capacity [kW]	Substation	Heat pump capacity [kW]	Substation	Heat pump capacity [kW]
G3	19	F4	35	A3	22
G9	25	F8	24	A7	16
G11	21	F14	16	B2	27
H7	13	D6	24	B7	25
H15	21	D11	29	B15	27
H14	23	D16	24	C6	34
H2	31	Sollia	38	E4	19

The heat pumps for the substations have a capacity between 13 kW and 38 kW. This is important for the economic analysis. The compressor power is calculated and given by CoolPack based on a COP of 5.7. The compressor power needs to be considered when it

comes to the electricity consumption and thus annual costs of heat pumps. The results are shown in Table 14.

Table 14 - Compressor power of each of the heat pumps Case 1

Substation	Compressor power [kW]	Substation	Compressor power [kW]	Substation	Compressor power [kW]
G3	3.33	F4	6.14	A3	3.86
G9	4.39	F8	4.21	A7	2.81
G11	3.68	F14	2.81	B2	4.74
H7	2.28	D6	4.21	B7	4.39
H15	3.68	D11	5.09	B15	4.74
H14	4.04	D16	4.21	C6	5.96
H2	5.44	Sollia	6.67	E4	3.33

Case 2 – Assuming a DHW demand of 41.13 kWh per m²

As it is introduced in Chapter 5.2, the heating demand for DHW is 48 $\frac{kWh}{m^2}$. This value can be used to calculate the size of the heat pump by

$$Floor\ area\ SS\ G9\ [m^2] * DHW\ demand\left[\frac{kWh}{m^2}\right] = DHW\ demand\ [kWh] \quad (6.16)$$

$$4887\ m^2 * 48.13\ \frac{kWh}{m^2} = 235211\ kWh$$

Assuming that the heat pump is running for 8760 hours per year, the capacity is calculated by

$$\frac{235211\ kWh}{8760\ h} = \mathbf{26.85\ kW} \quad (6.17)$$

The capacities for the heat pumps of each substation are given in Table 15.

Table 15 - Capacities of the heat pumps for DHW heating Case 2

Substation	Heat pump capacity [kW]	Substation	Heat pump capacity [kW]	Substation	Heat pump capacity [kW]
G3	20	F4	38	A3	24
G9	27	F8	26	A7	17
G11	23	F14	17	B2	30
H7	14	D6	26	B7	27
H15	23	D11	32	B15	29
H14	25	D16	26	C6	37
H2	34	Sollia	41	E4	21

If compared to Case 1, the compressor power for Case 2 increases slightly as it depends on the heat pump capacity. The compressor power based on a COP of 5.7 is shown in Table 16.

Table 16 - Compressor power of each of the heat pumps Case 2

Substation	Compressor power [kW]	Substation	Compressor power [kW]	Substation	Compressor power [kW]
G3	3.51	F4	6.67	A3	4.21
G9	4.74	F8	4.56	A7	2.98
G11	4.04	F14	2.98	B2	5.26
H7	2.46	D6	4.56	B7	4.74
H15	4.04	D11	5.61	B15	5.09
H14	4.39	D16	4.56	C6	6.49
H2	5.96	Sollia	7.19	E4	3.68

Comparing the results of both cases, it is obvious that the heat pump capacities calculated after Case 2 are slightly higher than for Case 1. They are also assumed to be more accurate because they are based on existing data provided by RBL.

6.5 Integration of DHW storage tanks

It is necessary to integrate water storage tanks into the system, if heat pumps and solar collectors are used for DHW heating. From the heat pump point-of-view, this is done in order to prevent multiple starts and stops of the compressor in times of low heating demands [23], whereas from the solar system point-of-view an accumulator tank has an impact on the overall efficiency of the system. Furthermore, energy demand and availability are usually not met. Solar energy is available during the day, but DHW is needed in the morning or evenings when people take showers. However, low fluid temperature from the accumulator towards the solar collector increases the efficiency of the solar system because the heat transferring fluid can absorb more heat before it rejects heat to the storage tank again [16]. According to Qvistgaard [16], a stratified accumulator improves the performance of a solar system compared to a fully-mixed water tank by two to three times because the temperature at the bottom of the tank is lower and thus a lower collector inlet temperature can be provided. Stene [23] investigated a DHW CO_2 heat pump system including a storage tank with a movable insulation plate which separates the hot water from the cold water of the tank and found that it improves the thermal performance of the storage tank. A possible system design for the integration of hot water storage tanks is proposed in Figure 44. The number of vessels is different for each substation and depends on the number of people living there. The storage tanks are operated in series [19] which means that the coldest water is at the bottom of the first storage tank and the hottest water at the top of the last storage tank. If DHW is needed, it is taken from the vessel with the hottest temperature and cold water flows into the coldest storage tank so that a flow circuit is established. Cold city water either flows into the vessel with the coldest water or enters the CO_2 heat pump after being pre-heated by a heat exchanger.

The size of the storage tanks depends on the DHW water demand of the substation. A typical DHW storage tank has a capacity of 800 to 1000 liters [23] [56]. It is assumed that the average DHW consumption is 40 liters per person per day [57]. As it was calculated for the simulations in SIMIEN, the DHW demand in Risvollan is 48.13 $\frac{kWh}{m^2}$. This specific demand is used for calculating the DHW demand per substation in order to get the number of storage tanks which have to be installed at each sub-station applying Equation (6.18).

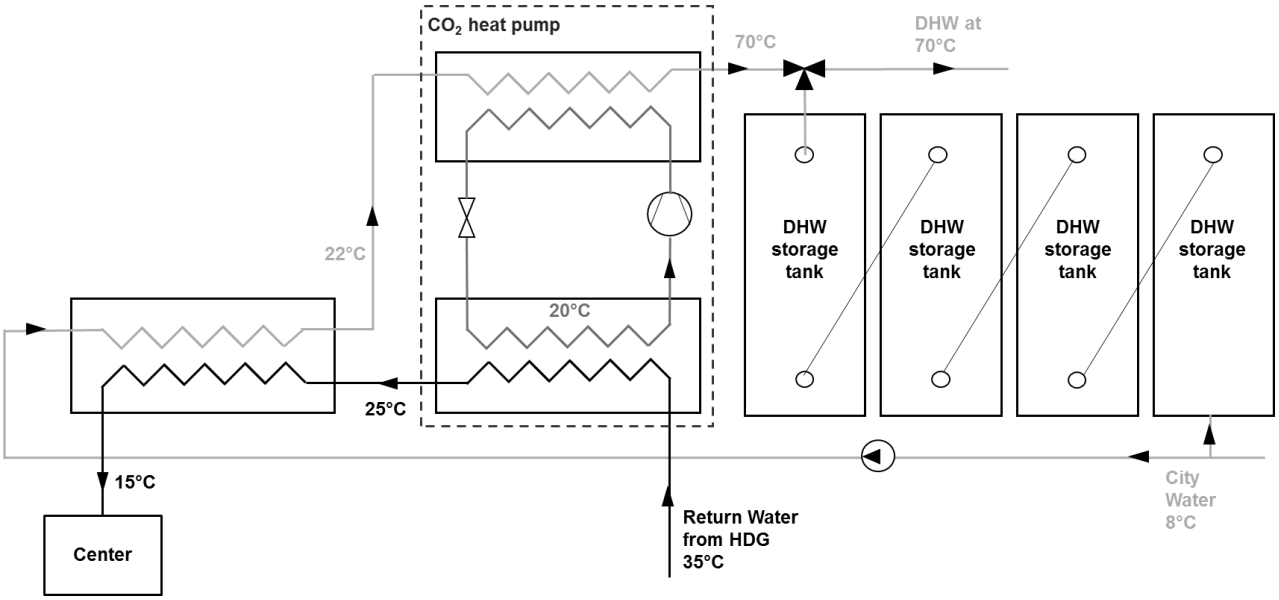

Figure 44 - Principle design of the integrated DHW storage tanks

The annual DHW heating demand is presented in Table 17.

Table 17 - DHW demand per substation per year

Substation	DHW demand [kWh]	Substation	DHW demand [kWh]	Substation	DHW demand [kWh]
G3	177118	F4	333685	A3	212205
G9	235211	F8	224430	A7	149925
G11	202002	F14	148289	B2	259661
H7	122443	D6	229003	B7	237666
H15	199740	D11	278384	B15	253068
H14	216922	D16	229003	C6	323722
H2	295470	Sollia	362082	E4	182413

An example calculation for getting the number of storage tanks per substation is carried out for Substation H7 assuming a storage tank size of 1000 liter.

The number of storage tanks is calculated from

$$N = \frac{Q}{m * c_p * \Delta T} \tag{6.18}$$

N Number of storage tanks

m Mass (volume) of the storage tank

c_p Heat capacity of water

ΔT Temperature difference of the water to be heated up

Q DHW demand of the substation

This leads to

$$N = \frac{122443\,\frac{kWh}{year} * 3.6\,\frac{MJ}{kWh} * 1000\,\frac{kJ}{MJ}}{12\,\frac{months}{year} * 30\,\frac{days}{month} * 1000\,l * 1\,\frac{kg}{l} * 4.2\,\frac{kJ}{kg * K} * (70 - 8)K}$$

$$N = 4.70 \triangleq \mathbf{5}\ \boldsymbol{tanks}$$

This means that Substation H7 requires 5 storage tanks of a volume of 1000 liter assuming a daily recharging.

A volume of about 5000 liters can be confirmed, if it is assumed that the average DHW consumption is 40 $\frac{liter}{day*person}$ [57]. There are 25 apartments at SS H7 [56] and assuming 4 persons living in one apartment the average daily DHW consumption would be about 4000 liters which means that a water storage of 5000 liters would be sufficient.

The number of storage tanks to be installed at each substation is summarized in Table 18.

Table 18 - Number of DHW storage tanks per substation

Substation	Number of storage tanks [-]	Substation	Number of storage tanks [-]	Substation	Number of storage tanks [-]
G3	7	F4	13	A3	9
G9	9	F8	9	A7	6
G11	8	F14	6	B2	10
H7	5	D6	9	B7	9
H15	8	D11	11	B15	10
H14	9	D16	9	C6	13
H2	12	Sollia	14	E4	7

It is estimated that a total number of 196 DHW storage tanks with a volume of 1000 liter need to be installed in the houses of the RBL, if the total DHW volume needs to be stored at the same time. The available or required space for the vessels has to be investigated for each substation. It is a more practical approach that the total storage tank volume per

substation does not have to cover the whole water consumption of the substation because the DHW will most likely be used at different times during the day which means that the water can be heated during day and night and therefore not all of the DHW needs to be stored at one time. Otherwise the storage would be over-dimensioned leading to unnecessary high investment costs and efficiency losses in the system. SWECO suggests to use two 1000 l storage tanks per substation, although the water consumption of a substation is much higher, being 11000 l and 23000 l [56].

7. Economic analysis of the STG measures

After the energy analysis of the STG measures is done and the key parameters of the technologies to be integrated are known, an economic analysis is carried out. So far, heat is provided by DH where the hot water is produced in a waste incineration plant. The prices for DH in Norway are relatively low which makes DH a competitive technology. The current energy prices in Trondheim are 0.7 $\frac{NOK}{kWh}$. Renewable energy technologies, such as the investigated STG measures, are initially more expensive, but usually have low maintenance costs as well as no fuels costs during their lifetime. For conventional power plants on the other hand, maintenance costs and increasing fuel prices occur and need to be paid by the customer. Especially for customers who have a high heating demand, it can be beneficial to invest in new energy systems in order to save money in the long run. It is a challenge to determine the value of a project because there are several ways of measuring future cash flows.

7.1 The Net Present Value model

The Net Present Value is a key performance indicator and will therefore be discussed and used for investigating the profitability of the STG measures.
The NPV is the difference between the present value of cash inflows and the present value of cash outflows [58] and is an indicator for how much monetary value the investment/project adds to the firm. It predicts the profitability of an investment and can be calculated by [59]

$$NPV = \sum_{t=1}^{T} \frac{C_t}{(1+r)^t} - C_o \tag{7.1}$$

$$NPV = C_t * \left(\frac{1-(1+r)^{-T}}{r} \right) - C_0 \tag{7.2}$$

C_t	Net cash inflow during the period / Future savings [NOK]
C_o	Initial investment costs [NOK]
r	Real interest rate
T	Number of time periods

The interest rate r accounts for the time value of a currency. If the NPV calculated after

Equation (7.2) is positive, the project might be realized and if it is negative, it may be rejected. The real interest rate expresses the real value of the money and differs from the nominal interest rate because it incorporates corrections for inflation, changes of the energy prices and taxes. For externally financed projects, the nominal interest rate is the rate of interest on the loan (lending rate). The real interest rate r is calculated from

$$r = \frac{1}{1+e} * \left[\frac{r_n * (1-s) - i}{1+i} - e\right] \tag{7.3}$$

where

i	Inflation rate
s	Tax rate
e	Rate of price increase
r_n	Nominal interest rate

The lifetime of a renewable energy system is estimated to be 20 to 30 years [60]. The unit of the NPV is given in the local currency, for example in € or NOK. The discount rate r is calculated after Equation (7.2), where the rate of price increase e is 2.2% in Norway, the inflation rate i is 2.07% [52], the average of the nominal interest rate r_n is 2.5% [61] and a tax rate s of 0% is assumed. Therefore, the real interest rate r is

$$r = \frac{1}{1+0.022} * \left[\frac{0.021 * (1-0) - 0.0207}{1+0.0207} - 0.022\right] = \mathbf{-0.0174} \triangleq \mathbf{-1.74}\%$$

This real interest rate is used for each calculation of the NPVs of the different STG measures. Another characteristic parameter for the economic analysis is the Net Present Value Quotient Method (NPVQ) which is

$$NPVQ = \frac{NPV}{C_0} \tag{7.4}$$

The higher the NPVQ is, the more profitable it is. This method makes it possible to set up a ranking of the different measures or investments and shows which measures give highest capital gains for an investment.

7.2 The energy system applied for space heating

A short repetition of the energy analysis shows that space heating is provided by the GSHP. 90% of the space heating demand is covered by the heat pump, whereas the other

10% are covered by a DH back-up. If a total heating demand of 10600 MWh is provided, the ground requires 7050 MWh to recover its temperature. 4200 MWh can be provided by the solar system and thus 2850 MWh need to be provided by DH.

In general, a solar system is characterized by high investment costs, but low operational costs. It is beneficial, if energy costs for oil, gas electricity are high, so that a solar system becomes more competitive. Therefore, the future price development of energy costs should be considered. Costs for annual servicing and maintenance are about 1% to 5% of the initial investment costs [62].

The costs for drilling boreholes depends on the ground conditions mostly. Since there is a deep clay layer in Risvollan, the drilling is more expensive because a casing is needed for drilling. As a rule of thumb, it is three to five times more expensive to drill with casing [52]. The costs for rigging up, drilling boreholes and installing the ground source heat exchanger in bedrock is 150-250 $\frac{NOK}{m}$ [16] and an economic lifetime of the system of 50 years is assumed. According to Energy Saving Trust [63] the total system costs for a BTES are 10500 $\frac{NOK}{kW}$ to 19000 $\frac{NOK}{kW}$ which is why a cost of 15000 $\frac{NOK}{kW}$ is chosen for the calculations.

The costs of the Solar/BTES/DH system are summarized in Table 19.

Table 19 - Economic analysis of the Solar/BTES/DH system for space heating

	Initial costs [NOK]
Solar	32.142.210
BTES	46.665.000
Total	**78.807.210**
	Current energy costs per year [NOK]
DH only	7.426.300
	Annual costs of the Solar/BTES/DH [NOK]
BTES	1.540.016
Solar	321.422
DH	2.737.630
Total	4.599.070
Annual savings [NOK]	**2.827.230**
Payback time [years]	**27.87**

The calculations on the solar system are based on the prices of Wagner Solar [64]. The initial investment for the solar system includes prices for collectors as well as frames because it is necessary to erect the collectors since the buildings are flat-roofed. The initial

costs of the BTES include costs for drilling as well as installation and commissioning of the ground loop and the GSHP. The current energy costs are the DH costs that were paid by RBL for space heating in 2014. Annual costs include operation and maintenance costs for the solar system, heating costs for DH in order to cover 10% of the space heating demand and DH costs for recovering the ground temperature as well as electricity costs for the compressor. Therefore, the annual savings are the expenses that are saved compared to the current 100% DH application. Detailed calculations of all costs are presented in Appendix C. The NPV and NPVQ will be compared to the other cases in Chapter 7.4.

7.3 The energy system applied for DHW heating

The DHW demand will be fully covered by CO_2 heat pumps and no DH is necessary. The costs of the energy system for DHW heating are summarized in Table 20.

Table 20 - Economic analysis of the CO_2 heat pump and water storage system

	Initial costs incl. VAT [NOK]
CO_2 heat pumps	9.720.000
Water storage tanks	1.620.000
Total	**11.340.000**
	Current energy costs per year [NOK]
DH only	3.410.540
	Annual costs of the system [NOK]
CO_2 heat pumps	509.036
Water storage tanks	-
Total	509.036
Annual savings [NOK]	**2.901.504**
Payback time [years]	**3.91**

For a 20 kW CO_2 heat pump costs are estimated to 210.000 NOK, as 30 kW and 40 kW heat pumps cost about 240.000 NOK and 360.000 NOK respectively [65]. Based on the heating demand of the substations, the heat pumps are chosen. The initial costs for the heat pumps add up to 9.72 million NOK, also including costs for integration and installation, automation as well as for rigging up. Due to the storage vessel, the RATIO1000 tank from Wagner Solar is chosen as an example. One storage tank costs about 16200 NOK [64]. Assuming that a total number of 100 storage tanks is a sufficient number of vessels, the initial costs are 1.62 million NOK. The total annual expenses are calculated to be around 600.000 NOK resulting from the electricity consumption of the

compressor. A COP of 5.7 is chosen for the calculations based on the simulation results from CoolPack. The payback time of the energy system is 4 years based on the expenses for DHW coming from DH only.

7.4 The STG in Risvollan

An economic analysis combining both energy systems is presented in Table 21.

Table 21 - Economic analysis of all STG measures

	Initial costs incl. VAT [NOK]
Space heating system	78.807.410
DHW	11.340.000
Total	**90.147.410**
	Energy costs per year in 2014 [NOK]
DH for space heating	7.426.300
DH for DHW	3.410.540
Total	10.836.840
	Annual costs of the system [NOK]
Space heating	4.599.070
DHW	509.036
Total	5.108.106
	Annual savings [NOK]
Space heating	2.827.230
DHW	2.901.504
Total	**5.728.734**
Payback time [years]	**15.74**

The total investment is about 90 million NOK for 1300 apartments. A payback time of 16 years seems reasonable as such, but a payback time of 28 years for the Solar/BTES system is too much, as the economic lifetime of a solar system is assumed to be 20 to 25 years [16] meaning that new investments for solar collectors may be necessary after 25 years.

The installation of CO_2 heat pumps and storage tanks for DHW heating is recommended as a payback of 4 years seems reasonable although building-related costs, installation costs and costs for any adjustments of the heating system are not considered. These costs would increase the payback time, but due to limited information they are not included.

The NPVs and NPVQs have been calculated for each of the energy system and are presented in Figure 45 and Figure 46.

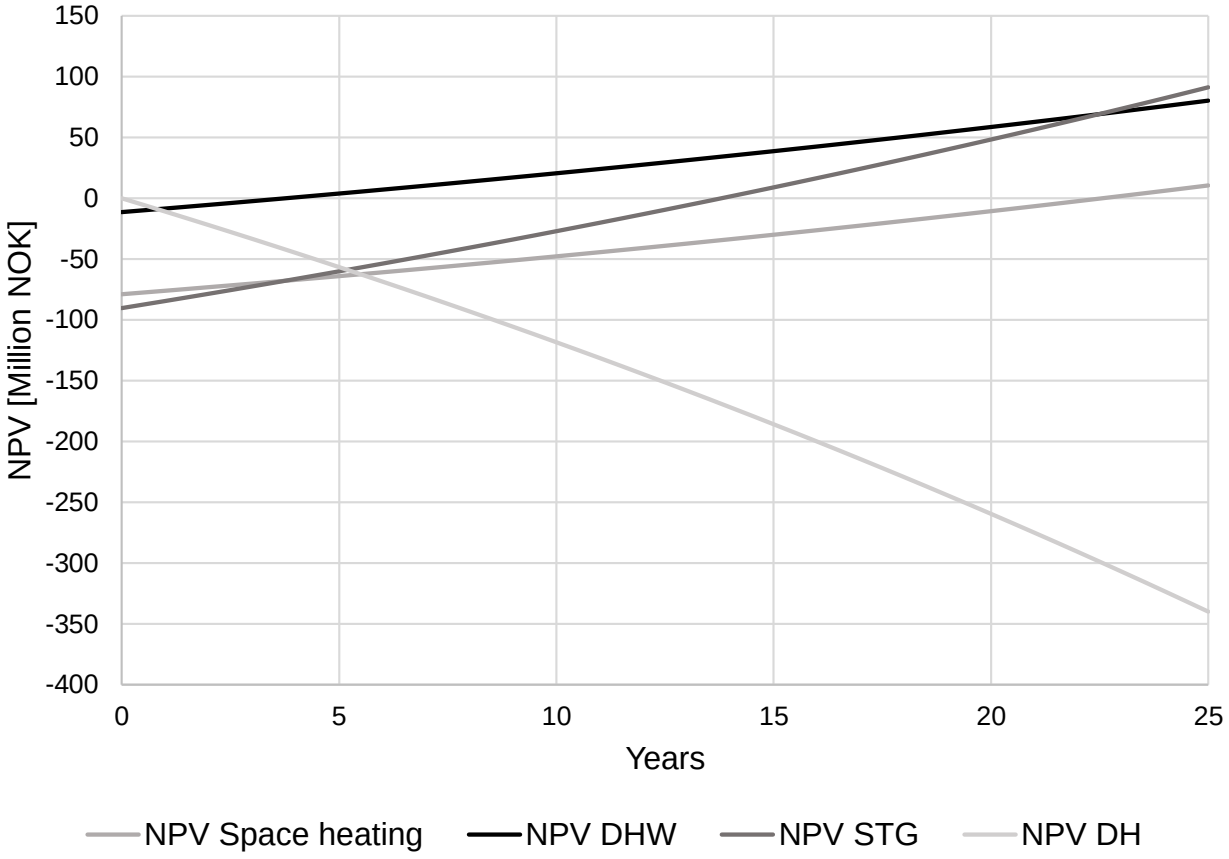

Figure 45 - NPV of the energy systems

As it can be seen from Figure 45, the NPV of the current system is the lowest for a system lifetime of 30 years. Although there are no initial investment costs, the NPV decreases each year since there are high annual expenses for DH.

Of the proposed new systems the one for DHW heating has the highest NPV for the first 25 years of operation; the energy system for space heating has a much lower NPV and the combination of both systems pays off after 25 years from a theoretical point-of-view, but since the lifetime of a solar system is estimated to be 25 years, the system is only feasible, if further measures are taken. The NPVs in year 25 are presented in Table 22.

Table 22 - NPV of the energy systems in year 25

	NPV in year 25 [Million NOK]
Space heating (Solar/BTES/DH)	10.71
DHW (CO_2 heat pump/storage tanks)	80.53
Combined system (STG)	91.24
Staying with DH	-339.84

As a conclusion from Figure 46, it can be said that it is reasonable to install a sustainable energy system because the NPVQs are positive after 25 years of operation. In year 25 it is 7.10 for the DHW heating system, 0.14 for the space heating system and 1.01 for the whole STG system.

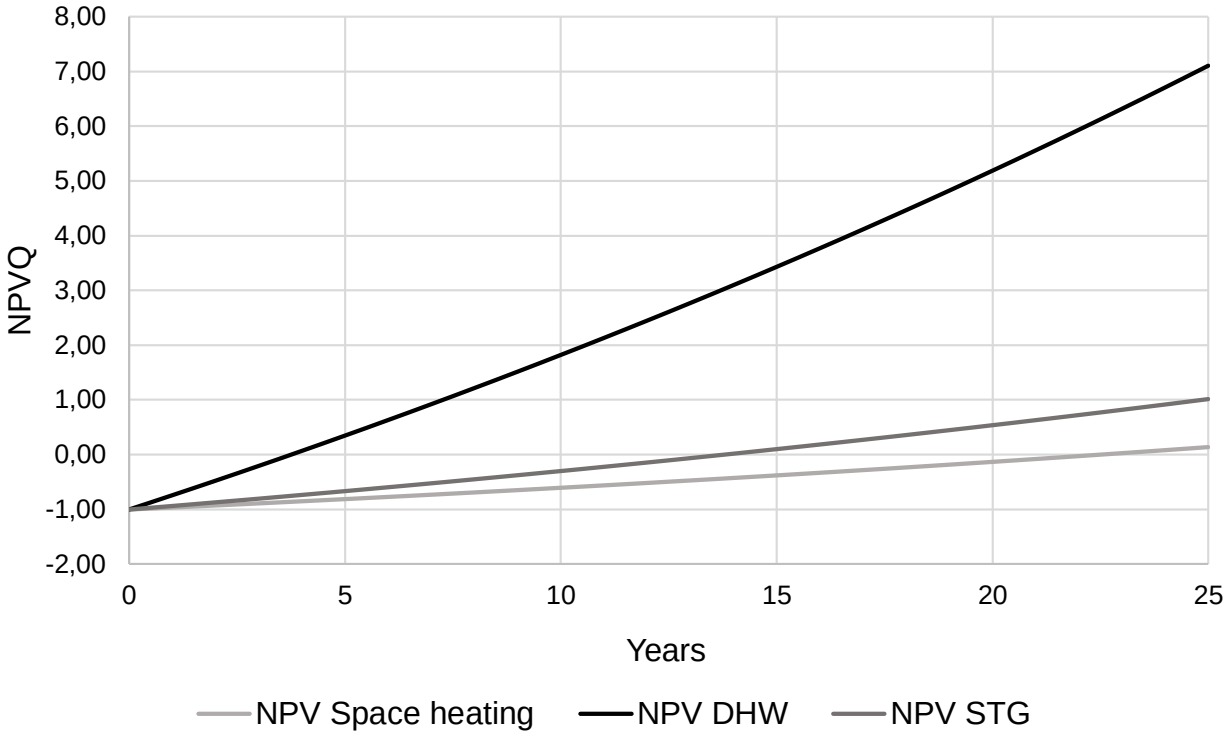

Figure 46 - NPVQ of the energy systems

8. Summary and discussion of the STG measures

This project investigated the feasibility of a local low-temperature heat distribution grid for Risvollan neighborhood. The grid is owned by the housing cooperative Risvollan Borettslag and is connected to about 1300 apartments in more than 150 houses where several houses constitute to a substation. Until now, the already existing local grid is directly coupled to the DH grid for space heating and DHW heating. Each substation is connected to the local grid via a heat exchanger where heat can be extracted whenever needed.

In order to reduce the energy use, the idea of a low-temperature grid primarily supported by renewable energy sources is investigated from an energetic as well as an economic point of view. There are several measures which were introduced and discussed and which can be seen as a first step towards a smart thermal grid. These measures include

- the integration of solar collectors
- a borehole thermal energy storage for seasonal heat storage
- the integration of a NH_3 – GSHP in connection with the BTES
- the installation of CO_2 heat pumps for DHW heating and
- the integration of DHW storage tanks.

An economic analysis of all proposed measures has been carried out based on the NPV and NPVQ. Initial costs, annual costs, annual savings as well as the payback time of the energy systems have been calculated.

<u>The smart thermal grid in Risvollan</u>

For the LTDG it is assumed that the supply temperature is about 45°C and the return temperature is around 15°C although these temperature might be different for summer and winter time. The water is heated by a ground source NH_3 heat pump. The CO_2 heat pumps for DHW heating are connected to the return line of the LTDG assuming a temperature of the return of about 35°C. The CO_2 heat pump extracts heat and thus the water leaves the heat exchanger of the CO_2 heat pump with a temperature of about 15°C. It then flows back to the energy center where it is heated up to 45°C by the GSHP. Solar thermal collectors are integrated in order to use solar energy for recovering the ground temperature of the BTES which is used to sustain a constant supply temperature the LTDG of 45°C. The proposed temperatures are based on literature data [66] and could be somewhat different in reality.

Current heating demand in Risvollan

All calculations are based on the total heat demand of RBL in year 2014. It is assumed that the heat demand is of the same range every year although it has to be mentioned that 2014 was a very warm year. From the data provided by RBL, a space heating demand of 105 $\frac{kWh}{m^2}$ and a DHW demand of 48 $\frac{kWh}{m^2}$ have been found. These heating demands are well in accordance with literature data which states that the average total heating demand of a apartment block is about 140 $\frac{kWh}{m^2}$ [67]. The heating demand share is 69% for space heating and 31% for DHW heating, respectively. The houses were renovated in the 1990s which is why TEK87 applies as the building standard.

The total peak heating load of all houses was modeled in SIMIEN because it was required for the simulations of the BTES in EED later on. The simulations were based on TEK87 which proposes standards for building insulation and heat losses of buildings. The simulation resulted in a peak heating load of 5185 kW which is the heating capacity that needs to be covered by the low-temperature distribution grid.

Energy system for space heating

The energy system for space heating combines a solar thermal system, BTES and DH. For solar collectors two scenarios were investigated; to either heat up DHW, or a more likely one, to recover the ground temperature of the BTES. Also, the possibility of auxiliary space heating from solar energy was introduced (Figure 39), but not investigated in detail. The calculations are based on solar data of Trondheim and on the solar collector L20AR from Wagner Solar chosen as an example collector assuming that collectors of the same type and size would lead to an equal solar gain. It is suggested to install solar collectors at the roof of each building. All buildings are flat-roofed. Results show that a number of 2663 collectors of type L20AR could be installed on top of the buildings leading to a total collector area of 6958 m^2 considering spacing effects, inclination angle of the collectors and solar altitude. The solar gain is about 4200 MWh when considering recovering the ground temperature of the BTES. On the other hand, the solar gain could cover the DHW demand of the neighborhood from May to September. In order to cover the whole energy demand which is required for recovering the ground temperature, about 1730 additional solar collectors would have to be installed. This is not feasible from an economic point-of-view which is why it is suggested to get the remaining energy for the GTR from DH. It should be investigated whether surplus heat from the supermarket in Risvollan Center can

be rejected to the ground. In that way less DH would be needed and thus costs as well as payback time could be reduced. On top of that, surplus heat from DH could be purchased at a lower cost during summer time and transferred to the ground.

The BTES was modeled in EED which calculates the mean fluid temperature of the brine and thus gives an idea of the ground temperature. The goal of the simulations is a constant fluid temperature over several years of operation. Different parameters, such as borehole spacing, base heating and cooling loads of the ground or the heat carrier fluids were examined and optimized. A BTES with 300 boreholes of 280 m depth is chosen. It is found that a heating load of 6000 MWh can be covered by recovering the ground with a solar gain of 4000 MWh. This corresponds to about half of the current space heating demand of RBL. In order to cover the total space heating demand of 10600 MWh, a solar gain of 7050 MWh is required, if only solar energy is assumed to be used for the ground temperature recovery. Both scenarios lead to a stable fluid temperature and thus ground temperature. The minimum fluid temperature of a year is around -1°C whereas the maximum temperature is 11°C. Both temperatures are well within an acceptable temperature difference of 11K or 17K from the undisturbed ground temperature of 4.7°C (from EED database) for base load operation or peak load operation, respectively. Other ideas for recovering the ground temperature are the application of a heat exchanger in the sewage water of the buildings as well as using surplus heat of the local supermarket. In both ways, low-temperature heat which is already available can lead to a more efficient energy system.

An ammonia GSHP was modeled in CoolPack/EES. This heat pump is used for space heating purposes and therefore supposed to heat up the water of the LTDG from about 15°C to 45°C. 45°C is a sufficient supply temperature for space heating and 15°C is a reasonable return temperature of the distribution grid after extraction of heat for space heating and DHW heat pumps. It is found that the SPF of the GSHP is 4.34, if a condensation temperature of 48°C and an evaporation temperature of 2°C is used. Heat pumps are usually designed to cover 60% of the peak load and therefore, the heating capacity is assumed to be 3111 kW. DH can be used as a back-up for covering peak heating loads.

The initial investment costs for the energy system used for space heating add up to 79 million NOK and the payback time is 28 years. After 25 years of operation, it has a NPV of

around 11 million NOK and a NPVQ of 0.14. The costs do not include investments for any extra pipe systems, pumps, refrigerants for the GSHP or costs for the absorber fluid of the solar collectors.

Energy system for DHW heating

The energy system for DHW heating consists of CO_2 heat pumps and water storage tanks with a capacity of 1000 l. CO_2 heat pumps use the return line of the LTDG as a heat source and are designed to heat up water from 22°C to 70°C. The incoming city water at 8°C is preheated to 22°C using the return flow from the CO_2 heat pumps. It is assumed that it cools the water of the LTDG from about 35°C to 15°C. The CO_2 cycle is modeled in CoolPack/EES. The evaporation temperature is set to around 20°C (57 bar), the gas cooling pressure to 115 bar (78.7°C) and the gas cooler outlet temperature of the CO_2 is 25°C. A pressure of 115 bar is required in order to keep a temperature difference to the water which is heated up. The COP of the system was 5.7. It is assumed that there is one heat pump at each substation which is sized depending on the heating demands of the substation in question. It is found that the heat pumps need to have capacities between 15 kW and 40 kW in order to cover the DHW demand of the different substations.

So far, there are no storage tanks installed in the houses, but this is necessary, if heat pumps will be integrated for DHW heating. Storage tanks with a volume of 1000 liters are common [23] [56] which is why this volume is used for calculating the number of storage tanks which need to be installed. The DHW demand [Liter] is calculated for each substation based on the average DHW demand per person per day (40 liter [57]), the number of apartments per substation and a number four persons living in one apartment. Results show that a total number of 196 storage tanks needs to be installed in Risvollan assuming that the tanks are recharged once per day. It has to be mentioned that 196 storage tanks is the maximum number of vessels, whereas the real number of installed storage tanks should be less assuming, for instance, that people take showers at different times and thus there is time for recharging the storage tanks again.

The initial investment for the DHW heating system is estimated to 11.5 million NOK and the payback time is 4 years assuming that 100 storage tanks with a capacity of 1000 l are installed. After 25 years of operation, the NPV is around 80 million NOK and the NPVQ is 7.10.

Sensitivity analysis

A sensitivity analysis has been carried out in order to evaluate how the payback time of the STG energy system is influenced by several input parameters, such as

- Number of solar collectors +20%
- Efficiency of the solar collectors ±3%
- Initial investment costs ±10%
- Annual costs savings of the STG measures ±10%
- Annual space heating demand ±20%

If 20% more solar collectors are installed, the initial investment costs increase, but on the other hand the solar gain and thus the annual energy savings increase. A modification of the initial investment costs by ±10% can come from installations of additional equipment as well as from the uncertainty of the exact costs of the investigated energy system. The annual savings highly depend on the space heating demand and the solar gain from the solar collectors, where the space heating demand depends on the outdoor temperatures throughout a year (cold or hot year). Therefore, the energy demand for space heating is modeled as well. If the heating demand is high, but the solar gain is low, more DH needs to be used in order to recover the ground temperature and thus the annual cost savings may be decreased. Figure 47 shows the results of the sensitivity analysis.

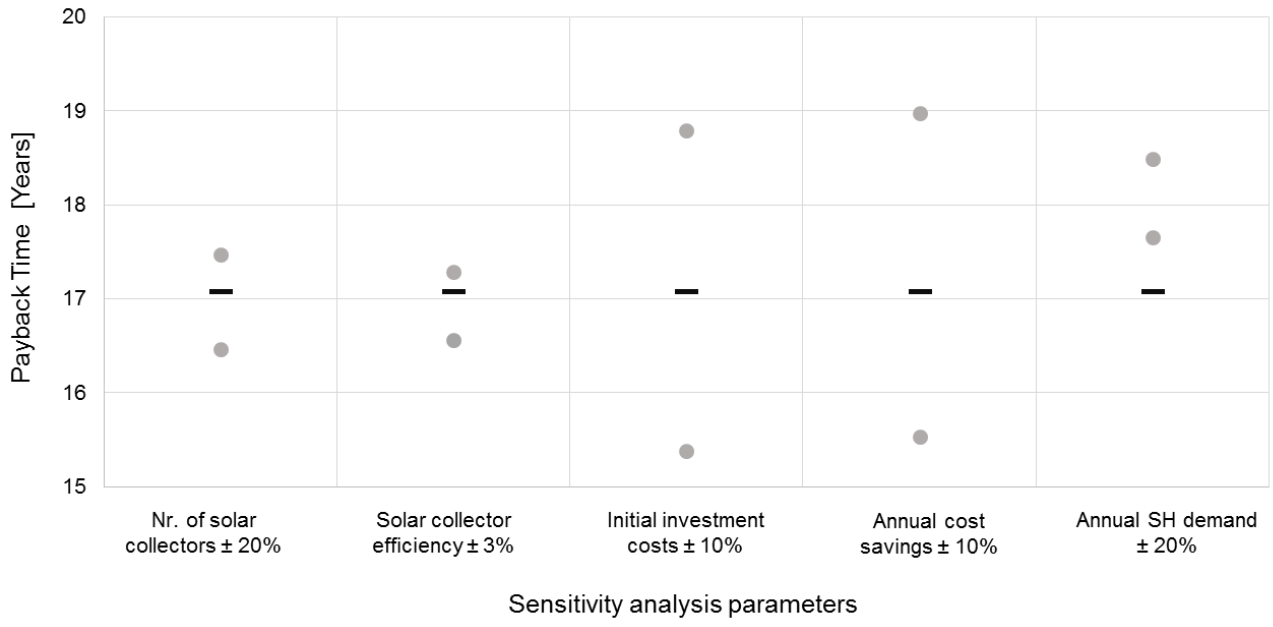

Figure 47 - Sensitivity analysis based on payback time of the energy system

The payback time for the whole energy system decreases by 4%, if 20% (553 collectors) more solar collectors are installed in Risvollan and increases by 3%, if 553 fewer collectors are installed. This is due to increased/decreased initial costs as well as an increased or decreased solar gain which can be used for ground temperature recovery. If more solar collectors are integrated, more solar energy can be absorbed and then be transferred to the ground. If fewer collectors are used, less solar energy is gained and thus more DH needs to be used for the GTR.

The payback time decreases by 3%, if the solar collector efficiency is increased by 3%. It increases by 1%, if the collector efficiency decreases by 3%.

Changing the initial investment costs as well as annual cost savings by ± 10%, the payback time changes by ± 10% accordingly.

When it comes to changes in the annual space heating demand, the payback time increases by 8%, if the demand increases by 20%. It increases by 3% in case of a 20% decrement of the space heating demand because the effect of the renewable energy system on annual savings decreases accordingly.

9. Conclusion

This feasibility study investigated different measures for upgrading a local heat distribution network of an existing building complex to a STG. The proposed measures considered a combination of a solar thermal system and a borehole geothermal energy storage for space heating as well as an application of heat pumps for DHW production.

It is found that it is not feasible to invest in the proposed energy system for space heating because the payback time (28 years) of the system is longer than the lifetime of the solar thermal system. Furthermore, the solar gain from the solar collectors is not sufficient for recovering the ground temperature of the BTES with solar energy only which is why DH would be needed for supplying the rest of the energy needed to recover the ground temperature.

Results show that an integration of CO_2 heat pumps and water storage tanks for DHW production is very promising as the payback time for the investigated system is only 4 years which is why this idea should be investigated further.

Financial support for the upgrade would be provided by ENOVA. They are supporting the integration of solar thermal systems [68] and heat pumps for DHW production [69].

10. Further work

Suggestions for further work are based on the results and conclusions and include:

- For the whole STG in Risvollan:
  - Modeling the proposed energy system with a software, for instance in IDA ICE or Wanda 4 heat. Wanda 4 heat is a dynamic pipeline simulation tool and can be applied for simulating the low-temperature distribution grid [70].
  - Designing a control system of the whole energy system, for instance in LEA. LEA (Low-Energy Architecture) can be used to calculate the energy demand of the buildings in order to see whether/how buildings can cope with low-grade heat.
  - Performing an advanced life cycle cost analysis or a life cycle analysis in order to cope with the environmental impact of the proposed measures
  - Investigating the total financial support from the incentive program of ENOVA

- For the space heating energy system:
  - Considering occupant behavior when it comes to calculating the energy consumption in buildings so that a more justified statement on the future energy consumption can be made.
  - Numerical simulations on the BTES because such a big geothermal storage may have an impact on the ground that cannot be modeled by EED. For instance, SPRING is a software tool which can be used to simulate a borehole thermal energy storage based on finite-element method.
  - Looking into different borehole drilling techniques, such as using vibration instead of drilling with hard cases around the pipe which is to be installed into the clay.
  - Investigating the possibility of taking heat from sewage water for space heating. This can result in energy savings and might make the proposed space heating system more feasible. It should be looked into the possibility of connecting the space heating with the DHW system via heat exchangers.
  - Using surplus heat from the local supermarket for ground temperature recovery

- For the DHW heating energy system:
  - Investigating whether a propane heat pump is more feasible than the proposed CO_2 heat pump, from an energetic as well as an economic point of view.
  - Calculating a reasonable number of water storage tanks based on the current water consumption in Risvollan

Bibliography

[1] Trondheim Kommune, "Trondheim SmartCity Energy Efficiency," Trondheim, 2007.

[2] Schmidt, "Key to Innovation Integrated Solution - Smart Thermal Grids," European Commission, 2013.

[3] H. L. David Connolly, "Smart Energy Systems," 2013. [Online]. Available: http://vbn.aau.dk/files/78422810/Smart_Energy_Systems_Aalborg_University.pdf. [Accessed 03 05 2015].

[4] SINTEF, "Analysis of Concerta energy concepts and guidelines for a whole building approach," Trondheim, 2007.

[5] R.-R. Schmidt, Writer, *The role of thermal grids in the smart city.* [Performance]. Austrian Institute of Technology, 2014.

[6] v. Vliet, "Flexibility in heat demand at the TU Delft campus smart thermal grid with phase change materials," TU Delft, Delft, 2013.

[7] Reyes Lastiri, "Design of Heating System with Geothermal Energy and CO2 capture," TU Delft, Delft, 2013.

[8] CONCERTO, "District heating and cooling networks," 2013.

[9] Fossum, "District heating in Statkraft," Trondheim, 2012.

[10] Statkraft, "http://www.statkraftvarme.no/Omstatkraftvarme/Vare-anlegg/," [Online]. Available: http://www.statkraftvarme.no/Omstatkraftvarme/Vare-anlegg/. [Accessed 01 04 2015].

[11] Statkraft, "Growth in pure energy," Trondheim, 2014.

[12] Å. Utne, Interviewee, *Discussion about DH in Trondheim.* [Interview]. 25 03 2015.

[13] L. Aichmayer, "Solar Power Technologies Low Temperature Solar Thermal Power," Stockholm, 2013.

[14] BoschClimate, "bosch-climate.cn," Bosch, [Online]. Available: http://www.bosch-climate.cn/web/product/product_detail.jsp?navId=229. [Accessed 23 06 2015].

[15] Apricus, "apricus.com," [Online]. Available: http://www.apricus.com/flat-plate-solar-collectors-3/#.VYp3rfntmkY. [Accessed 23 06 2015].

[16] L. H. Qvistgaard, "Energy-economic optimization of heating system with solar

collectors," NTNU, Trondheim, 2014.

[17] H. Havtun, Sustainable Energy Utilisation, Stockholm: KTH Energy Technology, 2013.

[18] J. Stene, "Heat sources for heat pumps," NTNU, Trondheim, 2015.

[19] J. Stene, "Design and application of ammonia heat pump systems for heating and cooling of non-residential buildings," Copenhagen, 2008.

[20] M. Cardin, "Goodway," [Online]. Available: http://www.goodway.com/hvac-blog/2009/08/ammonia-as-a-refrigerant-pros-and-cons/. [Accessed 09 07 2015].

[21] The Engineering ToolBox, "The Engineering ToolBox," [Online]. Available: http://www.engineeringtoolbox.com/fluids-evaporation-latent-heat-d_147.html. [Accessed 09 07 2015].

[22] P. Nekså, "CO2-heat pump water heater: characteristics, system design and experimental results," ELSEVIER, 1998.

[23] J. Stene, "Residential CO2 heat pump system for combined space heating and hot water heating," ELSEVIER International Journal of refrigeration, 2005.

[24] J. Heier, "Energy Efficiency through Thermal Energy Storage - Possibilities for the Swedish Building Stock," KTH School of Industrial Engineering and Management, Stockholm, 2013.

[25] Compedu, "CompEdu," KTH, [Online]. Available: http://www.energy.kth.se/compedu/webcompedu/WebHelp/index.html. [Accessed 09 04 2015].

[26] A. Vadiee, "Compedu," KTH, ITM, EGI, HPT, [Online]. Available: http://www.energy.kth.se/compedu/webcompedu/WebHelp/index.html. [Accessed 08 04 2015].

[27] GeoForschungsZentrum, "forschung-energiespeicher.info," [Online]. Available: http://forschung-energiespeicher.info/en/project-showcase/versorgungsnetze/projekt-einzelansicht//Saisonale_Waermespeicherung_in_Aquiferen/. [Accessed 10 04 2015].

[28] Paksoy, "State-of-the-art Review of Aquifer Thermal Energy Storage Systems for Heating and Cooling Buildings," Stockholm, 2009.

[29] Kjellson, "Solar Collectors Combined with Ground-Source Heat Pumps in Dwellings," Lund University, Lund, 2009.

[30] Drake Landing, "Drake Landing Solar Community," [Online]. Available:

http://www.dlsc.ca/borehole.htm. [Accessed 09 04 2015].

[31] V. Trillat-Berdal, "Coupling of geothermal heat pumps with thermal solar collectors," ELSEVIER Applied Thermal Engineering, 2006.

[32] Heier, "Evaluation of a high temperature solar thermal seasonal borehole storage," Stockholm, 2011.

[33] H. Wang, "A case study of underground thermal storage in a solar-ground coupled heat pump system for residential buildings," ELSEVIER Renewable Energy, 2009.

[34] L. Gao, "A review on borehole seasonal solar thermal energy storage," ELSEVIER Energy Procedia, 2015.

[35] Drake Landing, "http://www.dlsc.ca/," [Online]. Available: http://www.dlsc.ca/images/contentphotos/Simple-District-loop.gif. [Accessed 10 04 2015].

[36] D. Mangold, "Seasonal storage - a German success story," Freiburg, 2007.

[37] S. Forrester, "Geothermal (GSHP) and solar thermal hybrid system," DMA Engineering, Colorado.

[38] SODA, "soda-is," [Online]. Available: http://www.soda-is.com/eng/index.html. [Accessed 17 04 2015].

[39] Bureau of Meteorology, "bom.gov.au," [Online]. Available: http://www.bom.gov.au/climate/austmaps/solar-radiation-glossary.shtml. [Accessed 09 07 2015].

[40] Trondheim Kommune, "Rapport fra Geoteknisk avdeling Risvollan," Trondheim, 2013.

[41] Norges geologiske undersøkelse, "Geo NGU," [Online]. Available: http://geo.ngu.no/kart/arealis/?Box=271180:7037328:272574:7037996. [Accessed 21 05 2015].

[42] M. Thyholt, "Energy Analysis of the Norwegian Dwelling Stock," IEA SHC, 2009.

[43] J. Stene, "Dimensioning of Heat Pumps for Heating and Cooling," Trondheim, 2015.

[44] E. Communities, "European Commission PVGIS," 2007. [Online]. Available: http://re.jrc.ec.europa.eu/pvgis/apps/pvreg.php?lang=en&map=europe. [Accessed 21 04 2015].

[45] L. Finocchiaro, "Trondheim - Climate analysis," Trondheim.

[46] Free Hot Water, "freehotwater.com," [Online]. Available:

https://www.freehotwater.com/solar-calculators/commercial-collector-spacing-calculator/. [Accessed 15 04 2015].

[47] D. Trier, "Solar disstrict heating guidelines," PlanEnergi, 2012.

[48] Wagner Solar, "wagner-solar.com," [Online]. Available: http://www.wagner-solar.com/en/heat/products/solar-collectors/euro-l20-ar.html. [Accessed 16 04 2015].

[49] C. Lampe, "Report of Performance Test according to EN 12975-2 for a Glazed Solar Collector," ISHF, Bangor, 2006.

[50] Climate-Data, "climate-data.org," [Online]. Available: http://de.climate-data.org/location/707/. [Accessed 17 04 2015].

[51] J. V. Orlikowski, "Vergleich der Berechnungsmethoden zur Auslegung eines geothermisch genutzten Erdwäremesondenfeldes zwischen EED und SPRING," Hochschule Ostwestfalen-Lippe, 2012.

[52] S. P. E. Schuhmacher, "Smart and Cost efficient Energy Interactions in Building Complexes," NTNU, Trondheim, 2015.

[53] Å. Utne, Interviewee, [Interview]. 28 05 2015.

[54] De Kleijn Energy Consulting b.v., "Industrial Heat Pumps R717 (Ammonia)," De Kleijn Energy Consulting b.v..

[55] J. Stene, "Heat Pump Plants for Heating and Cooling of Large Buildings, Lecture 8," NTNU, Trondheim, 2015.

[56] SWECO, "Risvollan Borettslag," Trondheim, 2011.

[57] Sustainable Energy Authority of Ireland, "Domestic solar systems for hot water: A Consumer Guide," seai.

[58] Investopedia, "INVESTOPEDIA," [Online]. Available: http://www.investopedia.com/terms/n/npv.asp. [Accessed 27 06 2015].

[59] H. M. Mathisen, "Economic Analysis for Energy Efficiency Projects," NTNU, Trondheim, 2014.

[60] REA, "Renewable Energy Advisers," [Online]. Available: http://www.renewable-energy-advisors.com/learn-more-2/levelized-cost-of-electricity/. [Accessed 27 06 2015].

[61] Norges Bank, "www.norges-bank.no," [Online]. Available: http://www.norges-bank.no/en/Statistics/Interest-rates/. [Accessed 07 07 2015].

[62] BINE, "Large-scale solar thermal systems for buildings," 2008.

[63] Energy Saving Trust, "Domestic Ground Source Heat Pumps: Design and installation of closed-loop systems - A guide for specifiers, their advisors and potential users," 2007.

[64] Wagner Solar, "Preisliste 03/2014 Solarwärme und Heiztechnik," 2014.

[65] S. Jenssen, "Email from 9th of July," Trondheim, 2015.

[66] S. Mohammadi, "Conversion of existing district heating grids to low-temperature operation and extension to new areas of buildings," Aalborg University, Aalborg, 2013.

[67] R. Siller, "EffCoBuild Total Energy Demand Country Report - Thalgau, Austria," 2006.

[68] ENOVA, "enova.no," [Online]. Available: http://www.enova.no/finansiering/privat/enovatilskuddet-/solfanger/911/0/. [Accessed 20 07 2015].

[69] ENOVA, "enova.no," [Online]. Available: http://www.enova.no/finansiering/privat/enovatilskuddet-/vannbaren-varme-/1033/0/. [Accessed 20 07 2015].

[70] Deltares, "Smart thermal grids," Deltares, 2013.

Appendix A – Maps of the Risvollan area

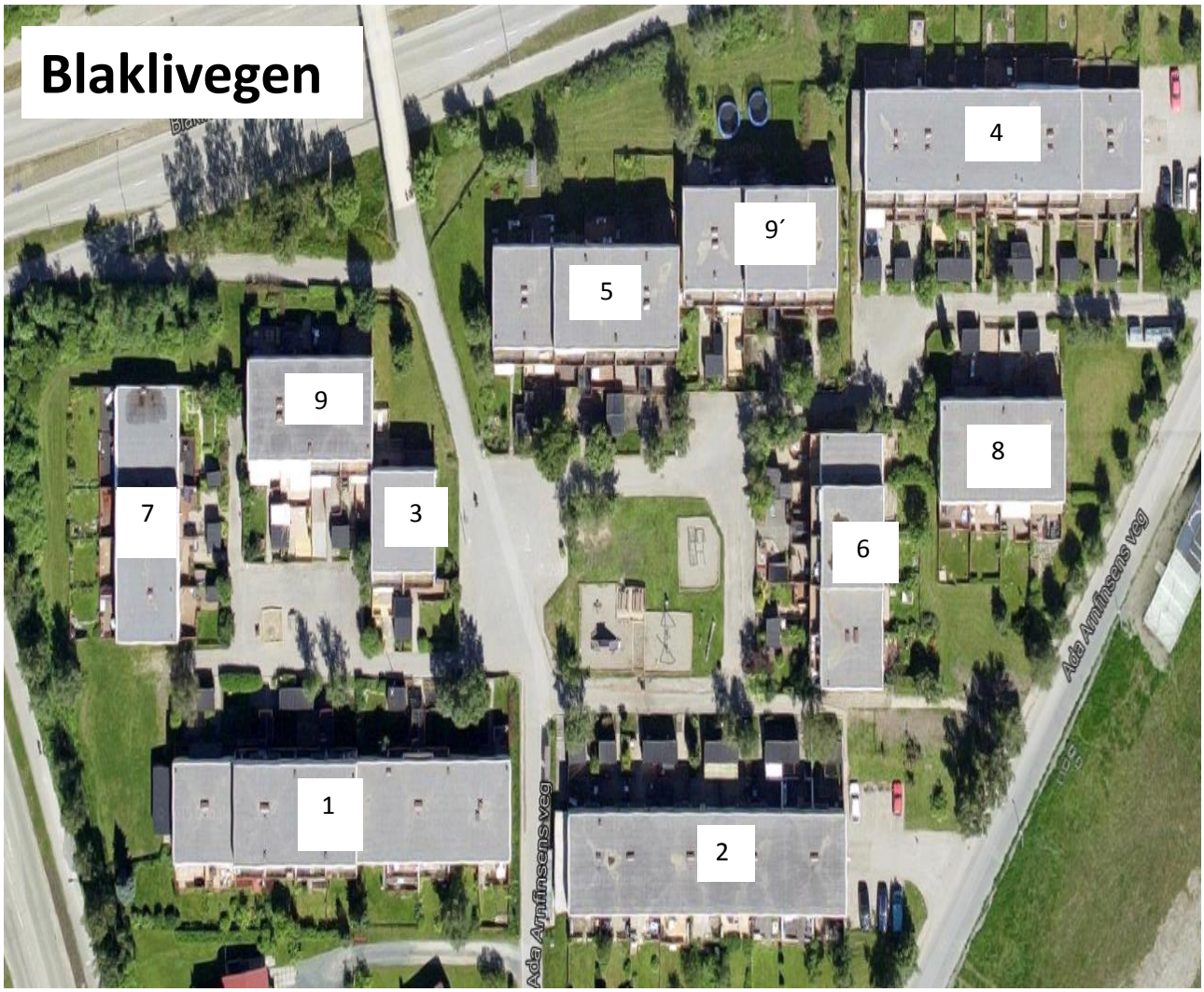

Figure A 1 - Blaklivegen

Figure A 2 - Marie Sørdals veg

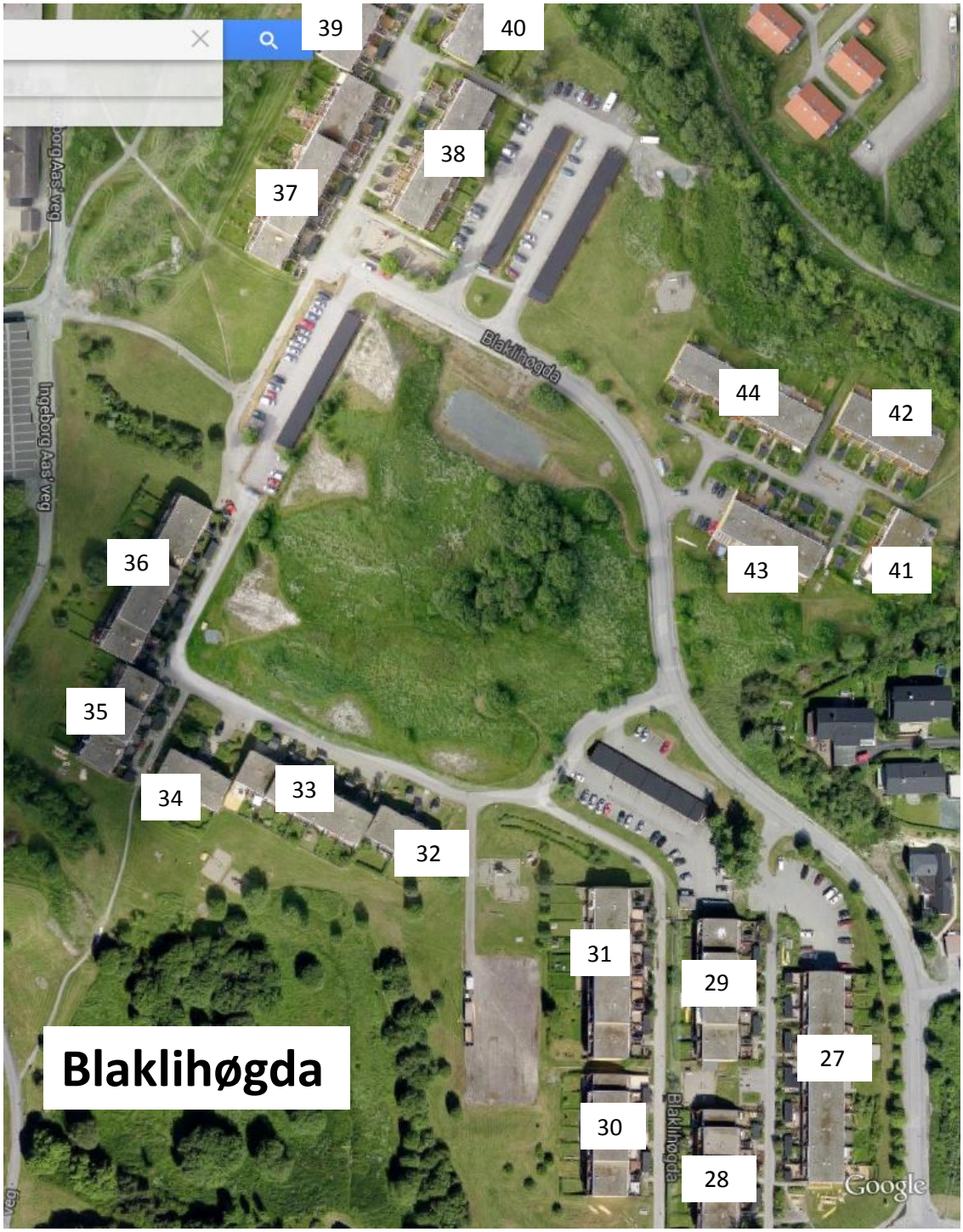

Figure A 3 - Blaklihøgda

Figure A 4 - Utleirtunet

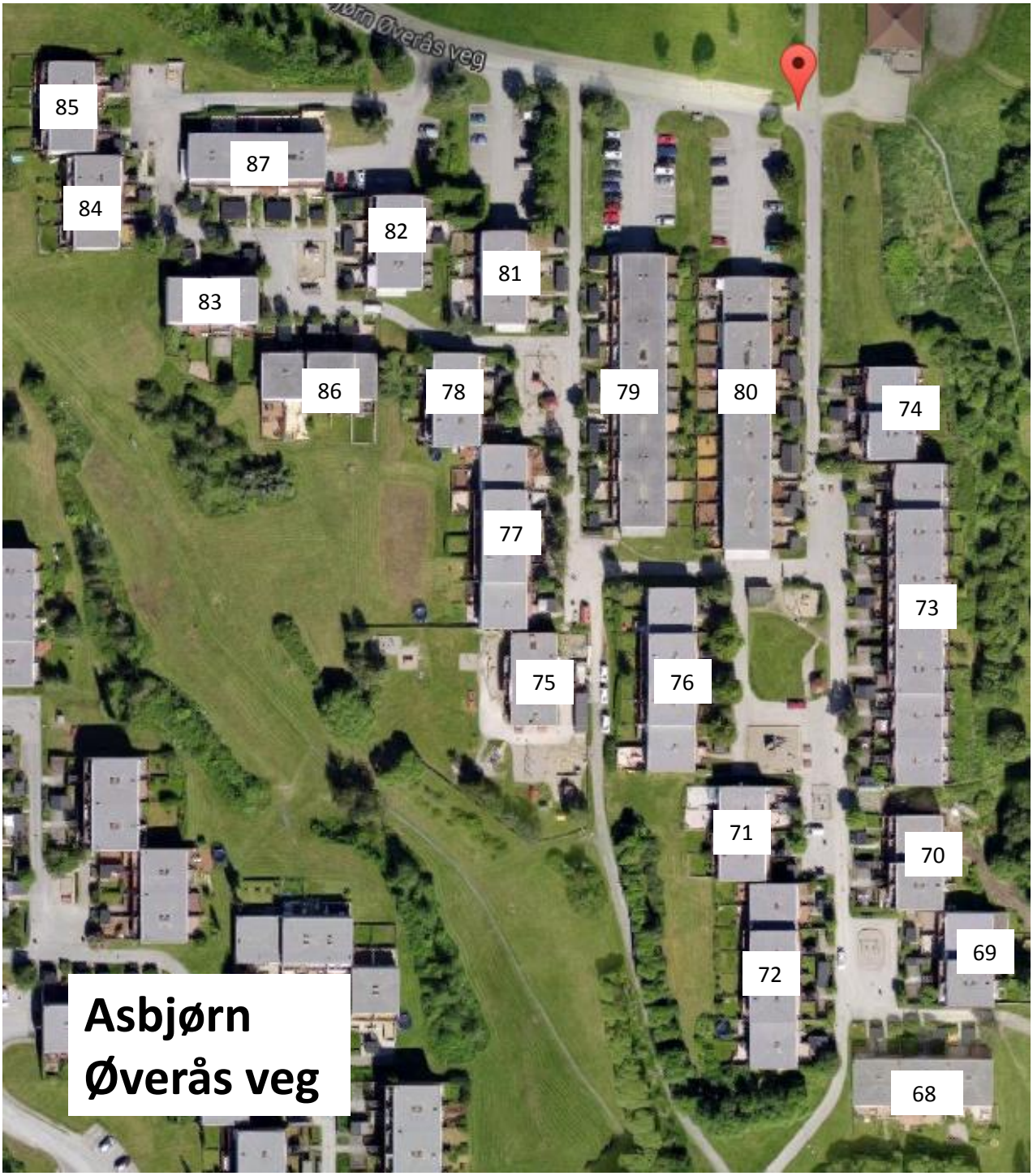

Figure A 5 - Asbjørn Øverås veg

Figure A 6 - Risvollvegen

Figure A 7 - Søndre Risvolltun

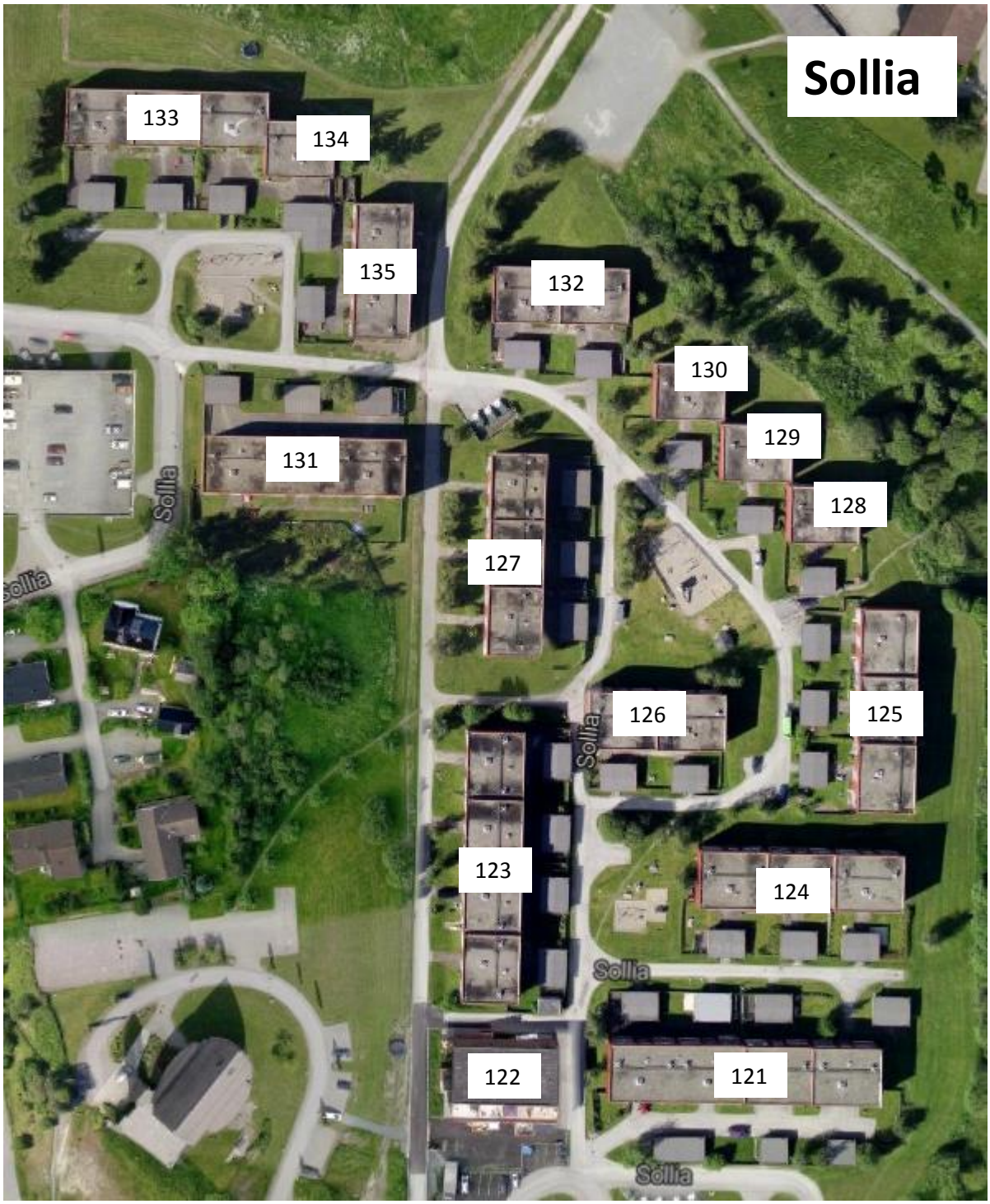

Figure A 8 - Sollia

Figure A 9 - Risvollan Center

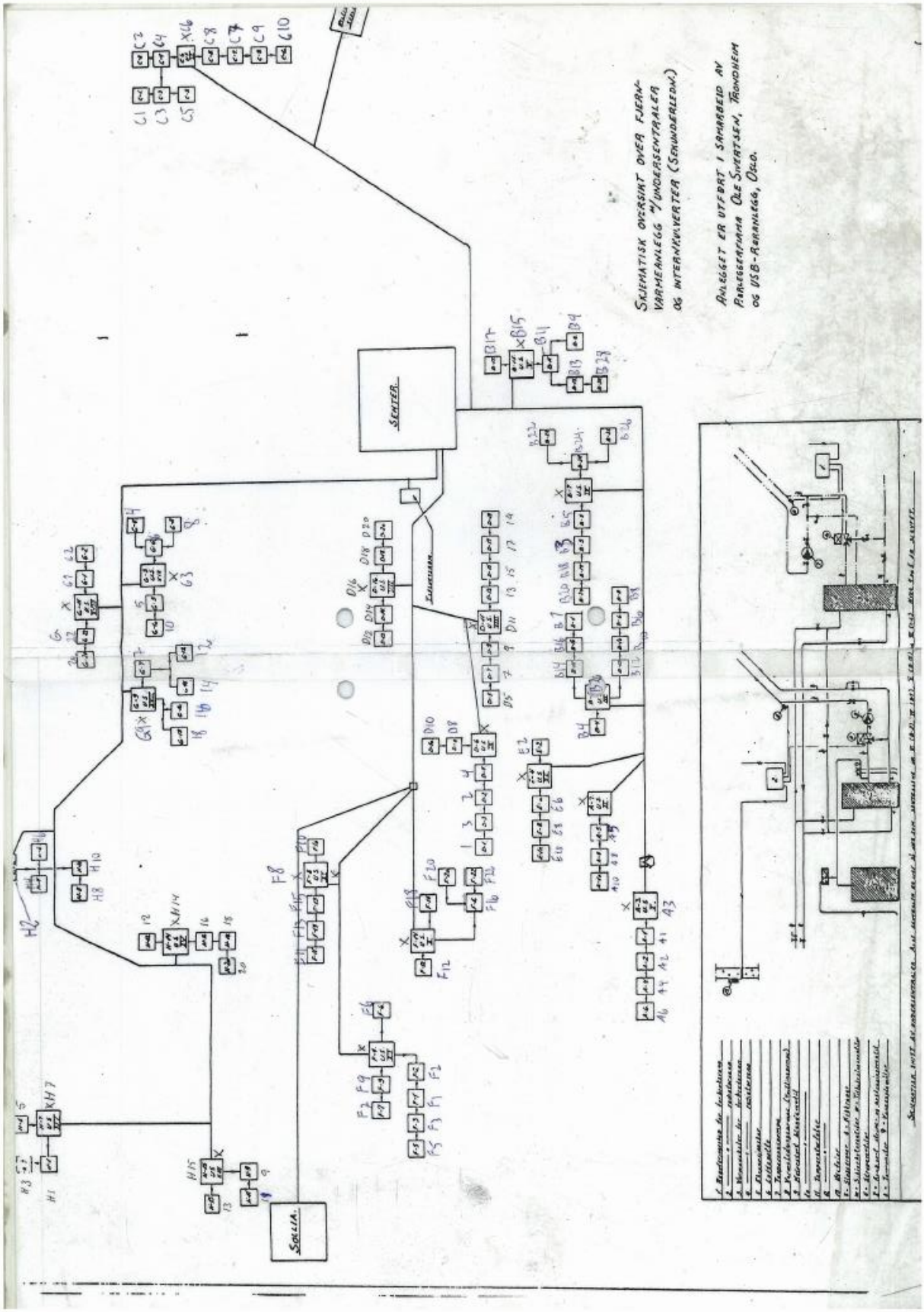

Figure A 10 – Original sketch of the distribution grid in Risvollan

Appendix B – BTES calculation specifications

Overview over sensible heat storage systems:

Table B 1 - Thermal and technical data for sensible TES systems *[25]*

	Concrete or steel tank	Basin with total insulation	Basin with top insulation	Rock cavern	Aquifer	Earth bed	Vertical tubes in clay	Drilled wells
Specific thermal capacity [Wh/m^{3}K]	1.16	1.16	1.16	1.16	0.75	0.70	0.89	0.63
Storage efficiency [-]	0.90	0.85	0.70	0.80	0.75	0.60	0.70	0.70
Conversion factor [kW/m^3]	57	54	45	51	31	23	8	24
Size range [m^3]	0-100000	0-75000	0-50000	50000-300000	50000-500000	0-100000	50000-300000	50000-400000

Test results of the simulations in EED investigating the mean HCF temperature as a function of several parameters:

set values:	Base load:	Heat	7000 MWh		HCF:	MPG 25%	
		Cool	3750 MWh		Configuration:	686 (338 bh)	
	SPF:	Heat	3,5				
		Cool	3				
		Constant mean fluid temperature [°C]					
		Peak (min)	Peak (max)	ΔT [K]	Base (min)	Base (max)	ΔT [K]
BH spacing [m]	6	-1	8	9	3	8	5
	7	-0,7	7,9	8,6	3,1	7,9	4,8
	8	-0,6	7,9	8,5	3,2	7,9	4,7
	9	-0,5	8	8,5	3,2	8	4,8

set values:	Base load:	Heat	7000 MWh		BH spacing:	7m	
		Cool	3750 MWh		Configuration:	686 (338 bh)	
	SPF:	Heat	3,5				
		Cool	3				
		Constant mean fluid temperature [°C]					
		Peak (min)	Peak (max)	ΔT [K]	Base (min)	Base (max)	ΔT [K]
HCF	Potassium carbonite	-0,7	7,9	8,6	3,1	7,9	4,8
	MEG 25%	-0,7	7,9	8,6	3,1	7,9	4,8
	MPG 25%	-0,7	7,9	8,6	3,1	7,9	4,8
	Ethanol 25%	-0,7	8	8,7	3,1	8	4,9
set values:	Base load:	Heat	7000 MWh		BH spacing:	7m	
	HCF	MPG 25%			Configuration:	686 (338 bh)	
	SPF:	Heat	3,5				
		Cool	3				
		Constant mean fluid temperature [°C]					
		Peak (min)	Peak (max)	ΔT [K]	Base (min)	Base (max)	ΔT [K]
Cooling Load (solar gain) [MWh]	3750	-0,7	7,9	8,6	3,1	7,9	4,8
	4000	not stable after 25 years					
	4250	not stable after 25 years					
	4500	not stable after 25 years					
set values:	Base load:	Heat	8150 MWh		BH spacing:	7m	
		Cool	4000 MWh		Configuration:	751 (576 bh)	
	HCF	MPG 25%					
	SPF:	Heat	3				
		Cool	3				
		Constant mean fluid temperature [°C]					
		Peak (min)	Peak (max)	ΔT [K]	Base (min)	Base (max)	ΔT [K]
HCF flow rate [l/s]	0,5	0,5	7,5	7	3,5	7,5	4
	1	1,8	6,9	5,1	3,9	6,9	3
	2	1,9	6,9	5	3,9	6,9	3
	3	2	6,8	4,8	4	6,8	2,8

Change heating and cooling load:			have biggest impact on the temperatures in the ground						
set values:	HCF	MPG 25%			BH spacing:	7m			
	SPF:	Heat	3,5		Configuration:	686 (338 bh)			
		Cool	3						
		Constant mean fluid temperature [°C]							
Heating Load [MWh]	**Cooling Load [MWh]**	Peak (min)	Peak (max)	ΔT [K]	Base (min)	Base (max)	ΔT [K]		
7100	3750	-0,9	7,6	8,5	3	7,6	4,6		
7600	4000	-1	7,7	8,7	2,9	7,7	4,8	this is 50% of the current heating	
8100	4250	-1,1	7,9	9	2,6	7,9	5,3		
10600	5200	1,6	7,2	5,6	3,4	7,2	3,8	if surplus DH is used to recover th	
set values:	Base load:	Heat	7600 MWh		BH spacing:	7m			
		Cool	4000 MWh		HCF:	MPG 25%			
	SPF:	Heat	3,5						
		Cool	3						
		Constant mean fluid temperature [°C]							
		Peak (min)	Peak (max)	ΔT [K]	Base (min)	Base (max)	ΔT [K]		
BH conf.	686 (338bh)	-1	7,7	8,7	2,9	7,7	4,8		
	720 (405 bh)	0,3	7,4	7,1	3,2	7,4	4,2		
	755 (784 bh)	2,75	6,5	3,75	4,4	6,5	2,1		
	751 (576 bh)	1,8	6,7	4,9	3,9	6,9	3		
set values:	Base load:	Cool	4000 MWh		BH spacing:	7m			
					HCF:	MPG 25%			
					BHConf:	751 with 576 bh			
		Constant mean fluid temperature [°C]							
SPF Heat	**SPF Cool**	Peak (min)	Peak (max)	ΔT [K]	Base (min)	Base (max)	ΔT [K]		
3,5	3	1,75	6,7	4,95	2,9	7,7	4,8	with heating 7600MWh	
2,5	2,5	2,2	6,9	4,7	3,9	6,9	3	with heating 9500MWh	
3	3	1,9	6,9	5	3,9	6,9	3	with heating 8150MWh	
4	3	1,6	6,9	5,3	4	6,9	2,9	with heating 7200MWh	
5	3,5	1,4	6,7	5,3	3,9	6,7	2,8	with heating 6600MWh	
5	2,5	1,4	6,9	5,5	3,9	6,9	3	with heating 7100MWh	

Appendix C – Economic analysis calculations

The economic analysis calculations are done in EXCEL and will be presented here. The cells shaded in yellow are the values which are varied in the sensitivity analysis.

Discount rate:

e	0,022			
i	0,0207			
r_n	0,025	$r = \frac{1}{1+e} * \left[\frac{r_n * (1-s) - i}{1+i} - e\right]$		
s	0			
r	**-0,0174**			

Solar thermal system:

Solar						
Total collector area in RBL			6958	m^2		
Annual solar gain			4200000	kWh		
> assuming these number for collectors from any provider						
Collector Wagner Solar L20AR						
Size	2,61	m^2				
Price	1141,308	€	10200	NOK	incl taxes	
	438,96	€/m^2	3209	NOK/m^2		
Nr of coll.	2663			4390	(for 7050 MWh solar gain)	
Total price	**27162600**	**NOK**		44778000	NOK	
Price for erection per collecto		213,98	Euro			
		1870	NOK			
Total price erection		**4979810**	**NOK**	8209300	NOK	
TOTAL	**32142410**	**NOK**	**Initial investment**	52987300	NOK	without taxes
O&M costs	321424,1	NOK		529873	NOK	
Ground temperature recovery						
7050	MWh needed for recovering		10600	MWh	(other nr are 8950 and 5950)	
4200	MWH from solar					
2850	MWh from DH		Costs for DH	1995000	NOK for DH for GTR	

$$Total\ price = (10200\ NOK + 1870\ NOK) * 2663\ collectors = 32.142.410\ NOK$$

BTES:

BTES							
Clay depth	51	m					
Bedrock depth	229	m					
Drilling cost clay	1000	NOK/m					
Drilling cost bedrock	250	NOK/m					
Nr. of boreholes	300						
Drilling cost per borehole		108250	NOK				
Total dr. Costs	**32475000**	**NOK**					
COP	4,34						
Space heating							
Energy				**Costs**			
Total SH demand	10609000	kWh		Total energy costs DH only	7426300	NOK	
90% from BTES	9548100	kWh		BTES	6683670	NOK	Savings on DH only
10% from DH	1060900	kWh		DH	742630	NOK	Annual Costs
				Costs for DH GTR	1995000	NOK for DH for GTR	
Ecomp	2200023	kWh		Compressor	1540016	NOK	Annual Costs
Annual energy savings	7348077	kWh		Total annual savings	3148654	NOK	2737630
Power							
Heating power	3111	kW		**BTES**	**46665000**	**NOK**	**Initial Investment**

$$Drilling\ costs\ per\ borehole = 51m * 1000\frac{NOK}{m} + 229m * 250\frac{NOK}{m} = 108250\ NOK$$

$$Total\ drilling\ costs = 108250\ NOK * 300\ boreholes = 32475000\ NOK$$

COP = 4.34 (from CoolPack COP = 3.34 + 1)

Space heating BTES:

$Costs\ BTES = 15000\frac{NOK}{kW} * 3111kW = 46.665.000\ NOK$ Initial investment

$$Savings\ on\ DH\ only = 0.9 * 10609000kWh * 0.7\frac{NOK}{kWh} = 6.683.670\ NOK$$

$$DH\ costs = (0.1 * 10609000kWh + 2850000kWh) * 0.7\frac{NOK}{kWh} = 2.737.630\ NOK$$

➔ 2850000 kWh are for ground temperature recovery

$$E_{Comp} = \frac{0.9 * 10609000\ kWh}{4.34} = 2.200.023\ kWh$$

CO_2 heat pumps:

	CO2 Heat Pumps						
					assumed COP	5,7	
	Initial costs per heat pump						
	20 kW hp	175000	NOK		DHW demand	4872200	kWh
	30 kW hp	200000	NOK		**DHW costs**	**3410540**	**NOK**
	40 kW hp	305000	NOK			This is what I am going to safe	
					Ecomp	727194	kWh
Compressor capacity [kW]	Heat Pump capacity [kW]	Costs estimation [NOK]	Costs incl. MVA [NOK]		**Compressor**	**509036**	**NOK**
3,33	19	175000	210000				Annual costs
4,39	25	200000	240000		**Storage tanks**		
3,68	21	200000	240000				
2,28	13	175000	210000		Total nr	196	
3,68	21	200000	240000		Price per 1000 l tan	13500	NOK
4,04	23	200000	240000				
5,44	31	305000	366000		Nr of tanks chosen	100	
0,00					**Total price for storage tanks**	**1350000**	**NOK**
6,14	35	305000	366000			Initial investment	
4,21	24	200000	240000				
2,81	16	175000	210000				
4,21	24	200000	240000				
5,09	29	305000	366000				
4,21	24	200000	240000				
6,67	38	305000	366000				
0,00							
3,86	22	200000	240000				
2,81	16	175000	210000				
4,74	27	200000	240000				
4,39	25	200000	240000				
4,74	27	200000	240000				
5,96	34	305000	366000				
3,33	19	175000	210000				
	Costs for all hp	4600000	5520000	NOK			
	Other costs	200000		NOK			
	Inst. Costs for all hp	4200000	4200000	NOK			
	Total cost heat pump	**8800000**	**9720000**	**NOK**			

Space heating and DHW heating concept:

Space heating concept						
	Initial costs [NOK]			**Payback Time**	**27,87**	**years**
BTES	46665000					
Solar	32142410					
SUM	**78807410**					
	Energy costs per year [NOK]					
DH only	7426300					
	Annual costs of the new system [NOK]					
BTES	4277646					
Solar	321424	Pumping costs are not included				
SUM	4599070					
Annual Savings [NOK]	2827230					

$$Annual\ savings = Energy\ costs\ per\ year\ DH\ only - Annual\ costs\ of\ the\ new\ system$$

$$Payback\ time = \frac{Sum\ of\ initial\ costs}{Annual\ savings} = 27.87\ years$$

DHW concept					
	Initial costs [NOK]		**Payback Time**	**3,91**	**years**
CO2 heat pumps	9720000				
Storage tanks	1620000				
SUM	**11340000**				
	Energy costs per year [NOK]				
DH only	3410540				
	Annual costs of the new system [NOK]				
CO2 heat pumps	509036				
Storage tanks	-				
SUM	509036				
Annual Savings [NOK]	2901504				

Analysis for the whole project:

Analysis for the whole project					
	Initial costs [NOK]		**Payback Time**	**15,74**	**years**
Space heating	78807410				
DHW	11340000				
SUM	**90147410**				
	Energy costs per year [NOK]				
DH only SH	7426300				
DH only DHW	3410540				
DH only SUM	10836840				
	Annual costs of the new system [NOK]				
SH	4599070				
DHW	509036				
SUM	5108106				
	Annual Savings [NOK]				
SH	2827230				
DHW	2901504				
SUM	5728734				

Sensitivity analysis:

Sensitivity analysis					
	New characteristic nr	Payback Time [Years]	"Normal" PT [Years]	x-Axis value	Part from Normal
Nr of coll ±20% [-]	3196	16,46	17,08	0,5	3,63
Nr of coll ±20% [-]	2130,4	17,47	17,08	0,5	-2,28
Coll efficiency +3% [MWh]	4434	16,56	17,08	1,5	3,04
Coll efficiency -3% [MWh]	4112	17,29	17,08	1,5	-1,23
Initial inv costs [NOK]	97314151	18,79	17,08	2,5	-10,01
	79620669	15,38	17,08	2,5	9,95
Annual cost savings [NOK]	5696181	15,53	17,08	3,5	9,07
	4660512	18,98	17,08	3,5	-11,12
Annual SH demand +20%	8950	18,49	17,08	4,5	-8,26
Annual SH demand -20%	5950	17,65	17,08	4,5	-3,34

NPV and NPVQ:

$$NPV = Annual\ savings\ [kWh] * Energy\ Price\left[\frac{NOK}{kWh}\right] * \left(\frac{1-(1+r)^{-T}}{r}\right) - C_0$$

	NPV Space heating		NPV DHW		NPV STG	
Year	NPV	NPV Q	NPV	NPV Q	NPV	NPV Q
0	-79	-1,00	-11	-1,00	-90	-1,00
1	-76	-0,96	-8	-0,74	-84	-0,94
2	-73	-0,93	-5	-0,47	-78	-0,87
3	-70	-0,89	-2	-0,20	-72	-0,80
4	-67	-0,85	1	0,07	-66	-0,73
5	-64	-0,81	4	0,35	-60	-0,66
6	-61	-0,77	7	0,63	-54	-0,59
7	-58	-0,73	10	0,92	-47	-0,52
8	-54	-0,69	14	1,22	-41	-0,45
9	-51	-0,65	17	1,52	-34	-0,37
10	-48	-0,60	21	1,82	-27	-0,30
11	-44	-0,56	24	2,13	-20	-0,22
12	-41	-0,52	28	2,45	-13	-0,14
13	-37	-0,47	31	2,77	-6	-0,06
14	-34	-0,43	35	3,10	2	0,02
15	-30	-0,38	39	3,43	9	0,10
16	-26	-0,33	43	3,77	17	0,18
17	-22	-0,28	47	4,11	24	0,27
18	-18	-0,23	51	4,46	32	0,36
19	-14	-0,18	55	4,82	40	0,45
20	-10	-0,13	59	5,18	48	0,54
21	-6	-0,08	63	5,55	57	0,63
22	-2	-0,03	67	5,93	65	0,72
23	2	0,03	72	6,31	74	0,82
24	6	0,08	76	6,70	82	0,91
25	10,71	0,14	80,53	7,10	91,24	1,01